Measurement of the suppression and azimuthal anisotropy of muons from heavy-flavor decays in Pb+Pb collisions at $\sqrt{s_{NN}} = 2.76$ TeV with the ATLAS detector

M. Aaboud *et al.**
(ATLAS Collaboration)

ATLAS measurements of the production of muons from heavy-flavor decays in $\sqrt{s_{NN}} = 2.76$ TeV Pb+Pb collisions and $\sqrt{s} = 2.76$ TeV pp collisions at the LHC are presented. Integrated luminosities of 0.14 nb^{-1} and 570 nb^{-1} are used for the Pb+Pb and pp measurements, respectively, which are performed over the muon transverse momentum range $4 < p_T < 14$ GeV and for five Pb+Pb centrality intervals. Backgrounds arising from in-flight pion and kaon decays, hadronic showers, and misreconstructed muons are statistically removed using a template-fitting procedure. The heavy-flavor muon differential cross sections and per-event yields are measured in pp and Pb+Pb collisions, respectively. The nuclear modification factor R_{AA} obtained from these is observed to be independent of p_T, within uncertainties, and to be less than unity, which indicates suppressed production of heavy-flavor muons in Pb+Pb collisions. For the 10% most central Pb+Pb events, the measured R_{AA} is approximately 0.35. The azimuthal modulation of the heavy-flavor muon yields is also measured and the associated Fourier coefficients v_n for $n = 2, 3$, and 4 are given as a function of p_T and centrality. They vary slowly with p_T and show a systematic variation with centrality which is characteristic of other anisotropy measurements, such as that observed for inclusive hadrons. The measured R_{AA} and v_n values are also compared with theoretical calculations.

I. INTRODUCTION

Heavy quarks, especially bottom quarks, provide an important probe of the properties of the quark-gluon plasma created in high-energy nuclear ($A+A$) collisions [1–8]. The masses of the charm and bottom quarks are much larger than the temperatures of 200–500 MeV attained in the plasma (Ref. [9] and references therein). As a result, the heavy quarks are mostly produced early in the collision at rates that are, in principle, calculable using perturbative QCD, and their subsequent interactions with the plasma give experimentally observable signatures. At transverse momenta (p_T) much greater than the mass of the bottom quark, heavy quarks are expected to lose energy similarly to light quarks but with mass-dependent modifications to the pattern of collisional and radiative energy loss [3,10–15]. At lower transverse momenta, $p_T \lesssim m_b$, the quarks are expected to diffuse in the plasma [4,7,16], losing energy and partially thermalizing [1,17]. As a result of their interactions with the collectively expanding medium, the heavy quarks may acquire an azimuthal anisotropy. Previous measurements of heavy-flavor production in $A+A$ collisions at RHIC and the LHC, using semileptonic decays [18–21] and direct reconstruction of heavy-flavor mesons [22–26],

have shown both substantial suppression in the yield of heavy quarks due to energy loss and significant azimuthal anisotropy. Measurements of the heavy-quark yield and azimuthal anisotropy in Pb+Pb collisions at the LHC can provide valuable constraints on plasma transport parameters, such as the heavy-quark diffusion coefficient, and potentially distinguish between weak- and strong-coupling models for heavy-quark interactions in the plasma [5,27–31].

The yield of particles produced in hard-scattering processes in $A+A$ collisions is often characterized using the nuclear modification factor

$$R_{AA} = \frac{1}{\langle T_{AA} \rangle} \frac{\frac{1}{N_{\text{evt}}} \frac{d^2 N}{dp_T d\eta}\big|_{\text{cent}}}{\frac{d^2 \sigma^{pp}}{dp_T d\eta}}, \tag{1}$$

where η is the pseudorapidity, the numerator is the differential per-event yield in $A+A$ collisions for a given centrality interval, the denominator is the pp differential cross section for producing the given particles, and $\langle T_{AA} \rangle$ represents the nuclear overlap function averaged over the centrality interval [32]. In the absence of significant modification to the nuclear parton distributions and of final-state interactions of the outgoing partons, R_{AA} should be unity. Measurements of the production of vector bosons [33–37] in Pb+Pb collisions at the LHC have verified this expectation. In contrast, measurements of R_{AA} for jets [38,39] and single hadrons [40–42] have shown a centrality-dependent suppression that is understood to result from the energy loss of the parent quarks and gluons (Refs. [43–45] and references therein). Measurements of D-meson production in Pb+Pb collisions at the LHC [24] have shown a centrality- and p_T-dependent suppression similar to

---

*Full author list given at the end of the article.

that observed for single hadrons. A measurement of *b*-hadron production, via their inclusive decays to J/ψ mesons, has also shown significant suppression [46]. Separate measurements of the production of forward heavy-flavor electrons [47] and muons [20] that are predominantly produced in semileptonic *B*- and *D*-meson decays give R_{AA} values that are significantly larger than those observed for inclusive hadrons. However, the $b \to J/\psi X$ and forward muon measurements are statistically limited and insufficient to test theoretical calculations.

The azimuthal anisotropy of particles produced in an $A+A$ collision is often characterized by harmonic coefficients v_n in a Fourier expansion of the particle yield as a function of azimuthal angle ϕ [48],

$$\frac{dN}{d\phi} = \left\langle \frac{dN}{d\phi} \right\rangle \left(1 + 2 \sum_{n \geqslant 1} v_n \cos(n[\phi - \Phi_n]) \right), \qquad (2)$$

where Φ_n represents the event-plane angle for the *n*th harmonic. In noncentral collisions, the azimuthal anisotropy is usually dominated by the $n = 2$ term due to the almondlike shape of the collision geometry in the transverse plane resulting from the nonzero impact parameter. Measurements of inclusive [49–53] and identified hadron [54,55] v_n values in $A+A$ collisions at the LHC and at RHIC show the presence of significant azimuthal anisotropies, which are well reproduced by hydrodynamic calculations. These results provide the basis for the interpretation that the medium created in heavy-ion collisions is strongly coupled. The elliptic flow of heavy-flavor hadrons depends both on the coupling of the heavy quark with the medium and on the transfer of the collective motion of the medium to the heavy-flavor hadron in the hadronization process [56]. The measurements of *D*-meson elliptic flow at midrapidity at the LHC [25,26] give v_2 values that are similar to those measured for light hadrons, while the forward-rapidity heavy-flavor v_2 values measured using semileptonic decays to muons are significantly smaller. However, those measurements are statistically limited and, thus, do not provide stringent constraints on theoretical calculations of the heavy-flavor elliptic flow. This paper presents ATLAS measurements of muons from heavy-flavor semileptonic decays (heavy-flavor muons, hereafter) in *pp* collisions at $\sqrt{s} =$ 2.76 TeV and Pb+Pb collisions at $\sqrt{s_{NN}} = 2.76$ TeV. The Pb+Pb data were recorded during 2011, and the *pp* data were recorded during 2013. The measurements are performed using data sets with integrated luminosities of 570 and 0.14 nb^{-1} for *pp* and Pb+Pb collisions, respectively. They are performed for several intervals of collision centrality, characterized using the total transverse energy measured in the forward calorimeters, and for different muon p_T intervals spanning the range 4–14 GeV. Heavy-flavor muons are statistically separated from background muons resulting from pion and kaon decays and from hadronic interactions using a "momentum-imbalance" variable (Sec. III C) that compares the momenta of the muons measured in the inner detector and muon spectrometer.

Over the p_T range of the measurement, the residual irreducible contamination by non-heavy-flavor muons, including contributions from J/ψ decays [57,58], is less than 1% and is neglected in the following. The heavy-flavor muon differential per-event yields in Pb+Pb collisions and differential cross

sections in *pp* collisions measured over the pseudorapidity interval $|\eta| < 1$ are used to calculate the heavy-flavor muon R_{AA} as a function of p_T in different Pb+Pb centrality intervals. In addition, heavy-flavor muon v_n values are measured for $n = 2-4$ as a function of p_T and collision centrality over $|\eta| < 2$ using both the event-plane and scalar-product [59] methods. The scalar-product method has become the *de facto* standard procedure for v_n measurements using event-plane reconstruction. However, the method introduces additional complexity to the background subtraction procedure (see Sec. III D), so results obtained using both methods are provided. The results presented in this paper provide significantly improved statistical precision over previous measurements of the suppression and the anisotropic flow of semileptonically decaying heavy-flavor hadrons in Pb+Pb collisions at the LHC.

This paper is structured as follows. Section II describes the components of the ATLAS detector and trigger system used in the measurement, Sec. III describes the data analysis, Sec. IV discusses the systematic uncertainties, and the results are discussed in Sec. V. Section VI provides a summary and outlook.

II. ATLAS DETECTOR

The measurements presented in this paper use the ATLAS muon spectrometer (MS), inner detector (ID), calorimeter, trigger, and data acquisition systems. A detailed description of these detectors and their performance in *pp* collisions is given in Ref. [60]. Muons are reconstructed by combining independent measurements of the muon trajectories from the ID and the MS. The ID measures charged particles within the pseudorapidity interval[1] $|\eta| < 2.5$ using silicon pixel detectors, silicon microstrip detectors (SCTs), and a straw-tube tracker, all immersed in a 2-T axial magnetic field. A charged particle typically traverses three layers of silicon pixel detectors, four layers of double-sided microstrip sensors, and 36 straws. The ID is surrounded by electromagnetic and hadronic calorimeters that absorb efficiently the copious charged and neutral hadrons produced in Pb+Pb collisions. A muon typically loses 3–5 GeV of energy, depending on the muon pseudorapidity, while crossing the calorimeters. The MS surrounds the calorimeters and provides tracking for muons within $|\eta| < 2.7$ in the magnetic field produced by three air-core toroid magnet systems. Muon momenta are measured in the MS using three stations of precision drift chambers. Fast tracking detectors are used to trigger on muons in the MS.

Two forward calorimeters (FCal) are placed symmetrically with respect to $z = 0$ and cover $3.2 < |\eta| < 4.9$. They are composed of tungsten and copper absorbers with liquid argon

---

[1]ATLAS uses a right-handed coordinate system with its origin at the nominal interaction point (IP) in the center of the detector and the *z* axis along the beam pipe. The *x* axis points from the IP to the center of the LHC ring, and the *y* axis points upward. Cylindrical coordinates (r, ϕ) are used in the transverse plane, ϕ being the azimuthal angle around the *z* axis. The pseudorapidity is defined in terms of the polar angle θ as $\eta = -\ln \tan(\theta/2)$.

as the active medium; each calorimeter has a total thickness of about ten interaction lengths.

Minimum-bias Pb+Pb collisions are identified using the zero-degree calorimeters (ZDCs) and the minimum-bias trigger scintillator (MBTS) counters [60]. The ZDCs are located symmetrically at $z = \pm 140$ m and cover $|\eta| > 8.3$. They are used only in Pb+Pb collisions where they primarily measure "spectator" neutrons, which originate from the incident nuclei and do not scatter hadronically during the collision. The MBTS system detects charged particles over $2.1 < |\eta| < 3.9$ using two hodoscopes of 16 counters each, placed at $z = \pm 3.6$ m. The MBTS counters provide measurements of both the pulse heights and arrival times of ionization energy depositions in each hodoscope.

The ATLAS trigger system [61] consists of a first-level (L1) trigger implemented using a combination of dedicated electronics with programmable logic, and a software-based high-level trigger (HLT). Data used for this analysis were selected using a combination of minimum-bias triggers, which provided a uniform sampling of the Pb+Pb inelastic cross section, and triggers that selected rare physics signatures such as muons. The measurements presented here are primarily obtained from muon triggers. Events from the minimum-bias triggers are used only for cross checks.

The muon triggers are formed using a combination of a L1 trigger and an HLT muon trigger whose configuration differed between Pb+Pb and *pp* operation. For the Pb+Pb data, the L1 trigger selected events having a total transverse energy of more than 50 GeV, and the HLT trigger selected events containing a track in the MS whose p_T, when corrected for the average muon energy loss in the calorimeter, is greater than 4 GeV. In *pp* data, the muon trigger required a stand-alone muon track in the MS at L1, and a muon track reconstructed using both the ID and MS with $p_T > 4$ GeV at the HLT. The muon trigger was unprescaled throughout the Pb+Pb run and sampled essentially all of the delivered luminosity. In the *pp* run, the trigger was prescaled such that it sampled $\sim$14% (570 nb^{-1}) of the 4 pb^{-1} delivered luminosity.

III. DATA ANALYSIS

A. Event selection

Charged-particle tracks and vertices are reconstructed from hits in the ID using a track reconstruction algorithm [62] whose configuration changed between the *pp* and Pb+Pb measurements to account for the high hit density in heavy-ion collisions [50]. To remove noncollision backgrounds, Pb+Pb events are required to have a reconstructed primary vertex, at least one hit in each MBTS counter, and a time difference between the two MBTS time measurements of less than 5 ns; *pp* events are required to have at least one reconstructed primary vertex.

The centrality of Pb+Pb collisions is characterized by $\Sigma E_T^{\mathrm{FCal}}$, the total transverse energy measured in the FCal [50]. For the results presented in this paper, the minimum-bias $\Sigma E_T^{\mathrm{FCal}}$ distribution is divided into centrality intervals according to the following percentiles of the $\Sigma E_T^{\mathrm{FCal}}$ distribution ordered from the most central to the most peripheral col-

TABLE I. The $\langle T_{AA} \rangle$ values and their systematic uncertainties [38] in each centrality interval used in this analysis. For the 40–60% centrality interval, the $\langle T_{AA} \rangle$ values are obtained by averaging the values for 40–50% and 50–60% centrality intervals from Ref. [38].

Centrality interval (%)	$\langle T_{AA} \rangle$ (mb^{-1})
0–10	23.45 ± 0.37
10–20	14.43 ± 0.30
20–30	8.73 ± 0.26
30–40	5.04 ± 0.22
40–60	2.02 ± 0.15

lisions: 0–10%, 10–20%, 20–30%, 30–40%, and 40–60%. A Glauber Monte Carlo analysis [63] is used to estimate $\langle T_{AA} \rangle$ for each of the centrality intervals [38]. The results are provided in Table I.

B. Muon reconstruction

Muons in this analysis are formed by combining tracks reconstructed in the MS [57] with the tracks measured in the ID. The associated ID tracks are required to satisfy criteria for the number of hits in the SCT and pixel detectors which are the same for the *pp* and Pb+Pb data, but which are optimized for the Pb+Pb analysis [50]. In particular, for both data sets, ID tracks are required to have transverse and longitudinal impact parameters relative to the reconstructed primary vertex of less than 5 mm and to have a momentum $p > 3$ GeV. The requirements on the longitudinal and transverse impact parameters are relaxed to 5 mm, compared to the 1 mm (or 1.5 mm) typically used in heavy-ion analyses [50,52], to allow selection of muons from off-vertex heavy-flavor decays. The ID tracks are also required to have at least one pixel hit, with the additional requirement of a hit in the first pixel layer when one is expected,[2] at least seven SCT hits, and at most one hit that is expected but not found in the pixel and SCT detectors taken together. The transverse momentum measured in the MS (p_T^{MS}) is required to be greater than 1.2 GeV for both the *pp* and Pb+Pb data. In the Pb+Pb analysis, this selection removes muons for which the Pb+Pb trigger efficiency is less than 50%.

The results presented here use muons having $4 < p_T < 14$ GeV and having $|\eta| < 1$ for the heavy-flavor-suppression analysis or $|\eta| < 2$ for the flow measurements. The lower limit of the p_T range is constrained by the p_T dependence of the muon trigger and reconstruction efficiencies, while the upper limit is determined by the number of events available in the Pb+Pb data. For the R_{AA} measurements, a muon η interval of $|\eta| < 1$ is chosen, as the muon trigger and reconstruction have optimal performance over this η range. The η range is extended to $|\eta| < 2$ for the v_n measurements,

---

[2] A hit is expected if the extrapolated track crosses an active region of a pixel module that has not been disabled.

as they are not sensitive to the effects of trigger and tracking efficiency. A total of 9.2 million (1.8 million) muons are reconstructed within these kinematic ranges from 8.7 million (1.8 million) events recorded using the Pb+Pb (*pp*) muon triggers. The performance of the ATLAS detector and offline analysis in measuring muons in *pp* collisions is evaluated by a GEANT4 [64] simulation of the ATLAS detector [65] using Monte Carlo (MC) $\sqrt{s} = 2.76$ TeV *pp* events produced with the PYTHIA event generator [66] (version 6.423 with parameters chosen according to the AUET2B set of tuned parameters [67]). The reconstruction performance in Pb+Pb collisions is evaluated by "overlaying" simulated PYTHIA *pp* events on minimum-bias Pb+Pb events. In this overlay procedure, the simulated hits are combined with the data from minimum-bias events to produce the final sample. The minimum-bias Pb+Pb events used in the overlay procedure were recorded by ATLAS during the same data-taking period as the data used in this analysis. For both the *pp* and Pb+Pb measurements, the muon reconstruction efficiency increases by about 30% from $p_T = 4$ GeV to $p_T = 6$ GeV, above which it is approximately constant at 0.80 and 0.77 for the *pp* and Pb+Pb data, respectively. The Pb+Pb muon reconstruction efficiency is independent of the centrality within uncertainties.

The Pb+Pb muon trigger efficiency is measured for fully reconstructed muons using the minimum-bias Pb+Pb data set. The efficiency is evaluated as the fraction of reconstructed muons for which the HLT finds a matching muon with $p_T > 4$ GeV. It is observed to be independent of centrality, within statistical uncertainties, and increases from about 0.6 at $p_T = 4$ GeV to about 0.8 at 6 GeV, above which it is approximately constant. The *pp* muon trigger efficiency is similarly evaluated using *pp* events selected by a set of minimum-bias triggers. The efficiency increases from 0.40 for $p_T = 4$ GeV to 0.75 for $p_T = 12$ GeV.

C. Heavy-flavor-suppression measurement

The muons measured in the *pp* and Pb+Pb data sets contain background from in-flight decays of pions and kaons, muons produced from the decays of particles produced in hadronic showers in the material of the detector, and misassociations of ID and MS tracks. Previous studies have shown that the signal and background contributions to the reconstructed muon sample can be discriminated statistically [57]. This analysis relies solely on the fractional momentum imbalance $\Delta p / p_{\mathrm{ID}}$, which quantifies the difference between the ID and MS measurements of the muon momentum after accounting for the energy loss of the muon in the calorimeters. It is defined as

$$\frac{\Delta p}{p_{\mathrm{ID}}} = \frac{p_{\mathrm{ID}} - p_{\mathrm{MS}} - \Delta p_{\mathrm{calo}}(p, \eta, \phi)}{p_{\mathrm{ID}}},$$

where p_{ID} and p_{MS} represent the reconstructed muon momenta from the ID and MS, respectively, and Δp_{calo} represents the momentum- and angle-dependent average momentum loss of muons in the calorimeter obtained from simulations. Muons resulting from background processes typically have p_{MS} values smaller than would be expected for a muon
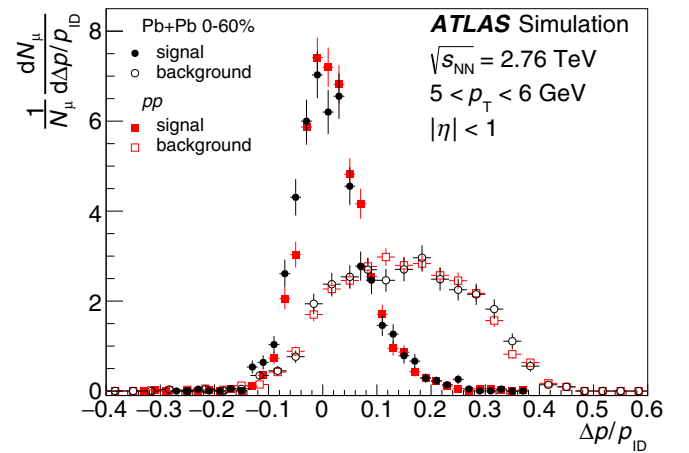

FIG. 1. Signal and background template distributions in *pp* collisions (square points) and Pb+Pb collisions (circular points) in the 0–60% centrality interval for muons having $5 < p_T < 6$ GeV and $|\eta| < 1$. The signal and background distributions are separately normalized such that their integral is unity. For clarity, the background distribution is binned more coarsely.

produced directly in *pp* or Pb+Pb collisions or via the decays of heavy-flavor hadrons. This is because the background muons from pion/kaon decays or from hadronic interactions in the calorimeter have, on average, smaller p_T compared to the parent particle. As a result, background muons are expected to have $\Delta p / p_{\mathrm{ID}} > 0$.

Distributions for $\Delta p / p_{\mathrm{ID}}$ are obtained from the simulated samples separately for signal muons and for background muons. The signal muons include muons directly produced in electromagnetic decays of hadrons, in decays of τ leptons, in decays of W and Z bosons, in decays of top quarks, and in semileptonic decays of heavy-flavor hadrons; this last contribution dominates the signal sample, contributing about 99% of the muons over the p_T range measured in this analysis (Ref. [57] and references therein). The different contributions to the background—pion decays in flight, kaon decays in flight, muons produced by secondary interactions of prompt particles, and misassociations—are evaluated separately. Figure 1 shows MC distributions of $\Delta p / p_{\mathrm{ID}}$ for signal and background muons having $5 < p_T < 6$ GeV for Pb+Pb collisions in the centrality range 0–60% and for *pp* collisions. The $\Delta p / p_{\mathrm{ID}}$ distribution for signal muons is centered at zero while the distribution for background muons is shifted to positive values. The signal distributions show only modest differences between *pp* and Pb+Pb collisions. Similarly, when making separate templates for different Pb+Pb collision centralities, a weak dependence of the signal templates on centrality is observed. The background $\Delta p / p_{\mathrm{ID}}$ distributions are much broader and are insensitive to the centrality-dependent effects seen in the signal distributions.

A template-fitting procedure is used to estimate statistically the signal fraction for each kinematic and centrality selection used in the analysis. The measured $\Delta p / p_{\mathrm{ID}}$ distribution is assumed to result from a combination of signal and background
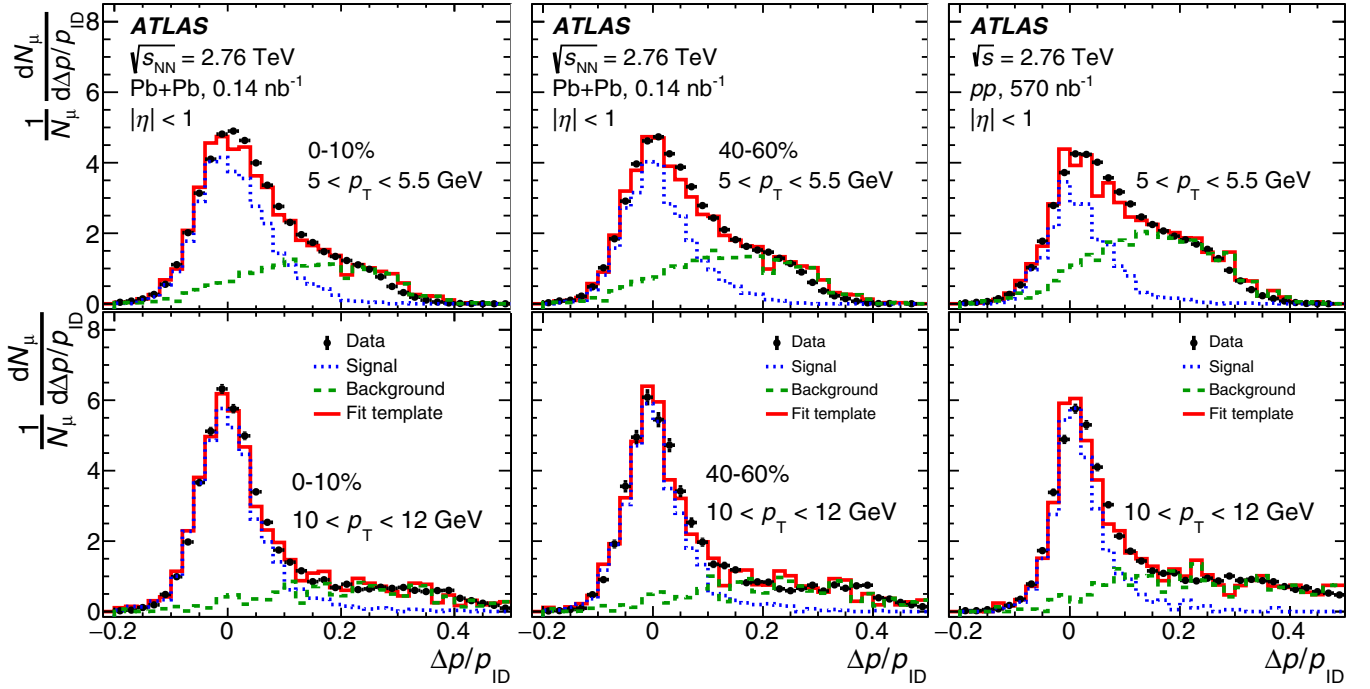
FIG. 2. Examples of template fits to Pb+Pb and *pp* data. The top panels show results for $5 < p_T < 5.5$ GeV and the bottom panels show results for $10 < p_T < 12$ GeV. The left, middle, and right panels show results for Pb+Pb 0–10%, Pb+Pb 40–60%, and *pp*, respectively. The black points represent the data. The dotted and dashed lines represent the signal and background template distributions weighted by f^{sig} and $(1 - f^{\text{sig}})$, respectively (see text) and the continuous lines represent the summed template distributions.

distributions,

$$\frac{1}{N_\mu} \frac{dN_\mu}{d\Delta p/p_{\text{ID}}} = f^{\text{sig}} \frac{dP^{\text{sig}}}{d\Delta p/p_{\text{ID}}} + (1 - f^{\text{sig}}) \frac{dP^{\text{bkg}}}{d\Delta p/p_{\text{ID}}},$$

where N_μ is the total number of muons in the sample, $dP^{\text{sig}}/d\Delta p/p_{\text{ID}}$ and $dP^{\text{bkg}}/d\Delta p/p_{\text{ID}}$ represent the signal and background $\Delta p/p_{\text{ID}}$ probability distributions, respectively, and f^{sig} represents the signal fraction.

For Pb+Pb data, centrality-dependent templates are used for the signal while centrality-integrated templates are used for the background. The latter is motivated by the observed centrality independence of the background templates and the limited size of the background sample. Template fits are performed using binned χ^2 fits that account for the statistical precision of the signal and background templates. The fits are performed using MINUIT [68] with f^{sig} as the free parameter. The uncertainties from the fits are used as statistical uncertainties of the yields and propagated into the final results. Example template fits are shown for two muon p_T intervals in Fig. 2 for Pb+Pb events in the 0–10% and 40–60% centrality intervals and for *pp* data. As shown in Fig. 2, the measured $\Delta p/p_{\text{ID}}$ distributions are well described by a combination of the signal and background templates, and this holds for all studied kinematic and centrality intervals.

The signal fractions f^{sig} obtained from the template fits using these intervals are shown in Fig. 3 for the Pb+Pb and *pp* data. The signal fractions increase with p_T for $p_T > 5$ GeV, indicating that at higher p_T a larger fraction of the recon-

structed muons are heavy-flavor (HF) muons. The increase in f^{sig} at low p_T results from the trigger, which is less efficient for background muons that have low p_T^{MS}. Such an increase is not observed when repeating this analysis using the minimum-bias Pb+Pb data set. This increase in the f^{sig} due to the trigger does not affect the measurement, as is demonstrated by studies of variations in the p_T^{MS} criterion in Sec. IV A.

With the f^{sig} obtained from the template fits, the *pp* differential cross section for producing heavy-flavor muons is calculated according to

$$\frac{d^2\sigma_{\text{HF}\mu}}{dp_T d\eta} = \frac{1}{\mathcal{L}} \frac{\Delta N_\mu f^{\text{sig}}}{\Delta p_T \Delta \eta} \frac{1}{\varepsilon_{\text{trig}} \varepsilon_{\text{rec}}}, \qquad (3)$$

where $\mathcal{L}$ is the integrated luminosity of the *pp* measurement, Δp_T is the width of the given p_T interval, $\Delta \eta = 2$ is the size of the pseudorapidity interval, ΔN_μ represents the number of muons in the given p_T and η intervals, and $\varepsilon_{\text{trig}}$ and ε_{rec} represent the trigger and reconstruction efficiencies, respectively. The luminosity is calibrated using a set of beam-separation scans performed in February 2013. It has a relative uncertainty of 3.1% that was derived following a methodology similar to that detailed in Ref. [69].

The Pb+Pb differential per-event yields for producing heavy-flavor muons are calculated according to

$$\frac{1}{N_{\text{evt}}} \frac{d^2N_{\text{HF}\mu}}{dp_T d\eta} \bigg|_{\text{cent}} = \frac{1}{N_{\text{evt}}^{\text{cent}}} \frac{\Delta N_\mu^{\text{cent}} f^{\text{sig}}}{\Delta p_T \Delta \eta} \frac{1}{\varepsilon_{\text{trig}} \varepsilon_{\text{rec}}}, \qquad (4)$$
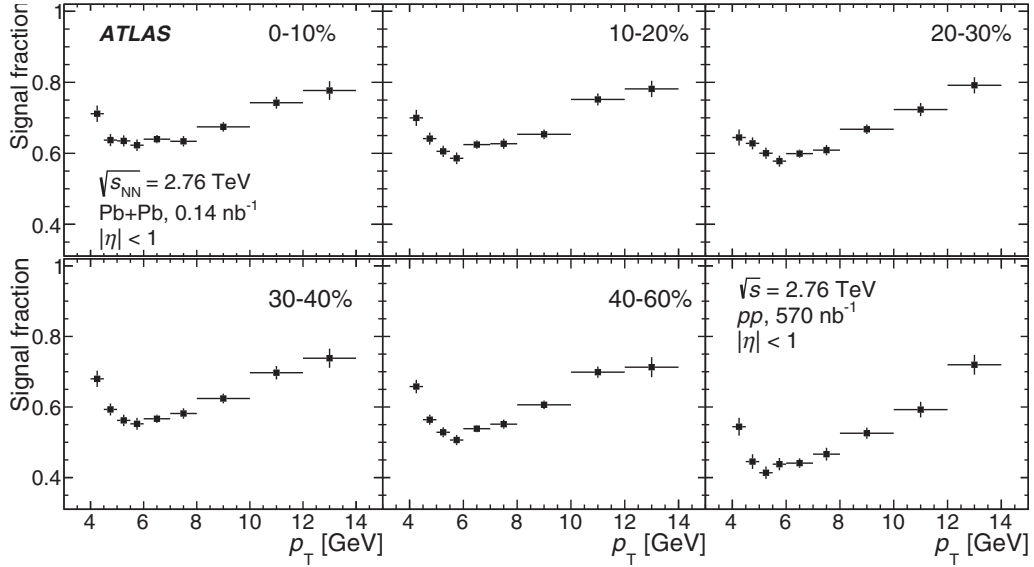
FIG. 3. Signal fraction values obtained from template fits to the Pb+Pb and *pp* data as a function of the muon p_T. Results are shown for different Pb+Pb centrality intervals and for *pp* collisions in the bottom right panel. The error bars correspond to statistical uncertainties only.

where $N_{\text{evt}}^{\text{cent}}$ is the number of Pb+Pb collisions in a given centrality interval, $\Delta N_\mu^{\text{cent}}$ represents the number of total muons with $|\eta| < 1$ measured in the given p_T and centrality interval, f^{sig} represents the corresponding signal fraction obtained from the template fits, and $\varepsilon_{\text{trig}}$ and ε_{rec} represent the trigger and reconstruction efficiencies, respectively.

D. Azimuthal anisotropy measurement

The v_n measurements additionally require determination of the event-plane (EP) angles Φ_n [Eq. (2)]. However, due to detector acceptance effects and finite particle multiplicity in an event, the measured EP angles, denoted Ψ_n, fluctuate event by event around the true EP angles [48]. The "observed" v_n, v_n^{obs}, is obtained by measuring the distribution of the particle directions relative to the Ψ_n planes:

$$\frac{dN}{d\phi} = N_0 \left[1 + 2 \sum_{n \geqslant 1} v_n^{\text{obs}} \cos[n(\phi - \Psi_n)] \right]. \quad (5)$$

The v_n^{obs} are smaller in magnitude than the true v_n because they are calculated around the Ψ_n planes rather than the Φ_n planes. To account for this, the v_n^{obs} are corrected by the EP resolution factor $\text{Res}\{n\Psi_n\}$, which accounts for the smearing of Ψ_n relative to Φ_n [48]:

$$v_n = \frac{v_n^{\text{obs}}}{\text{Res}\{n\Psi_n\}}, \quad \text{Res}\{n\Psi_n\} = \langle\cos[n(\Psi_n - \Phi_n)]\rangle_{\text{evts}}, \quad (6)$$

where, the $\langle\ldots\rangle_{\text{evts}}$ indicates averaging over all events in a given centrality class. In this analysis, the Ψ_n angle is determined using the flow vector or "q-vector" method [48], in which the q vector is calculated from the E_T deposited in

the FCal according to

$$q_{n,x} = \frac{\Sigma E_{\text{T},i} \cos(n\phi_i) - \langle\Sigma E_{\text{T},i} \cos(n\phi_i)\rangle_{\text{evts}}}{\Sigma E_{\text{T},i}},$$

$$q_{n,y} = \frac{\Sigma E_{\text{T},i} \sin(n\phi_i) - \langle\Sigma E_{\text{T},i} \sin(n\phi_i)\rangle_{\text{evts}}}{\Sigma E_{\text{T},i}}, \quad (7)$$

where the sum is over all the calorimeter towers[3] in the FCal, $E_{\text{T},i}$ is the transverse energy deposited in the ith tower, and ϕ_i denotes the azimuthal angle of the position of the center of the tower. The event-averaged terms $\langle\Sigma E_{\text{T},i} \cos(n\phi_i)\rangle_{\text{evts}}$ and $\langle\Sigma E_{\text{T},i} \sin(n\phi_i)\rangle_{\text{evts}}$ are subtracted in order to remove detector effects [70]. From the q_n vectors, the EP angles Ψ_n, are determined as [71]

$$\tan(n\Psi_n) = \frac{q_{n,y}}{q_{n,x}}.$$

The parameter $\text{Res}\{n\Psi_n\}$ is determined by the two-subevents (2SE) method [48]. In the 2SE method, the signal from a detector used to measure the event plane is divided into two "subevents" covering equal pseudorapidity ranges in opposite η hemispheres, such that the two subevents nominally have the same resolution. The FCal detectors located at positive and negative η, FCal$^\text{P}$ and FCal$^\text{N}$, provide such a division. The resolution of the FCal$^{\text{P(N)}}$ is calculated from the correlation between the two subevents

$$\text{Res}\big(n\Psi_n^{\text{P(N)}}\big) = \sqrt{\big\langle \cos n\big(\Psi_n^\text{P} - \Psi_n^\text{N}\big)\big\rangle},$$

where $\Psi_n^{\text{P(N)}}$ is the event-plane angle determined from the positive (negative) side of the FCal. From the subevent resolution the full FCal resolution can be determined by the procedure

---

[3]Calorimeter towers are localized groups of calorimeter cells that have a $\delta\eta \times \delta\phi$ segmentation of 0.1×0.1.
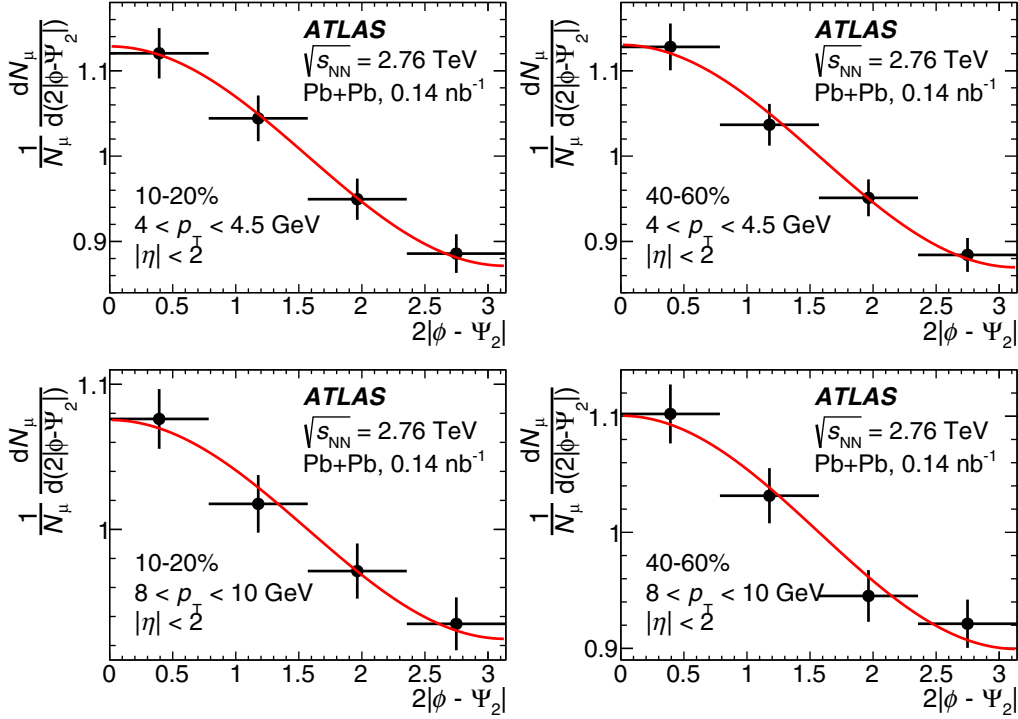
FIG. 4. Examples of heavy-flavor muon yields, expressed in thousands of muons, as a function of $2|\phi - \Psi_2|$ in intervals of $\pi/4$. The left and right columns show results for the 10–20% and 40–60% centrality intervals, respectively, and the top and bottom rows correspond to $4.0 < p_T < 4.5$ GeV and $8 < p_T < 10$ GeV, respectively. The error bars on the data points show statistical uncertainties from the fits. There are significant bin-to-bin correlations between the statistical uncertainties due to the use of the same signal and background templates in all $2|\phi - \Psi_2|$ intervals. The continuous lines indicate the results of fits of the data to Eq. (5).

described in Ref. [48]. The Res$\{n\Psi_n\}$ for the FCal and their associated systematic uncertainties were determined in a previous ATLAS analysis [52]. Those values and uncertainties are directly used in this paper. Depending on the centrality class, the EP resolution factor for the FCal varies between 0.7 and 0.9, 0.3 and 0.65, and 0.2 and 0.4 for v_2, v_3, and v_4, respectively. The uncertainties in the EP resolution factor are less than 3%, 4%, and 6% for v_2, v_3, and v_4, respectively, for all the centrality classes used in this analysis.

The heavy-flavor muon v_n^{obs} values are measured by evaluating the yields differentially relative to the Ψ_n plane. For this, the template-fitting procedure is repeated in intervals of $n|\phi - \Psi_n|$ for each p_T and centrality interval. Utilizing the n-fold symmetry of the Ψ_n plane and the fact that $\cos[n(\phi - \Psi_n)]$ is an even function, it is sufficient to bin only over the interval $(0, \pi)$ in $n|\phi - \Psi_n|$. Four intervals of $n|\phi - \Psi_n|$ $[(0,\pi/4), (\pi/4, \pi/2), (\pi/2, 3\pi/4),$ and $(3\pi/4, \pi)]$ are used. The same signal and background templates are used for the four $n|\phi - \Psi_n|$ intervals in a given p_T and centrality interval. As a result, there is a significant correlation between the statistical uncertainties of the signal fractions measured in the four $\cos[n(\phi - \Psi_2)]$ intervals. This correlation is accounted for in the statistical uncertainties of the final v_n values.

Figure 4 shows examples of the differential yields of heavy-flavor muons obtained from the template fits as a function of $2|\phi - \Psi_2|$ for two centrality and two p_T intervals.

A clear dependence of the yields on $2|\phi - \Psi_2|$ can be observed, with a larger yield in the "in-plane" direction $(2|\phi - \Psi_2| \sim 0)$ compared to the "out-of-plane" direction $(2|\phi - \Psi_2| \sim \pi)$, implying a significant v_2 signal. The differential yields are fitted with a second-order Fourier function of the form in Eq. (5) to obtain the v_2^{obs} values. In the fits, the χ^2 minimization takes into account the correlations between the statistical uncertainties of the yields in the different $2|\phi - \Psi_2|$ bins. These fits are indicated by the continuous lines in Fig. 4. The v_2^{obs} values are then corrected to account for the EP resolution [Eq. (6)] for the final results presented in Sec. V.

One drawback of the EP method is that there is an ambiguity in the interpretation of the v_n values obtained from it (from here on the v_n values obtained from the event-plane method are denoted by v_n^{EP}). In the limit of perfect EP resolution, Res$\{n\Psi_n\} \to 1$, $v_n^{\text{EP}} \to \langle v_n \rangle$, while in the limit of poor resolution, Res$\{n\Psi_n\} \to 0$, $v_n^{\text{EP}} \to \sqrt{\langle v_n^2 \rangle}$ where the $\langle \ldots \rangle$ indicates an average over all events [59]. In general, the v_n values measured with the EP method lie somewhere between $\langle v_n \rangle$ and $\langle \sqrt{v_n^2} \rangle$, depending on the value of the resolution. For this reason, the scalar-product (SP) method is considered to be a superior measurement technique, as it always measures the r.m.s. v_n value, i.e., $\sqrt{\langle v_n^2 \rangle}$ [59]. The ideal SP method entails weighting the contribution of each measured signal muon by the magnitude of the q vector [Eq. (7)] measured in the FCal,

giving

$$v_n^{\text{SP}} = \frac{\langle q_n \cos[n(\phi - \Psi_n)]\rangle_{\text{evts}}}{\text{Res}^{\text{SP}}\{n\Psi_n\}}, \qquad (8)$$

where $\text{Res}^{\text{SP}}\{n\Psi_n\}$ is the resolution for the SP method, given by

$$\text{Res}^{\text{SP}}(n\Psi_n) = \sqrt{\langle q_n^{\text{P}} q_n^{\text{N}} \cos n(\Psi_n^{\text{P}} - \Psi_n^{\text{N}})\rangle},$$

where $q_n^{\text{P(N)}}$ is the magnitude of the nth-order q vector measured in the positive z (negative z) side of the FCal. Previous ATLAS measurements for inclusive charged particles show that v_n^{EP} values differ by less than 5% from the r.m.s. v_n values for v_2, and harmonics of order $n \geqslant 3$ are consistent with the r.m.s. v_n within systematic uncertainties [72]. However, Eq. (8) cannot be directly used in the present analysis, since *a priori* it is not known whether a reconstructed muon is a signal or background muon; the number of signal muons is statistically extracted from the momentum imbalance distributions. Instead, the implementation of the SP method follows quite closely the EP method. The template fits are done in four intervals of $n|\phi - \Psi_n|$ with each muon weighted with the measured q_n in that event. These fits give the q_n-weighted signal muon yields in each $n|\phi - \Psi_n|$ interval. These weighted yields are then fitted with nth-order Fourier functions, similar to Fig. 4, to obtain the observed SP v_n values, which are then corrected by $\text{Res}^{\text{SP}}\{n\Psi_n\}$ to obtain the v_n^{SP}, presented later in Sec. V.

While the SP method has advantages over the EP method, only a modified version of the SP method can be used in the present analysis. Thus, the results obtained from both the SP and EP methods are presented.

E. Jet bias in the v_n measurement

The heavy-flavor muons measured in this analysis often result from heavy-flavor jets that have an associated back-to-back recoil jet. If the recoil jet is in the FCal, it can bias the orientation of the Ψ_n to be aligned with the azimuthal angle of the muon, yielding a larger measured v_n. This "jet bias effect" needs to be estimated and corrected for in the measurement. The magnitude of this effect is estimated using the simulated-data overlay events described in Sec. III B, where PYTHIA-generated events are overlaid on minimum-bias Pb+Pb data. The overlay is done independently of the Ψ_n angles and, thus, should yield a zero v_n value when the analysis procedure used in the data is applied to the simulated events. Any systematic deviation from $v_n = 0$ seen in the simulated data is, then, a result of jet bias. The procedure used to evaluate the jet bias in v_n values is as follows.

The presence of the recoil jet biases the observed q vector in the FCal as[4]

$$q_n^{\text{Biased}} = q_n e^{in\Psi_n} + k e^{in\phi^{\text{Jet}}},$$

where the first term on the right is the unbiased q vector, which only has the natural statistical smearing. The second term on the right is the bias introduced by the recoil jet, which shifts the event-plane angle to be aligned with the recoil jet direction. The factor k represents the strength of the bias and may depend on the p_T of the recoil jet as well as the centrality, and ϕ^{Jet} is the direction of the jet. Since the recoil jet is nominally back to back with the muon, its direction can be written as

$$\phi^{\text{Jet}} = \phi^\mu + \pi + \delta,$$

where ϕ^μ is the azimuthal angle of the muon and δ represents event-by-event fluctuations in the jet direction. This bias affects the numerator in the SP method [Eq. (8)]; the resolution [denominator in Eq. (8)] is not affected by the bias, as the resolution is calculated using minimum-bias events and not from events that are triggered by muons. The dot product between the muon's transverse direction and the biased q vector, averaged over many events, [numerator of Eq. (8)] now becomes

$$\begin{aligned} &\langle e^{in\phi^\mu}(q_n e^{-in\Psi_n} + k e^{-in(\phi^\mu + \pi + \delta)})\rangle_{\text{evts}} \\ &= \langle e^{in\phi^\mu} q_n e^{-in\Psi_n}\rangle_{\text{evts}} + \langle k e^{-in(\pi+\delta)}\rangle_{\text{evts}}. \end{aligned} \qquad (9)$$

The first term on the right is the numerator of Eq. (8) for no bias, and the second term is the bias, which conveniently separates out as an additive contribution. The second term on the right of Eq. (9) corrected by $\text{Res}^{\text{SP}}\{n\Psi_n\}$ is the jet bias in v_n^{SP}.

The bias determined in this manner is independent of p_T within statistical errors. The magnitude of the bias varies with centrality. It is smallest in the most central events—where the underlying event is quite large, and the additional energy deposited by the jet does not cause a significant perturbation—and increases with decreasing centrality. For v_2, the p_T-averaged value of this bias is 0.0025 in the 0–10% centrality interval; it increases to 0.011 in the 40–60% centrality interval. For comparison, the v_2 at $p_T = 4$ GeV in the 0–10% and 40–60% centrality intervals is about 0.04 and 0.07, respectively. Because the jet yield is suppressed by as much as a factor of 2 in Pb+Pb collisions [38], only half of this estimated bias is applied as a correction. Half of this estimated bias is also conservatively taken as the systematic uncertainty of the correction. In principle, the jet bias also affects the R_{AA} measurements since the correlated jet, if it falls within the FCal acceptance, also alters the centrality interval to which the event is assigned. However, this effect, estimated from the simulated-data overlay sample, is negligible compared to the systematic uncertainties in the R_{AA} measurement (Sec. IV A), and corrections for it are not applied.

IV. SYSTEMATIC UNCERTAINTIES

A. Yield, cross-section, and R_{AA} systematic uncertainties

The measurements of the heavy-flavor muon differential cross sections and per-event yields are subject to systematic uncertainties arising from the muon-trigger selection, muon-reconstruction efficiencies, the template-fitting procedure, muon p_T resolution, and the pp luminosity. They are

---

[4]In this section, the two-dimensional q vector is represented using complex numbers [73].

TABLE II. Relative systematic uncertainties in the heavy-flavor muon R_{AA}, quoted in percent, for selected p_T intervals.

p_T interval	$4 < p_T < 4.5$ GeV	$6 < p_T < 7$ GeV	$10 < p_T < 12$ GeV
Muon selection (%)	2.5	4	4
p_T^{MS} selection (%)	7.5	2	2
Background template variation (%)	0.5	0.5	0.5
Template fitting (%)	13	7	5
Efficiency (%)	2.5	1.5	1.5

described below. Where appropriate, the uncertainties are smoothed as a function of p_T, to reduce the statistical fluctuations in the uncertainty estimates. The systematic uncertainties for the Pb+Pb data do not show any significant variation with collision centrality.

The systematic uncertainty in the Pb+Pb muon-trigger efficiency is evaluated by varying the selections applied to the offline-reconstructed muons in the minimum-bias reference sample and re-evaluating the trigger efficiency. The resulting changes in the trigger efficiency are less than 0.5% over $4 < p_T < 14$ GeV and are taken as the estimate of the systematic uncertainty in $\varepsilon_{\mathrm{trig}}$. The uncertainty in the pp muon-trigger efficiency is evaluated similarly, and is less than 2.5% for $p_T < 6$ GeV and less than 1.5% for $p_T > 6$ GeV. The systematic uncertainty associated with the muon-reconstruction efficiency is evaluated by varying the muon selections, evaluating the reconstruction efficiency for the new selections, and repeating the analysis with the updated muon selection and reconstruction efficiency. This uncertainty is less than about

4% for the pp data and less than about 2.5% for the Pb+Pb data. Separately, the minimum p_T^{MS} (default value of 1.2 GeV, Sec. III B) is varied from 0.5 to 1.5 GeV, and the entire analysis is repeated. This variation affects the template fitting but also is sensitive to potential systematic uncertainties in the muon reconstruction and trigger efficiencies. The change in the Pb+Pb muon yields from varying the minimum p_T^{MS}, taken as a systematic uncertainty in the heavy-flavor muon yields, decreases with p_T from ∼10% to ∼1.5% over the measured p_T range. For the pp cross-section measurements, the systematic uncertainty decreases with p_T from ∼11.5% to ∼3%. The systematic uncertainty associated with the p_T^{MS} criterion is somewhat correlated with the systematic uncertainty associated with the trigger efficiency; however, they are conservatively treated as independent uncertainties.

Systematic uncertainties resulting from the construction of the templates, particularly the background template, are evaluated by changing the relative proportions of different background contributions. The pion and kaon decay-in-flight

TABLE III. Systematic uncertainties in the heavy-flavor muon v_n for selected p_T and centrality intervals. The values are for the EP method and are quoted either as absolute values or in percent. They are averaged over p_T intervals that are larger than the intervals used for the measurement.

|	p_T interval	$4 < p_T < 5$ GeV		$6 < p_T < 10$ GeV		$10 < p_T < 14$ GeV	
	Centrality	0–10%	40–60%	0–10%	40–60%	0–10%	40–60%
v_2	p_T^{MS} selection (10^{-3})	0.6	1.0	0.2	0.3	0.2	0.3
	Muon selection (10^{-3})	1.0	1.2	2.0	3.0	2.0	3.0
	Background template variation (10^{-3})	0.1	0.5	0.1	0.5	0.1	0.5
	Template fitting (10^{-3})	0.1	0.1	0.1	0.1	0.1	0.1
	Jet bias correction (10^{-3})	1.2	5.5	1.2	5.5	1.2	5.5
	p_T resolution (%)	1.0	1.0	1.0	0.4	0.6	0.6
	EP resolution (%)	3.7	3.3	3.7	3.3	3.7	3.3
v_3	p_T^{MS} selection (10^{-3})	0.3	0.2	0.3	0.2	0.3	0.2
	Muon selection (10^{-3})	0.8	3.0	0.8	3.0	0.8	3.0
	Background template variation (10^{-3})	0.5	0.5	0.5	0.5	0.5	0.5
	Template fitting (10^{-3})	0.1	0.1	0.1	0.1	0.1	0.1
	Jet bias correction (10^{-3})	1.7	11.0	1.7	11.0	1.7	11.0
	p_T resolution (%)	1	1	1	1	1	1
	EP resolution (%)	3.3	5.4	3.3	5.4	3.3	5.4
v_4	p_T^{MS} selection (10^{-3})	0.5	0.8	0.5	0.8	0.5	0.8
	Muon selection (10^{-3})	0.8	0.6	0.8	0.6	2.0	2.0
	Background template variation (10^{-3})	0.2	0.5	0.2	0.5	0.2	1.5
	Template fitting (10^{-3})	0.1	0.1	0.1	0.1	0.1	0.1
	Jet bias correction (10^{-3})	1.8	15	1.8	15	1.8	15
	p_T resolution (%)	1	1.0	1.0	1.0	1.0	1.0
	EP resolution (%)	4.1	5	4.1	5	4.1	5
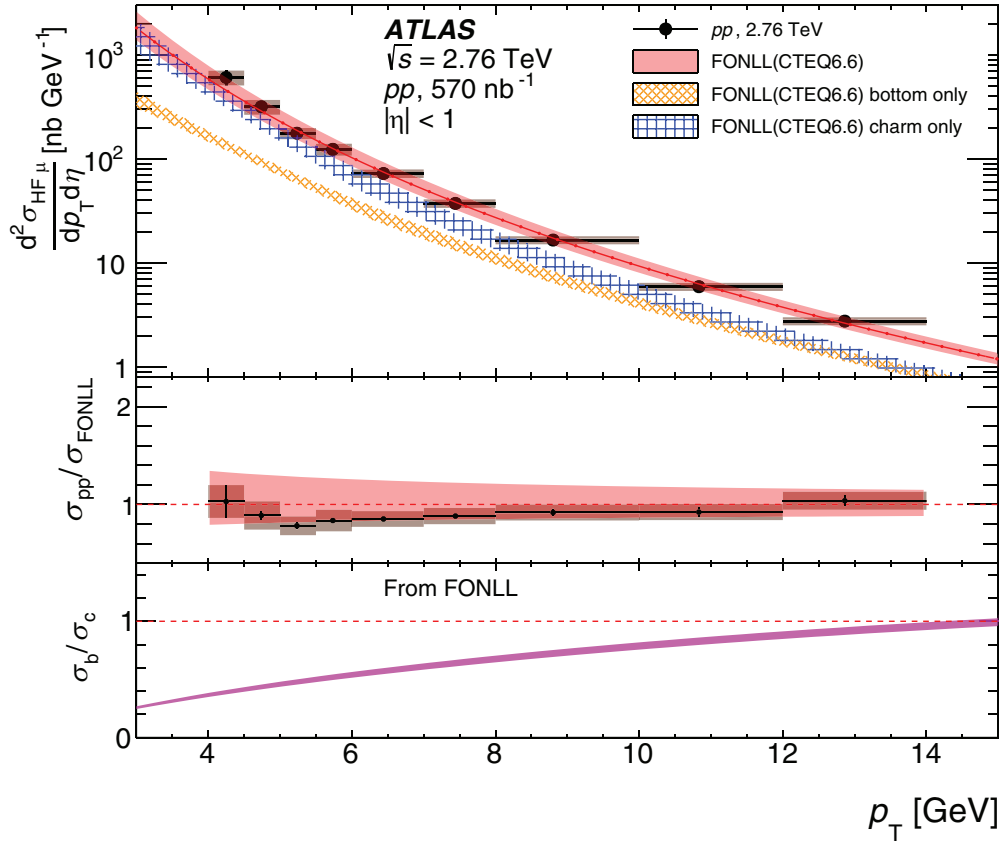
FIG. 5. Top panel: the p_T dependence of the measured heavy-flavor muon cross section in $\sqrt{s} = 2.76$-TeV pp collisions. The data points are plotted at the average muon p_T within a given p_T interval. The vertical bars and bands on the data points indicate statistical and systematic uncertainties, respectively. The cross section for heavy-flavor decays from FONLL calculations is also shown, along with the individual contributions from bottom and charm quarks. For the FONLL calculations, the vertical width of the band represents theoretical systematic uncertainties. Middle panel: the ratio of the measured and FONLL cross sections integrated over each p_T interval. Statistical and systematic uncertainties in the data are indicated by error bars and gray shaded boxes, respectively. The systematic uncertainty of the ratio from FONLL is indicated by the shaded band centered on unity. Bottom panel: the ratio of the bottom contribution to the charm contribution in the FONLL calculations. All results are averaged over $|\eta| < 1$.

components of the background are separately increased by a factor of 2 and then separately decreased by a factor of 2, as motivated by differences observed in the kaon to pion yields between PYTHIA—which is used to generate the MC templates—and data [74]. For each variation, the template fitting is performed, and a new value for f^{sig} is obtained. The average of the unsigned differences between the varied and nominal f^{sig} values is taken as the systematic uncertainty in the template fitting due to the background composition. This is less than 0.5% over the p_T range of the measurement for both the Pb+Pb and pp data.

In order to account for possible inconsistencies between the data and MC templates that may arise from the effect of the trigger, or other factors that may not be properly accounted for in the MC simulation, a separate systematic uncertainty in the template-fitting method is estimated using a "cut-and-correct" procedure applied to the $\Delta p/p_{\text{ID}}$ distributions. In this procedure, the fraction of muons having $\Delta p/p_{\text{ID}} < \Delta p/p_{\text{ID}}|_{\text{cut}}$, $f^<$, is measured in the data in each centrality and p_T interval. This fraction provides an estimate of the signal muon fraction, but it must be corrected for true muons

having $\Delta p/p_{\text{ID}} > \Delta p/p_{\text{ID}}|_{\text{cut}}$ (inefficiency) and background muons having $\Delta p/p_{\text{ID}} < \Delta p/p_{\text{ID}}|_{\text{cut}}$ (fakes). The corrections are obtained from the MC signal and background $\Delta p/p_{\text{ID}}$ distributions and are expressed in terms of the efficiencies, $\varepsilon_{\text{true}}$ and ε_{bkg}, for true and background muons, respectively, to pass the $p/p_{\text{ID}} < \Delta p/p_{\text{ID}}|_{\text{cut}}$. In terms of these efficiencies, $f^<$ is given by

$$f^< = f^{\text{sig}}\varepsilon_{\text{true}} + (1 - f^{\text{sig}})\varepsilon_{\text{bkg}}.$$

Inverting this equation, the signal fraction estimated using the cut-and-correct procedure is

$$f^{\text{sig}} = \frac{f^< - \varepsilon_{\text{bkg}}}{\varepsilon_{\text{true}} - \varepsilon_{\text{bkg}}}.$$

If the MC exactly describes the signal and background $\Delta p/p_{\text{ID}}$ distributions in the data, then the cut-and-correct f^{sig} values will be identical to the signal fractions obtained from the template fitting. Differences from the template-fit signal fractions quantify the impact of inaccuracies in the MC templates and are taken as a systematic uncertainty. The cut-and-correct f^{sig} values were evaluated using
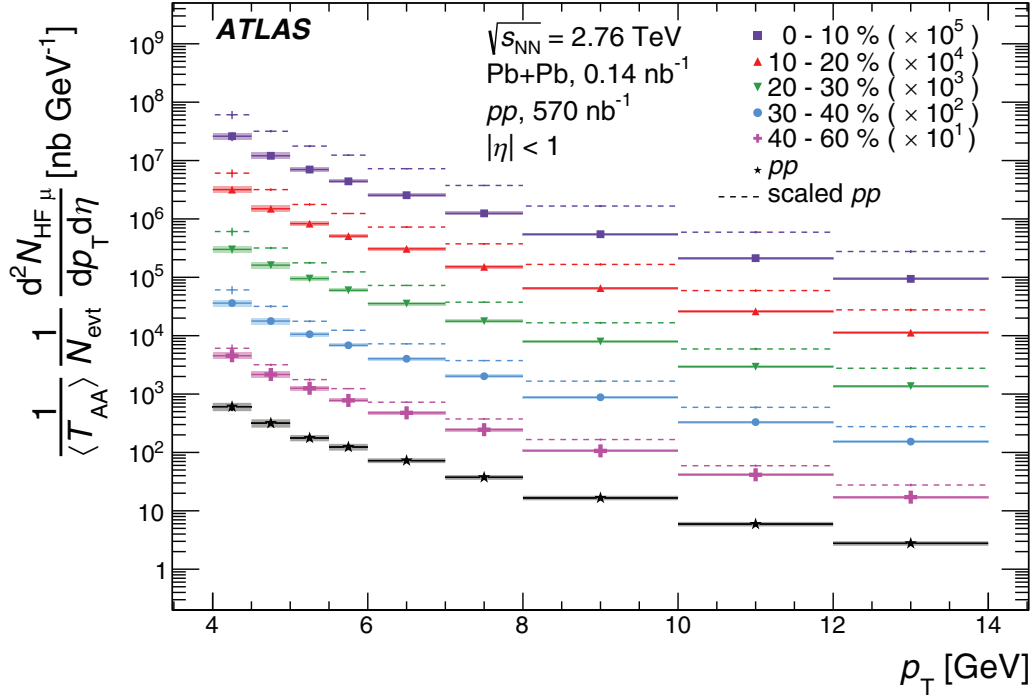
FIG. 6. The p_T dependence of the measured Pb+Pb heavy-flavor muon differential per-event yields for different centrality intervals scaled by the corresponding $\langle T_{AA} \rangle$. Also shown is the measured pp heavy-flavor muon differential cross section. For clarity, the results for the different centralities are multiplied by scale factors that are indicated in the legend. The pp cross section is replotted multiple times, as dashed lines, multiplied by these scale factors, for comparison with the results for the different Pb+Pb centralities. The error bars and shaded bands represent statistical and systematic uncertainties, respectively, and in many cases are too small to be seen.

$\Delta p / p_{ID}|_{cut} = 0.1$. The obtained signal fractions were found to be systematically higher than the results from the template fits at both low and high p_T and in both the pp and Pb+Pb data. The relative difference is largest in the lowest p_T interval where it is ~11% and 6% for the pp and Pb+Pb data, respectively. It decreases with increasing p_T, and for the highest p_T interval, is ~6% and 3% for the pp and Pb+Pb data, respectively.

The pp cross sections and Pb+Pb per-event yields are not corrected for any bin migrations that result from the muon momentum resolution. An evaluation of MC bin-by-bin correction factors gives values that are typically within 1% (2%) of unity for pp (Pb+Pb) data. These corrections are sufficiently small that they are not applied to the data. However, the deviations from unity are included in the systematic uncertainties of the cross sections and per-event yields.
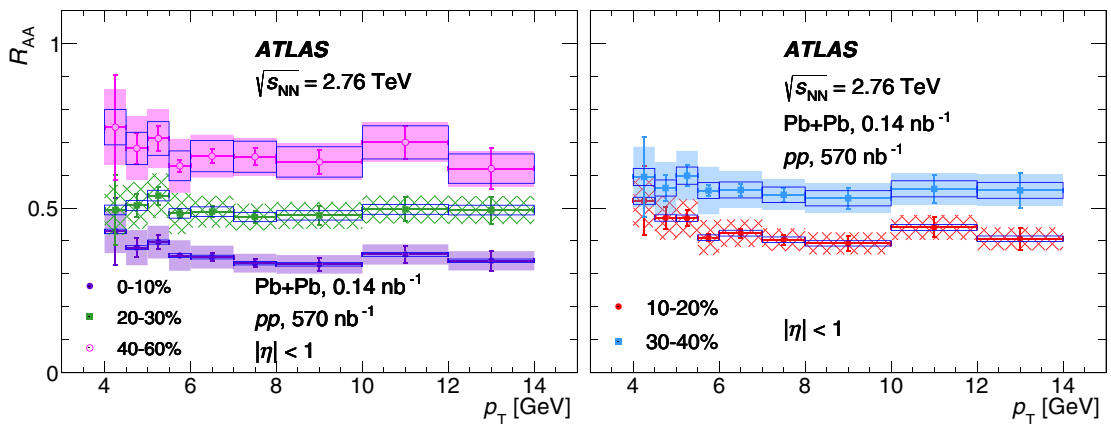

FIG. 7. The measured Pb+Pb heavy-flavor muon R_{AA} as a function of p_T. For clarity, the centrality intervals are split between the two panels. The left panel shows results for the 0–10%, 20–30%, and 40–60% centrality intervals while the right panel shows results for the 10–20% and 30–40% intervals. The error bars represent statistical uncertainties. The boxes indicate theoretical uncertainties of $\langle T_{AA} \rangle$. The shaded bands represent the experimental systematic uncertainties.
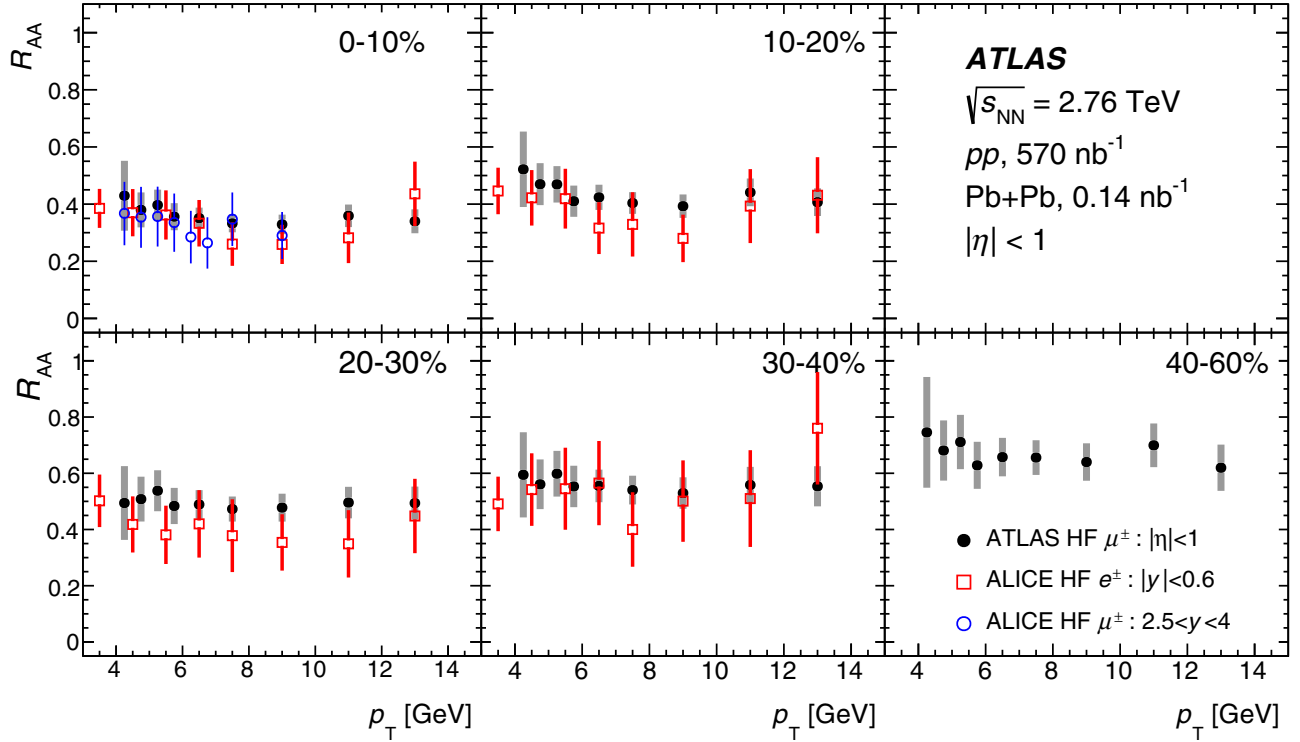
FIG. 8. Comparison of the Pb+Pb heavy-flavor muon R_{AA} measured in this analysis to similar measurements for muons at forward rapidity ($2.5 < y < 4$) and heavy-flavor electrons at midrapidity ($|y| < 0.6$) from the ALICE Collaboration. The error bars represent systematic and statistical uncertainties added in quadrature. The $\langle T_{AA} \rangle$ errors are identical between the three measurements and are excluded from the comparison.

FIG. 9. Comparison of the Pb+Pb heavy-flavor muon R_{AA} measured in this analysis to the R_{AA} for inclusive charged hadrons from ATLAS and the R_{AA} for identified D^0 mesons from the CMS Collaboration. The error bars represent systematic and statistical uncertainties added in quadrature. The $\langle T_{AA} \rangle$ errors are identical between the three measuremen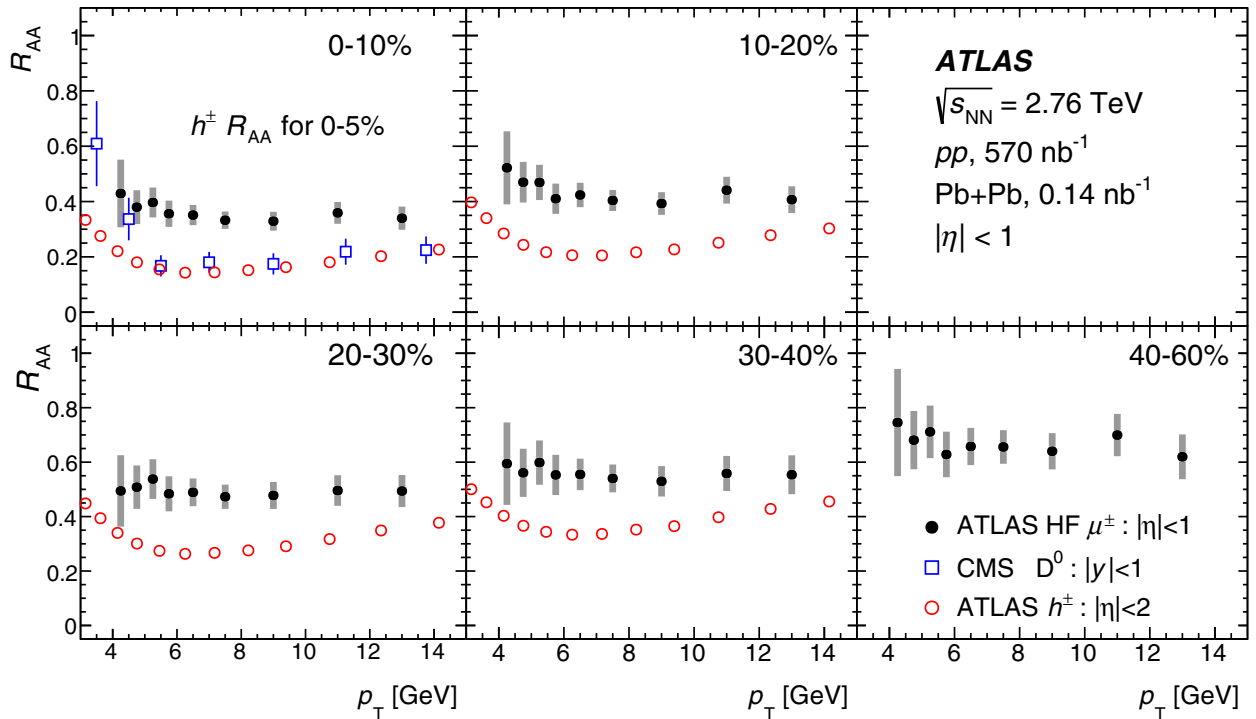ts and are excluded from the comparison. The inclusive charged hadron R_{AA} values shown in the top left panel are for the 0–5% centrality interval.
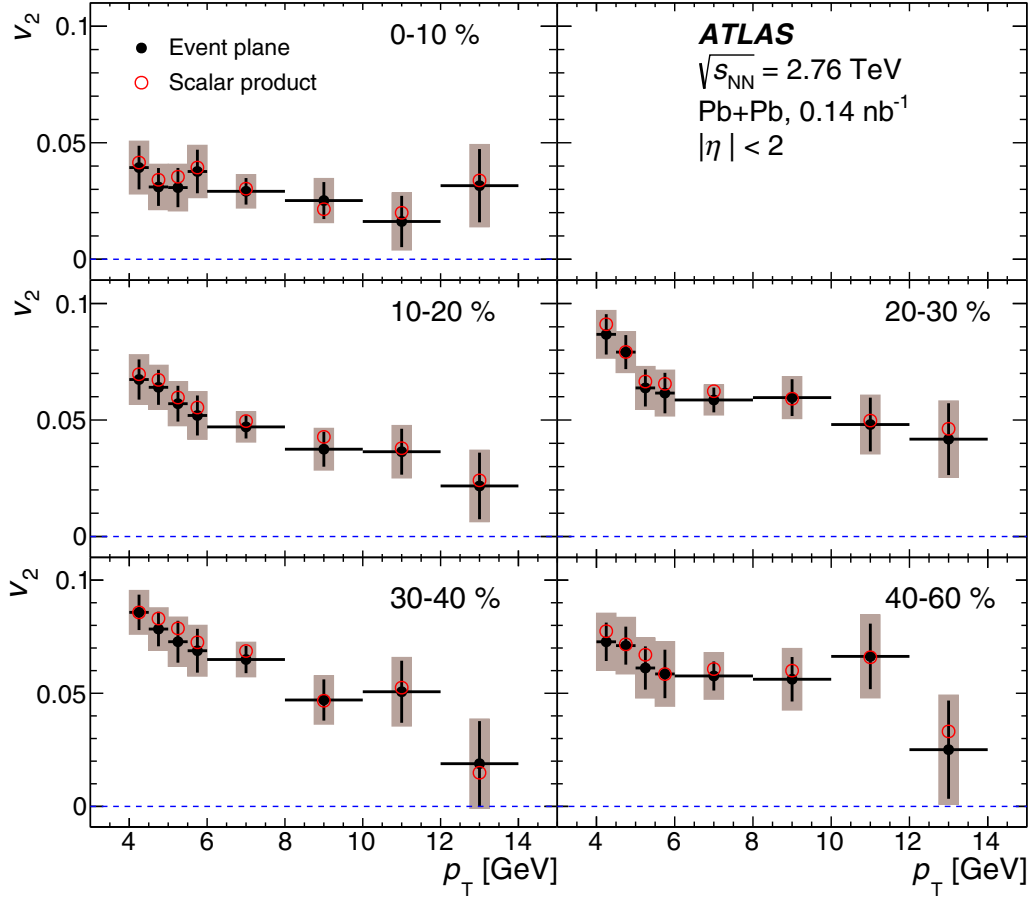
FIG. 10. The p_T dependence of the Pb+Pb heavy-flavor muon v_2. Results are shown for both the EP and SP methods. Each panel represents a different centrality interval. The error bars and shaded bands represent statistical and total uncertainties, respectively, and are shown only for the EP v_2. The horizontal dashed lines indicate $v_2 = 0$.

The measured pp cross section has an additional normalization systematic uncertainty of 3.1% due to uncertainties in the integrated luminosity.

For the R_{AA} measurement, the systematic uncertainties from the pp cross section and Pb+Pb per-event yields are propagated as if they are correlated, i.e., the systematic variations are simultaneously performed in the pp and Pb+Pb data and the change in the R_{AA} value is taken as the systematic uncertainty. Besides the systematic uncertainties from the pp cross section and Pb+Pb per-event yields, additional systematic uncertainties in the R_{AA} measurement come from theoretical uncertainties in $\langle T_{AA} \rangle$, which are listed in Table I. Table II summarizes the final experimental systematic uncertainties in R_{AA}. The total uncertainty is obtained by adding the individual uncertainties in quadrature.

B. Systematic uncertainties in v_n

The sources of the systematic uncertainties in the v_n measurements are primarily the same as those in the R_{AA} measurements (Sec. IV A). However, several sources of systematic uncertainty that affect R_{AA} do not have a significant effect on the v_n values. The v_n measurements are independent of

the trigger and tracking efficiencies. While these efficiencies have an impact on the absolute muon yields, the v_n values, which measure the relative or fractional modulation in yields, are insensitive to them. Therefore, the uncertainties in the efficiencies do not have any effect on the v_n measurements. Varying the muon selection as described in Sec. IV A changes the measured value of v_2 by $(1–2) \times 10^{-3}$ below p_T of 6 GeV. The p_T^{MS} criterion variation changes the measured value of v_2 by $(0.5–1) \times 10^{-3}$ for $p_T < 6$ GeV. At higher p_T the effect of this criterion on v_2 is about 0.2×10^{-3}. For v_3 and v_4 the effect of the p_T^{MS} criterion is $(0.5–1) \times 10^{-3}$ across the measured p_T range. The effects of the muon selection and the p_T^{MS} criterion are evaluated not just by applying the selection in the data but also by rebuilding the templates in the MC simulation while applying the variations, and then repeating the entire analysis. The variation in the shape of the background template, when varying the relative contribution of the pion and kaon backgrounds, results in variations in the v_n values that are less than 0.5×10^{-3} across most of the centrality and p_T ranges. The systematic uncertainty in v_n due to p_T-resolution effects is estimated to be less than 1% (relative) for $p_T < 10$ GeV. This estimate is obtained by first determining the p_T resolution using MC simulation
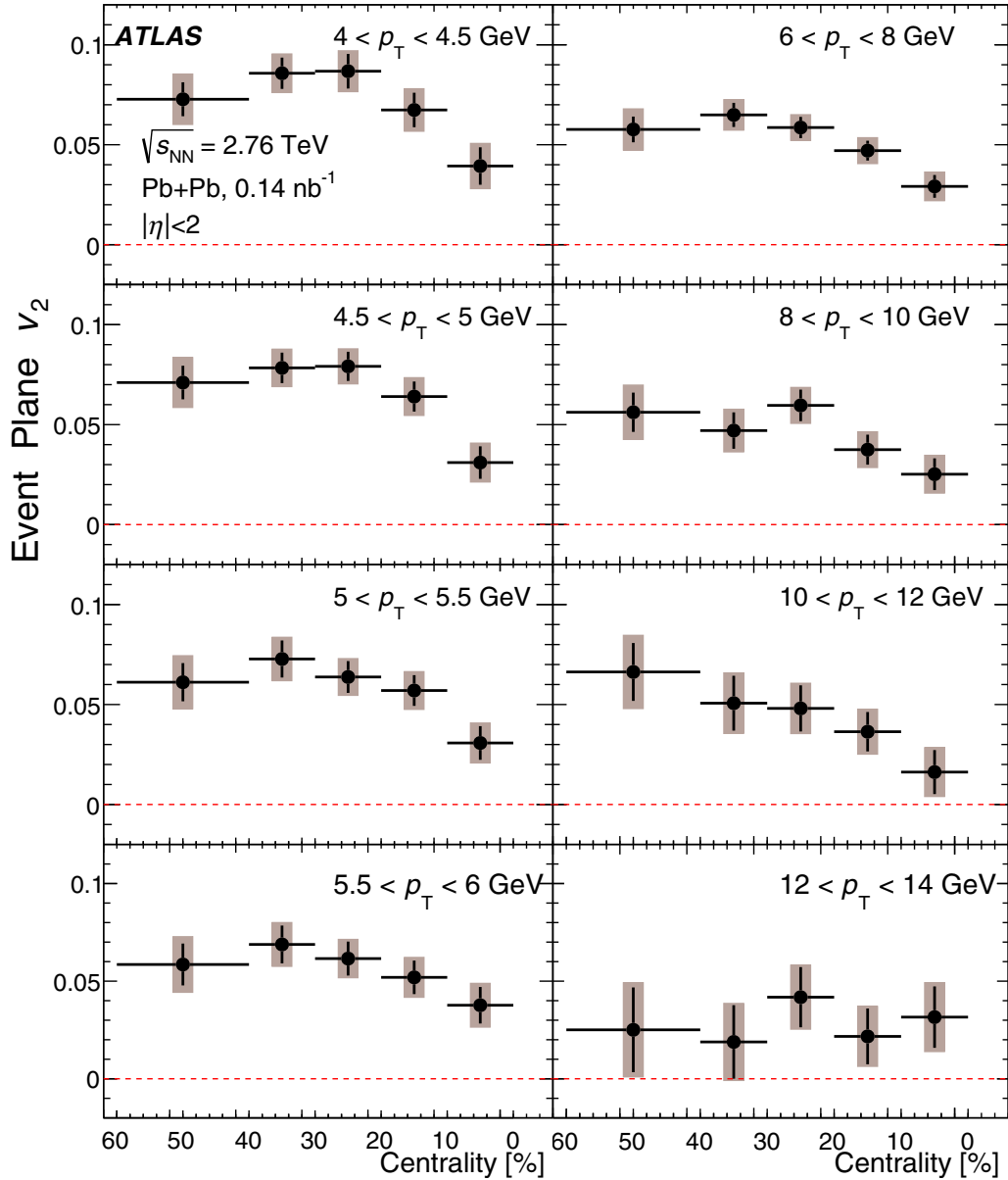
FIG. 11. The centrality dependence of the Pb+Pb heavy-flavor muon v_2 (the horizontal scale decreases in centrality). Each panel represents a different p_T interval. The error bars and shaded bands represent statistical and total uncertainties, respectively. The dashed lines indicate $v_2 = 0$. The results are for the EP method.

(Sec. III B), and then evaluating the change in the v_2 values when smearing the p_T of the reconstructed muons by this resolution. The uncertainty arising from the p_T resolution is treated as a fractional uncertainty; since if v_n changes, then the p_T resolution effects that result in migration of muons from one p_T interval to an adjacent one also increase proportionally. For $p_T > 10$ GeV, the systematic uncertainties from all the above sources are partially correlated with the statistical uncertainties, and are thus somewhat larger.

Additional systematic uncertainties that affect only the v_n but not the R_{AA} measurements are the uncertainty in the EP resolution for Ψ_n and the jet bias correction discussed in Sec. III D. The uncertainty in the EP resolution is a relative

uncertainty and depends only on the centrality. It varies between 1% and 5.5% depending on the harmonic and centrality. The systematic uncertainty associated with the jet bias correction is the leading uncertainty in the measurement. The absolute value of this uncertainty depends on the centrality and the harmonic order but is independent of p_T. It increases monotonically from central to peripheral events and is much larger for v_3 and v_4 than for v_2. Table III summarizes the systematic uncertainties for the v_n in three different p_T ranges and for two centrality intervals. The uncertainties associated with the p_T resolution and EP resolution are intrinsically fractional uncertainties and are listed as percentages. All other uncertainties are listed as absolute values.
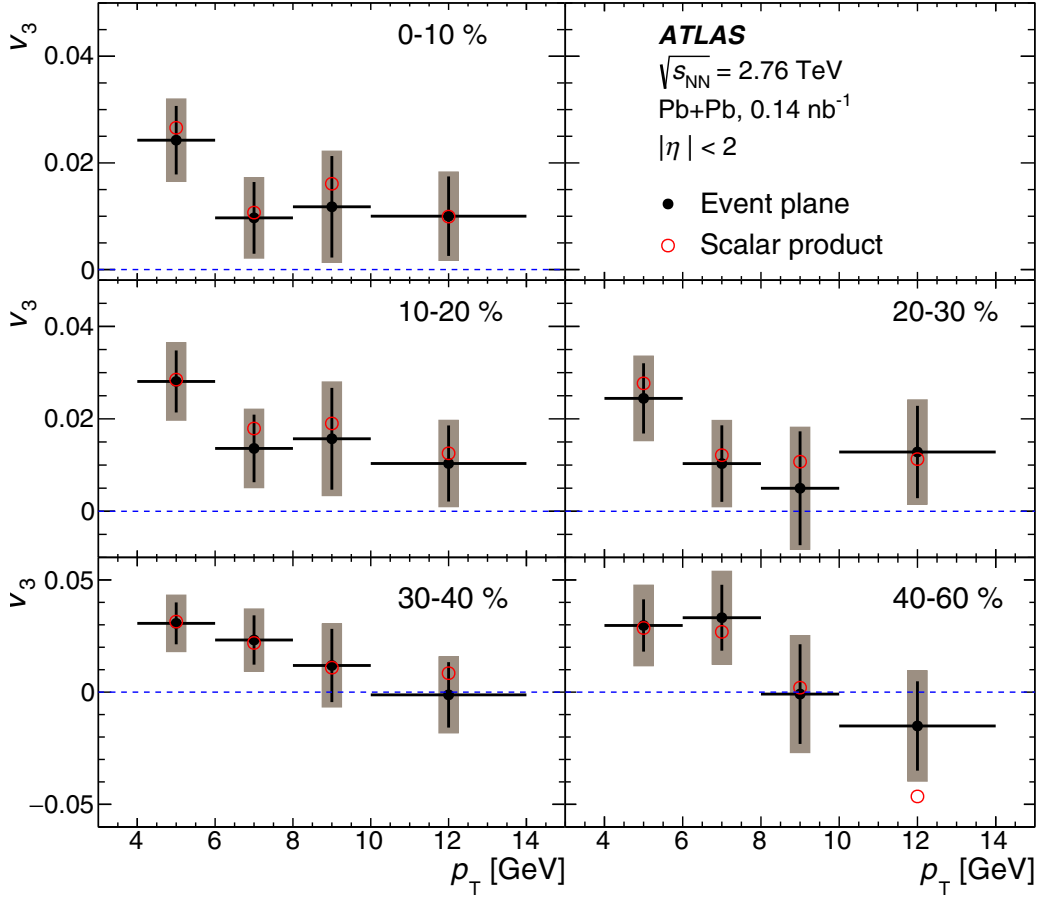
FIG. 12. The p_T dependence of the Pb+Pb heavy-flavor muon v_3. Results are shown for both the EP and SP methods. Each panel represents a different centrality interval. The error bars and shaded bands represent statistical and total uncertainties, respectively, and are shown only for the EP v_3. The horizontal dashed lines indicate $v_3 = 0$.

V. RESULTS

A. Heavy-flavor muon R_{AA}

Figure 5 shows the measured heavy-flavor muon cross sections, calculated via Eq. (3), in the $\sqrt{s} = 2.76$-TeV pp data as a function of the muon p_T. The error bars show statistical uncertainties resulting from combining the statistical uncertainties of ΔN_μ and f^{sig}. The measured cross sections are compared with fixed-order plus next-to-leading-logarithm (FONLL) [75–78] calculations using CTEQ 6.6 PDFs [79]. The FONLL calculations are based on three main components: (1) the heavy-quark production cross-section calculated in perturbative QCD by matching the fixed-order next-to-leading-order (NLO) terms with the next-to-leading-logarithms (NLLs) high-p_T resummation, (2) the nonperturbative heavy-flavor fragmentation functions determined from e^+e^- collisions and extracted in the same framework, and (3) the decays of the heavy hadrons to leptons using decay tables and form factors from B factories. The middle panel of Fig. 5 presents the ratios of the measured and FONLL cross sections. The FONLL calculation agrees with the data within systematic uncertainties. The individual contributions of the bottom and charm quarks to the heavy-flavor muon cross

section obtained from the FONLL calculations are compared in the lower panel of Fig. 5. It is seen that at 4 GeV the contribution of the bottom quark to the muon cross section is about 40% of that of the charm quark. The relative contribution increases monotonically with the muon p_T, and at $p_T = 14$ GeV, the contributions from bottom and charm decays are comparable.

Figure 6 shows the differential per-event heavy-flavor muon yields in Pb+Pb collisions [Eq. (4)] scaled by the corresponding $\langle T_{AA} \rangle$ for the centrality intervals in this analysis. The statistical uncertainties are the combined statistical uncertainties of ΔN_μ and f^{sig}. Figure 6 also compares the $\langle T_{AA} \rangle$ scaled yields to the measured pp cross section. There are significant differences between the scaled Pb+Pb yields and the pp cross section, which monotonically increase with increasing centrality.

The heavy-flavor muon R_{AA} is calculated according to Eq. (1) using the results in Fig. 6 and is shown in Fig. 7. The parameter R_{AA} does not depend on p_T within the uncertainties of the measurement. This is of note because the suppression of bottom and charm quarks in the quark-gluon plasma (QGP) is expected to be different, and the FONLL calculations show that the contribution of bottom and charm quarks changes
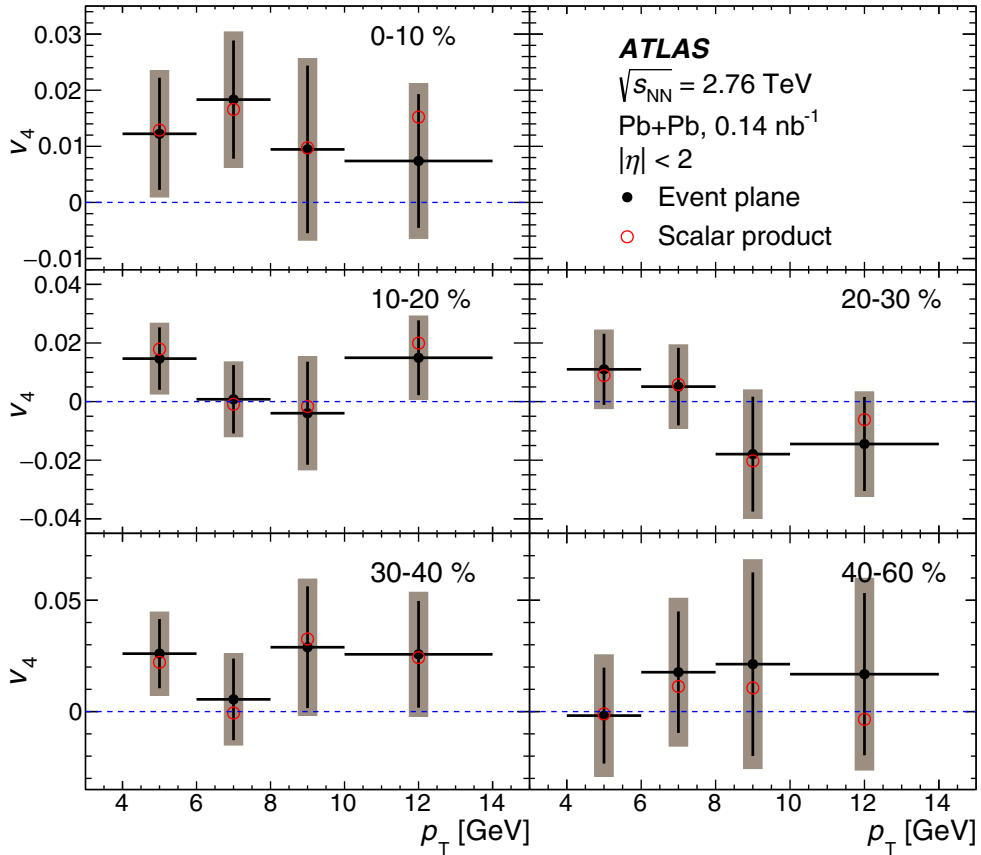
FIG. 13. The p_T dependence of the Pb+Pb heavy-flavor muon v_4. Results are shown for both the EP and SP methods. Each panel represents a different centrality interval. The error bars and shaded bands represent statistical and total uncertainties, respectively, and are shown only for the EP v_4. The horizontal dashed lines indicate $v_4 = 0$.

with p_T in the pp case, as shown in Fig. 5. The parameter R_{AA} decreases between peripheral 40–60% collisions, where it is about 0.65, to more central collisions, reaching a value of about 0.35 in the 0–10% centrality interval.

Figure 8 shows a comparison of the R_{AA} measurements in this paper with similar measurements for muons at forward rapidity ($2.5 < y < 4$) [20] and heavy-flavor electrons at midrapidity ($|y| < 0.6$) [47] from the ALICE Collaboration. In general, the results are consistent; however, the present measurements have considerably smaller uncertainties.

Figure 9 compares the R_{AA} measurement presented in this paper with the R_{AA} of inclusive charged hadrons [42] at $\sqrt{s_{NN}} = 2.76$ TeV and identified D^0 mesons [80] from the CMS Collaboration at $\sqrt{s_{NN}} = 5.02$ TeV. The R_{AA} from D^0 analyses is similar to that of inclusive hadrons for $p_T > 5$ GeV [80], implying that the charm suppression is very similar to that for the light quarks and gluons. On the other hand, the heavy-flavor muon R_{AA}, which includes contributions from bottom and charm, is observed to be larger than that of inclusive hadrons. This would imply a significantly smaller suppression for muons from the decays of b hadrons. One caveat is that the D^0 p_T and the HF muon p_T are related differently to the p_T of the HF quark that produced them. However, this effect is mitigated by the relatively weak

p_T dependence of both the D^0 and HF muon R_{AA} over the 4–14-GeV p_T range.

B. Heavy-flavor muon v_n

Figure 10 shows the v_2 values measured using the EP method as a function of p_T for the five centrality intervals in this analysis, including the statistical and total uncertainties. The evaluation of the total uncertainty includes the correlation between the statistical uncertainties and the systematic uncertainties that are proportional to v_n, i.e., the relative uncertainties associated with the EP and p_T resolutions. This correlation arises because as the measured v_n is varied within its statistical uncertainty, the relative uncertainties that are proportional to v_n also vary. The other (absolute) systematic uncertainties are added in quadrature to the correlated uncertainty to get the total uncertainty. Over the 10–40% centrality range, v_2 is largest at the lowest measured p_T of 4 GeV and decreases for higher p_T. However, in the 0–10% and 40–60% centrality intervals, no clear p_T dependence is visible. For all centralities, a significantly nonzero v_2 is observed up to a p_T of 12 GeV. Figure 10 also shows the v_2^{SP} values, which are slightly higher than the EP values. The systematic uncertainties and a significant fraction of the statistical
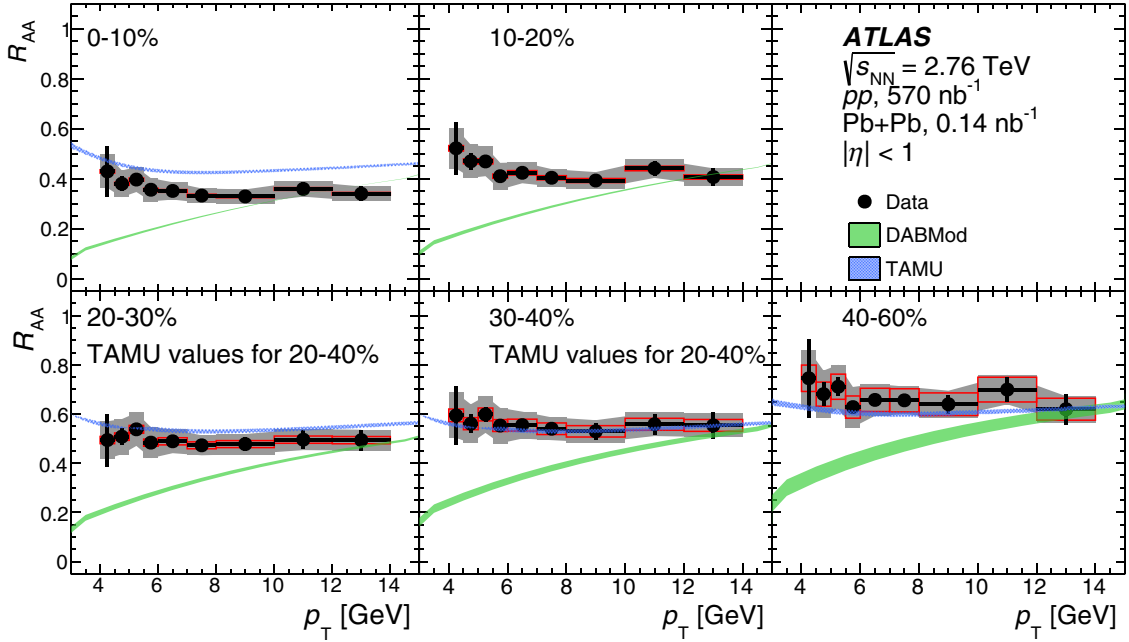
FIG. 14. Comparison of the measured heavy-flavor muon R_{AA} in Pb+Pb collisions with the values predicted from the TAMU transport model and the DABMod model. Each panel represents a different centrality interval. For the 20–30% and 30–40% centrality intervals, the plotted TAMU values correspond to the 20–40% centrality interval. For the data, the error bars represent statistical uncertainties, the shaded bands represent the experimental systematic uncertainties, and the boxes indicate theoretical uncertainties from $\langle T_{AA} \rangle$. For the model calculations the bands indicate the theoretical systematic uncertainties.

uncertainties are correlated between the EP and SP v_2 values, and for clarity are not shown for the v_2^{SP}. These measurements are consistent with previous v_2 measurements of heavy-flavor muons [21] and heavy-flavor electrons [81] from the ALICE Collaboration, but have significantly smaller statistical and systematic uncertainties, and are performed over wider centrality and p_T ranges.

Figure 11 shows the v_2 obtained from the EP method plotted as a function of centrality for different p_T intervals. For p_T in the range 4–8 GeV, the centrality dependencies of the heavy-flavor muon v_2 are qualitatively similar in shape, but considerably smaller in magnitude, to those for charged hadrons of similar p_T [50,52]. In this p_T range, the v_2 first increases from central to midcentral events, reaches a maximum between 20% and 40% centrality, and then decreases. Over the p_T range of 8–12 GeV, some deviation from this trend is observed, with the v_2 increasing monotonically from central to peripheral events. However, the associated statistical and systematic uncertainties are considerably larger. This monotonically increasing centrality dependence of the v_2 at high p_T is also seen in the inclusive charged hadron v_2 [50,52]. For the highest p_T interval of $12 < p_T < 14$ GeV, the statistical and systematic errors are too large to identify a clear centrality dependence of v_2.

Figure 12 shows the p_T dependence of v_3. At a given p_T and centrality, v_3 is a factor of 2–3 smaller than the corresponding v_2. As with v_2, v_3 also decreases with increasing p_T over the 4–8-GeV p_T range. At higher p_T, the statistical uncertainties are too large to observe clear p_T-dependent trends. The parameter v_3 shows a much weaker variation with centrality: the v_3 values at a given p_T are consistent within

uncertainties across the different centrality intervals. These features for the centrality and p_T dependence are consistent with observations of the inclusive charged-hadron v_3 [52]. Figure 13 shows the p_T dependence of v_4. The statistical uncertainties in v_4 do not allow inference of any significant p_T- or centrality-dependent trends.

C. Comparison with theoretical models

In this section, the measured R_{AA} and v_2 values are compared with calculations from the TAMU transport model [82] and the DABMod model [83]. TAMU is a transport model for heavy flavor within the QGP and subsequent hadronic phase. The initial heavy-quark spectra used in the model are obtained from FONLL calculations, accounting for shadowing effects in Pb+Pb collisions. The space-time evolution of the bulk QGP medium, in which the heavy quarks diffuse, is modeled using ideal relativistic hydrodynamics, tuned to reproduce the charged-hadron p_T spectra and inclusive elliptic flow measured in Pb+Pb collisions at the LHC. The initial conditions for the hydrodynamic modeling are obtained from the Glauber model and do not include initial state fluctuations or initial flow. After this tuning, there are no free parameters in the model. The hadronization of heavy-flavor quarks is done partially via recombination of heavy quarks with light-flavor hadrons in the QGP and partially by fragmentation. Finally, the diffusion of heavy-flavor hadrons in the hadronic phase is continued until kinetic freeze-out. DABMod is an energy-loss model for heavy quarks traversing the QGP. The energy loss is a parametrized analytic function of the velocity of the heavy quark and the local temperature. The initial p_T distribution of
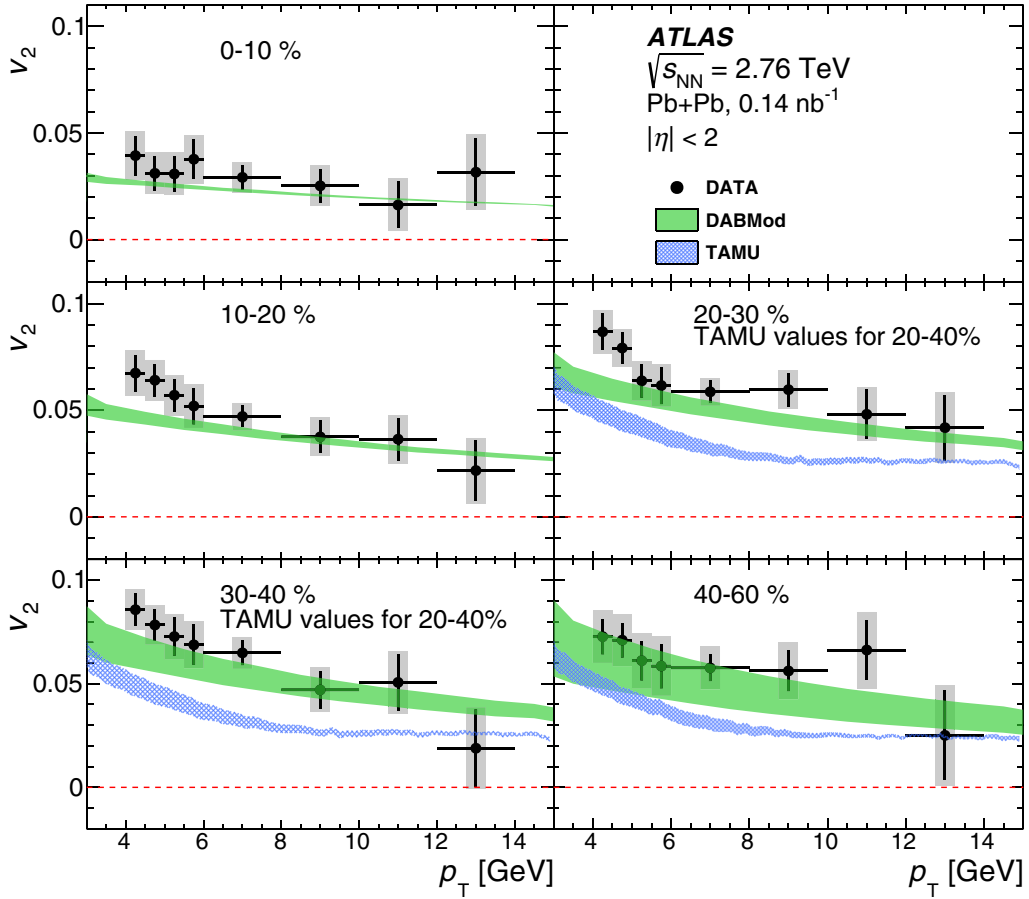
FIG. 15. Comparison of the Pb+Pb heavy-flavor muon v_2 with calculations from the TAMU and DABMod models. Each panel represents a different centrality interval. For the 20–30% and 30–40% centrality intervals, the plotted TAMU values correspond to the 20–40% centrality interval. For the data, the error bars and shaded bands represent statistical and total uncertainties, respectively. For the model calculations, the bands represent theoretical systematic uncertainties.

heavy quarks is obtained from FONLL calculations. The underlying QGP is modeled using (2+1)-dimensional relativistic viscous hydrodynamics including event-by-event fluctuations in the initial conditions and subsequent hydrodynamic expansion. All the hydrodynamic parameters are tuned to describe the experimental flow data at low p_T. The heavy quarks are evolved on top of the hydrodynamic underlying event until they reach a decoupling temperature below which they are hadronized via fragmentation. Any subsequent hadronic rescattering is neglected. The DABMod model calculations are available for R_{AA} and v_2–v_4 for all the centrality intervals over which the measurements are performed in this paper. The TAMU calculations for R_{AA} are available for the 0–10%, 20–40%, and 40–60% centrality intervals, and for v_2 for the 20–40% and 40–60% centrality intervals only.

Figure 14 compares the measured heavy-flavor muon R_{AA} values with theoretical calculations from the TAMU and DABMod models. Generally, the TAMU model describes many features of the data well, especially the weak p_T dependence of R_{AA}, while DABMod only reproduces the measured R_{AA} for $p_T > 12$ GeV. The failure of the DABMod model at low p_T is understood to result from incomplete modeling of heavy-flavor suppression for $p_T \lesssim m_b$. The TAMU model

predicts a larger suppression in the 40–60% centrality interval and a lower suppression in the 0–10% centrality interval than what is measured. Thus, the range of the suppression seen in the data is larger than in the TAMU model. As stated above, the TAMU model does not implement event-by-event fluctuations in the initial geometry, which are known to affect the dynamical evolution of bulk medium [63,84]. This may be one of the possible reasons for the smaller dynamical range of R_{AA} predicted by the model.

Figure 15 compares the measured heavy-flavor v_2 values with calculations from the TAMU and DABMod models. The DABMod v_2 values are systematically larger than the TAMU values and closer to the measured v_2. Unlike TAMU, the DABMod calculations include event-by-event fluctuations which are known to increase v_n [63,84]. This could be a possible reason for the systematically larger v_2 values obtained in the DABMod model. The DABMod calculations are consistent with the measured values for $p_T > 6$ GeV for all centralities. However, for $4 < p_T < 6$ GeV and for the 10–40% centrality range, the calculated values are significantly smaller than the measured v_2 values. The TAMU v_2 values are significantly smaller than the measured v_2 over the $4 < p_T < 10$ GeV p_T range. Figure 16 compares the measured v_3 values
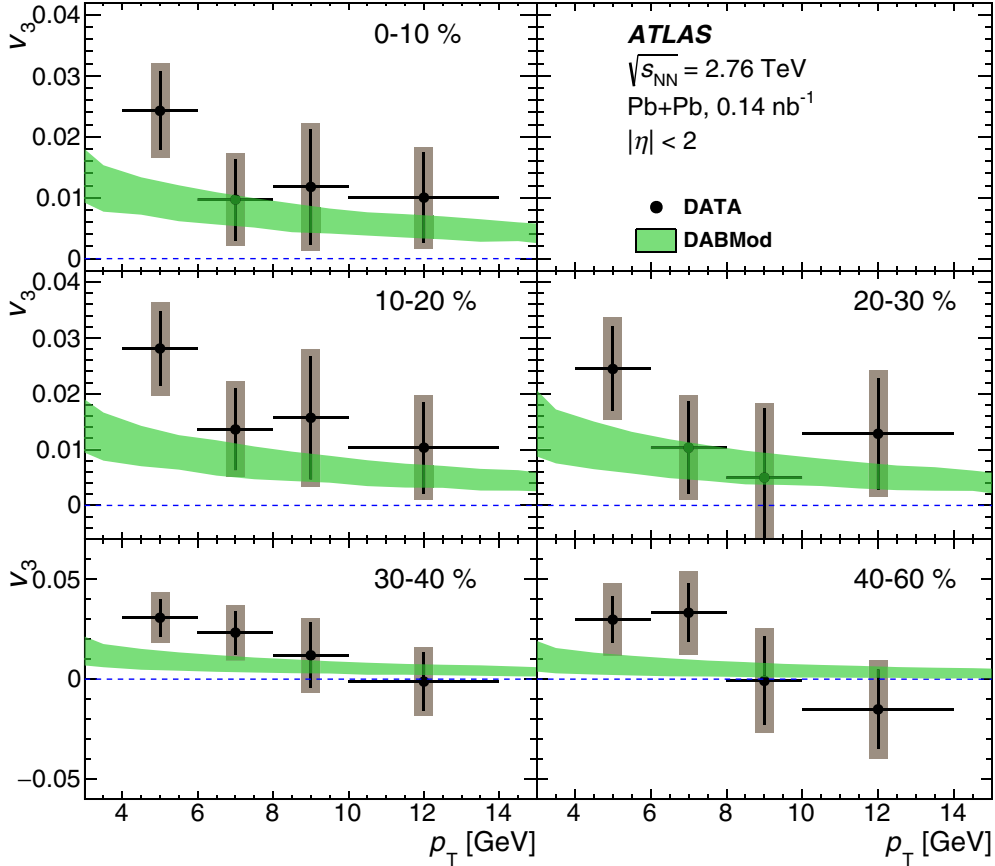
FIG. 16. Comparison of the Pb+Pb heavy-flavor muon v_3 with calculations from the DABMod model. Each panel represents a different centrality interval. For the data, the error bars and shaded bands represent statistical and total uncertainties, respectively. For the model calculations, the bands represent theoretical systematic uncertainties.

to calculations from the DABMod model. Features similar to the v_2 comparison are observed; the model predictions are smaller than the measured v_3 for $4 < p_T < 6$ GeV but become consistent with the data at higher p_T. The DABMod calculations are also compared with the v_4 measurements. However, the large experimental uncertainties do not allow detailed comparisons with the model predictions.

VI. CONCLUSION

This paper presents ATLAS measurements of heavy-flavor muon production in 0.14 nb^{-1} of $\sqrt{s_{NN}} = 2.76$ TeV Pb+Pb collisions and 570 nb^{-1} of $\sqrt{s} = 2.76$ TeV pp collisions at the LHC. The measurements are performed over the transverse momentum range of $4 < p_T < 14$ GeV. Backgrounds arising from in-flight pion and kaon decays, hadronic showers, and misreconstructed muons are statistically removed using a template-fitting procedure based on the relative difference between the muon track momenta in the muon spectrometer and inner detector, corrected for energy loss in the calorimeter system. The heavy-flavor muon differential cross sections and per-event yields are measured in pp and Pb+Pb collisions, respectively. The nuclear modification factor R_{AA} calculated from these quantities shows a centrality-dependent suppression that does not depend on p_T within uncertainties. In the

0–10% centrality interval, $R_{AA} \sim 0.35$. In Pb+Pb collisions, measurements of the heavy-flavor muon yields as a function of $\phi - \Psi_n$, the azimuthal angle of the muons relative to the event-plane angles, show a clear sinusoidal modulation of the yield in all centrality intervals. The heavy-flavor muon v_n, for $n = 2$–4, is measured in Pb+Pb collisions as a function of p_T for five centrality intervals covering the 0–60% centrality range. Significant v_2 values up to about 0.08 are observed at $p_T = 4$ GeV. In the 10–20%, 20–30%, and 30–40% intervals, the v_2 decreases with p_T but is still significant at 10 GeV. At fixed p_T, the v_2 values show a systematic variation with centrality which is typical of elliptic-flow measurements. For most centrality intervals, v_3 also decreases with increasing p_T over the 4–8-GeV p_T range. For $p_T > 8$ GeV, the statistical uncertainties in the measured v_3 values are too large to discern any p_T-dependent trends. At a given p_T and centrality, the v_3 values are smaller than the v_2 values by a factor of 2–4. Further, v_3 shows a much weaker centrality dependence than v_2. Conclusions about any p_T- or centrality-dependent trends in the v_4 are limited by the statistical precision.

The measured R_{AA} and v_2 are also compared with theoretical predictions from the TAMU and DABMod models. The R_{AA} values from the TAMU model show a weak p_T dependence over the 4–14-GeV p_T range, qualitatively

similar to the measured R_{AA}. However, the predicted R_{AA} values are smaller than the measured values in the 40–60% centrality interval, and larger than the measured values in the 0–10% centrality interval. On the other hand, the DABMod model predicts a strong p_T dependence for R_{AA}, which is not observed in the data. The R_{AA} value at $p_T = 4$ GeV predicted by DABMod is significantly smaller than the measured values but increases with increasing p_T and becomes comparable to the measured values at $p_T = 12$ GeV. For v_2, the TAMU and DABMod qualitatively reproduce the observed p_T dependence but the DABMod calculations are more consistent with the measured values. Thus both models fail to simultaneously reproduce v_2 and R_{AA} over the measured p_T range.

The R_{AA} values measured here for $|\eta| < 1$ and v_2 values for $|\eta| < 2$ are compatible with, but are substantially more precise than, similar measurements of heavy-flavor muons at forward rapidity ($2.5 < y < 4$) and heavy-flavor electrons at midrapidity ($|y| < 0.6$) from the ALICE Collaboration. Thus, they should provide improved insight into the propagation of heavy quarks in the quark-gluon plasma created in Pb+Pb collisions.

ACKNOWLEDGMENTS

[1] H. van Hees and R. Rapp, Thermalization of heavy quarks in the quark-gluon plasma, Phys. Rev. C **71**, 034907 (2005).

[2] H. van Hees, V. Greco, and R. Rapp, Heavy-quark probes of the quark-gluon plasma and interpretation of recent data taken at the BNL Relativistic Heavy Ion Collider, Phys. Rev. C **73**, 034913 (2006).

[3] C. P. Herzog, A. Karch, P. Kovtun, C. Kozcaz, and L. G. Yaffe, Energy loss of a heavy quark moving through $\mathcal{N} = 4$ supersymmetric Yang-Mills plasma, J. High Energy Phys. 07 (2006) 013.

[4] H. van Hees, M. Mannarelli, V. Greco, and R. Rapp, Nonperturbative Heavy-Quark Diffusion in the Quark-Gluon Plasma, Phys. Rev. Lett. **100**, 192301 (2008).

[5] W. A. Horowitz and M. Gyulassy, Heavy quark jet tomography of Pb + Pb at LHC: AdS/CFT drag or pQCD energy loss? Phys. Lett. B **666**, 320 (2008).

[6] J. Uphoff, O. Fochler, Z. Xu, and C. Greiner, Elliptic flow and energy loss of heavy quarks in ultrarelativistic heavy ion collisions, Phys. Rev. C **84**, 024908 (2011).

[7] M. He, R. J. Fries, and R. Rapp, Heavy-quark diffusion and hadronization in quark-gluon plasma, Phys. Rev. C **86**, 014903 (2012).

[8] S. Cao, G.-Y. Qin, and S. A. Bass, Heavy-quark dynamics and hadronization in ultrarelativistic heavy-ion collisions: Collisional versus radiative energy loss, Phys. Rev. C **88**, 044907 (2013).

[9] N. Armesto *et al.*, Heavy Ion Collisions at the LHC - Last Call for Predictions, J. Phys. G **35**, 054001 (2008).

[10] Y. L. Dokshitzer and D. E. Kharzeev, Heavy quark colorimetry of QCD matter, Phys. Lett. B **519**, 199 (2001).

[11] M. Djordjevic and M. Gyulassy, Heavy quark radiative energy loss in QCD matter, Nucl. Phys. A **733**, 265 (2004).

[12] N. Armesto, C. A. Salgado, and U. A. Wiedemann, Medium induced gluon radiation off massive quarks fills the dead cone, Phys. Rev. D **69**, 114003 (2004).

[13] M. Djordjevic, M. Gyulassy, R. Vogt, and S. Wicks, Influence of bottom quark jet quenching on single electron tomography of Au + Au, Phys. Lett. B **632**, 81 (2006).

[14] P. B. Gossiaux, J. Aichelin, T. Gousset, and V. Guiho, Competition of Heavy Quark Radiative and Collisional Energy Loss in Deconfined Matter, J. Phys. G **37**, 094019 (2010).

[15] P. B. Gossiaux and J. Aichelin, Tomography of the Quark-Gluon Plasma by Heavy Quarks, J. Phys. G **36**, 064028 (2009).

[16] J. Casalderrey-Solana and D. Teaney, Heavy quark diffusion in strongly coupled $\mathcal{N} = 4$ Yang-Mills, Phys. Rev. D **74**, 085012 (2006).

[17] G. D. Moore and D. Teaney, How much do heavy quarks thermalize in a heavy ion collision? Phys. Rev. C **71**, 064904 (2005).

[18] A. Adare *et al.* (PHENIX Collaboration), Energy Loss and Flow of Heavy Quarks in Au+Au Collisions at $\sqrt{s_{NN}}$ = 200 GeV, Phys. Rev. Lett. **98**, 172301 (2007).

[19] A. Adare *et al.* (PHENIX Collaboration), Heavy-quark production in $p + p$ and energy loss and flow of heavy quarks in Au + Au collisions at $\sqrt{s_{NN}}$ = 200 GeV, Phys. Rev. C **84**, 044905 (2011).

[20] ALICE Collaboration, Production of Muons from Heavy Flavor Decays at Forward Rapidity in *pp* and Pb-Pb Collisions at $\sqrt{s_{NN}}$ = 2.76 TeV, Phys. Rev. Lett. **109**, 112301 (2012).

[21] ALICE Collaboration, Elliptic flow of muons from heavy-flavour hadron decays at forward rapidity in Pb-Pb collisions at $\sqrt{s_{NN}}$ = 2.76 TeV, Phys. Lett. B **753**, 41 (2016).

[22] L. Adamczyk *et al.* (STAR Collaboration), Observation of D^0 Meson Nuclear Modifications in Au+Au Collisions at $\sqrt{s_{NN}}$ = 200 GeV, Phys. Rev. Lett. **113**, 142301 (2014).

[23] L. Adamczyk *et al.* (Star Collaboration), Measurement of D^0 Azimuthal Anisotropy at Midrapidity in Au+Au Collisions at $\sqrt{s_{NN}}$ = 200 GeV, Phys. Rev. Lett. **118**, 212301 (2017).

[24] ALICE Collaboration, Suppression of high transverse momentum D mesons in central Pb-Pb collisions at $\sqrt{s_{NN}}$ = 2.76 TeV, J. High Energy Phys. 09 (2012) 112.

[25] ALICE Collaboration, *D* Meson Elliptic Flow in Noncentral Pb-Pb Collisions at $\sqrt{s_{NN}}$ = 2.76 TeV, Phys. Rev. Lett. **111**, 102301 (2013).

[26] ALICE Collaboration, Azimuthal anisotropy of D-meson production in Pb-Pb collisions at $\sqrt{s_{NN}}$ = 2.76 TeV, Phys. Rev. C **90**, 034904 (2014).

[27] S. Caron-Huot and G. D. Moore, Heavy quark diffusion in QCD and $\mathcal{N}$ = 4 SYM at next-to-leading order, J. High Energy Phys. 02 (2008) 081.

[28] S. S. Gubser, S. S. Pufu, F. D. Rocha, and A. Yarom, Energy loss in a strongly coupled thermal medium and the gauge-string duality, in *Quark Gluon Plasma*, edited by R. Hwa and X.-N. Wang (World Scientific, Singapore, 2009), Vol. 4, Chap. 1.

[29] C. Hoyos, Drag and jet quenching of heavy quarks in a strongly coupled $\mathcal{N}$ = 2* plasma, J. High Energy Phys. 09 (2009) 068.

[30] J. Noronha, M. Gyulassy, and G. Torrieri, Conformal holography of bulk elliptic flow and heavy-quark quenching in relativistic heavy ion collisions, Phys. Rev. C **82**, 054903 (2010).

[31] M. Chernicoff, D. Fernandez, D. Mateos, and D. Trancanelli, Drag force in a strongly coupled anisotropic plasma, J. High Energy Phys. 08 (2012) 100.

[32] R. J. Glauber and G. Matthiae, High-energy scattering of protons by nuclei, Nucl. Phys. B **21**, 135 (1970).

[33] ATLAS Collaboration, Measurement of Z Boson Production in Pb+Pb Collisions at $\sqrt{s_{NN}}$ = 2.76 TeV with the ATLAS Detector, Phys. Rev. Lett. **110**, 022301 (2013).

[34] CMS Collaboration, Study of W boson production in PbPb and *pp* collisions at $\sqrt{s_{NN}}$ = 2.76 TeV, Phys. Lett. B **715**, 66 (2012).

[35] CMS Collaboration, Measurement of isolated photon production in *pp* and PbPb collisions at $\sqrt{s_{NN}}$ = 2.76 TeV, Phys. Lett. B **710**, 256 (2012).

[36] ATLAS Collaboration, Measurement of the production and lepton charge asymmetry of W bosons in Pb+Pb collisions at $\sqrt{s_{NN}}$ = 2.76 TeV with the ATLAS detector, Eur. Phys. J. C **75**, 23 (2015).

[37] ATLAS Collaboration, Centrality, rapidity and transverse momentum dependence of isolated prompt photon production in lead–lead collisions at $\sqrt{s_{NN}}$ = 2.76 TeV measured with the ATLAS detector, Phys. Rev. C **93**, 034914 (2016).

[38] ATLAS Collaboration, Measurements of the Nuclear Modification Factor for Jets in Pb+Pb Collisions at $\sqrt{s_{NN}}$ = 2.76 TeV with the ATLAS Detector, Phys. Rev. Lett. **114**, 072302 (2015).

[39] ALICE Collaboration, Measurement of jet suppression in central Pb-Pb collisions at $\sqrt{s_{NN}}$ = 2.76 TeV, Phys. Lett. B **746**, 1 (2015).

[40] CMS Collaboration, Study of high-p_T charged particle suppression in PbPb compared to *pp* collisions at $\sqrt{s_{NN}}$ = 2.76 TeV, Eur. Phys. J. C **72**, 1945 (2012).

[41] ALICE Collaboration, Centrality dependence of charged particle production at large transverse momentum in Pb–Pb collisions at $\sqrt{s_{NN}}$ = 2.76 TeV, Phys. Lett. B **720**, 52 (2013).

[42] ATLAS Collaboration, Measurement of charged-particle spectra in Pb+Pb collisions at $\sqrt{s_{NN}}$ = 2.76 TeV with the ATLAS detector at the LHC, J. High Energy Phys. 09 (2015) 050.

[43] M. Gyulassy, I. Vitev, X. N. Wang, and B.-W. Zhang, Jet quenching and radiative energy loss in dense nuclear matter, in *Quark Gluon Plasma* (Ref. [28]),Vol. 3, Chap. 3.

[44] A. Majumder and M. Van Leeuwen, The theory and phenomenology of perturbative QCD based jet quenching, Prog. Part. Nucl. Phys. A **66**, 41 (2011).

[45] J. Casalderrey-Solana and C. A. Salgado, Introductory lectures on jet quenching in heavy ion collisions, Acta Phys. Pol. B **38**, 3731 (2007).

[46] CMS Collaboration, Suppression of non-prompt J/ψ, prompt J/ψ, and $\Upsilon(1S)$ in PbPb collisions at $\sqrt{s_{NN}}$ = 2.76 TeV, J. High Energy Phys. 05 (2012) 063.

[47] ALICE Collaboration, Measurement of the production of high-p_T electrons from heavy-flavour hadron decays in Pb-Pb collisions at $\sqrt{s_{NN}}$ = 2.76 TeV, Phys. Lett. B **771**, 467 (2017).

[48] A. M. Poskanzer and S. A. Voloshin, Methods for analyzing anisotropic flow in relativistic nuclear collisions, Phys. Rev. C **58**, 1671 (1998).

[49] ALICE Collaboration, Elliptic Flow of Charged Particles in Pb-Pb Collisions at $\sqrt{s_{NN}}$=2.76 TeV, Phys. Rev. Lett. **105**, 252302 (2010).

[50] ATLAS Collaboration, Measurement of the pseudorapidity and transverse momentum dependence of the elliptic flow of charged particles in lead–lead collisions at $\sqrt{s_{NN}}$ = 2.76 TeV with the ATLAS detector, Phys. Lett. B **707**, 330 (2012).

[51] ALICE Collaboration, Harmonic decomposition of two particle angular correlations in Pb-Pb collisions at $\sqrt{s_{NN}}$ = 2.76 TeV, Phys. Lett. B **708**, 249 (2012).

[52] ATLAS Collaboration, Measurement of the azimuthal anisotropy for charged particle production in $\sqrt{s_{NN}}$ = 2.76 TeV lead–lead collisions with the ATLAS detector, Phys. Rev. C **86**, 014907 (2012).

[53] CMS Collaboration, Multiplicity and transverse momentum dependence of two- and four-particle correlations in pPb and PbPb collisions, Phys. Lett. B **724**, 213 (2013).

[54] ALICE Collaboration, Elliptic flow of identified hadrons in Pb-Pb collisions at $\sqrt{s_{NN}} = 2.76$ TeV, J. High Energy Phys. 06 (2015) 190.

[55] ALICE Collaboration, Anisotropic flow of charged hadrons, pions and (anti-)protons measured at high transverse momentum in Pb-Pb collisions at $\sqrt{s_{NN}} = 2.76$ TeV, Phys. Lett. B **719**, 18 (2013).

[56] V. Greco, C. M. Ko, and R. Rapp, Quark coalescence for charmed mesons in ultrarelativistic heavy ion collisions, Phys. Lett. B **595**, 202 (2004).

[57] ATLAS Collaboration, Measurements of the electron and muon inclusive cross-sections in proton–proton collisions at $\sqrt{s} = 7$ TeV with the ATLAS detector, Phys. Lett. B **707**, 438 (2012).

[58] ATLAS Collaboration, Measurement of the differential cross-sections of prompt and non-prompt production of J/ψ and $\psi(2S)$ in pp collisions at $\sqrt{s} = 7$ and 8 TeV with the ATLAS detector, Eur. Phys. J. C **76**, 283 (2016).

[59] M. Luzum and J. Y. Ollitrault, Eliminating experimental bias in anisotropic-flow measurements of high-energy nuclear collisions, Phys. Rev. C **87**, 044907 (2013).

[60] ATLAS Collaboration, The ATLAS Experiment at the CERN Large Hadron Collider, JINST **3**, S08003 (2008).

[61] ATLAS Collaboration, Performance of the ATLAS Trigger System in 2010, Eur. Phys. J. C **72**, 1849 (2012).

[62] ATLAS Collaboration, Charged-particle multiplicities in pp interactions measured with the ATLAS detector at the LHC, New J. Phys. **13**, 053033 (2011).

[63] M. L. Miller, K. Reygers, S. J. Sanders, and P. Steinberg, Glauber modeling in high energy nuclear collisions, Annu. Rev. Nucl. Part. Sci. **57**, 205 (2007).

[64] S. Agostinelli, GEANT4 - a simulation toolkit, Nucl. Instrum. Methods A **506**, 250 (2003).

[65] ATLAS Collaboration, The ATLAS Simulation Infrastructure, Eur. Phys. J. C **70**, 823 (2010).

[66] T. Sjostrand, S. Mrenna, and P. Z. Skands, PYTHIA6.4 physics and manual, J. High Energy Phys. 05 (2006) 026.

[67] ATLAS Collaboration, ATLAS tunes of PYTHIA6 and PYTHIA8 for MC11, ATL-PHYS-PUB-2011-009, http://cdsweb.cern.ch/record/1363300

[68] F. James and M. Roos, Minuit: A System for Function Minimization and Analysis of the Parameter Errors and Correlations, Comput. Phys. Commun. **10**, 343 (1975).

[69] ATLAS Collaboration, Improved luminosity determination in pp collisions at $\sqrt{s} = 7$ TeV using the ATLAS detector at the LHC, Eur. Phys. J. C **73**, 2518 (2013).

[70] S. Afanasiev *et al.* (PHENIX Collaboration), Systematic studies of elliptic flow measurements in Au+Au collisions at $\sqrt{s_{NN}} = 200$ GeV, Phys. Rev. C **80**, 024909 (2009).

[71] ATLAS Collaboration, Measurement of event-plane correlations in $\sqrt{s_{NN}} = 2.76$ TeV lead–lead collisions with the ATLAS detector, Phys. Rev. C **90**, 024905 (2014).

[72] ATLAS Collaboration, Measurement of the distributions of event-by-event flow harmonics in lead–lead collisions at $\sqrt{s_{NN}} = 2.76$ TeV with the ATLAS detector at the LHC, J. High Energy Phys. 11 (2013) 183.

[73] ATLAS Collaboration, Measurement of multi-particle azimuthal correlations in pp, p+Pb and low-multiplicity Pb+Pb collisions with the ATLAS detector, Eur. Phys. J. C **77**, 428 (2017).

[74] ALICE Collaboration, Measurement of pion, kaon and proton production in proton-proton collisions at $\sqrt{s} = 7$ TeV, Eur. Phys. J. C **75**, 226 (2015).

[75] M. Cacciari, M. Greco, and P. Nason, The p_T spectrum in heavy-flavor hadroproduction, J. High Energy Phys. 05 (1998) 007.

[76] M. Cacciari, S. Frixione, and P. Nason, The p_T spectrum in heavy-flavor photoproduction, J. High Energy Phys. 03 (2001) 006.

[77] M. Cacciari, S. Frixione, N. Houdeau, M. L. Mangano, P. Nason, and G. Ridolfi, Theoretical predictions for charm and bottom production at the LHC, J. High Energy Phys. 10 (2012) 137.

[78] M. Cacciari, M. L. Mangano, and P. Nason, Gluon PDF constraints from the ratio of forward heavy-quark production at the LHC at $\sqrt{S} = 7$ and 13 TeV, Eur. Phys. J. C **75**, 610 (2015).

[79] P. M. Nadolsky, H.-L. Lai, Q.-H. Cao, J. Huston, J. Pumplin, D. Stump, W.-K. Tung, and C.-P. Yuan, Implications of CTEQ global analysis for collider observables, Phys. Rev. D **78**, 013004 (2008).

[80] CMS Collaboration, Nuclear modification factor of D^0 mesons in PbPb collisions at $\sqrt{s_{NN}} = 5.02$ TeV, Phys. Lett. B **782**, 474 (2018).

[81] ALICE Collaboration, Elliptic flow of electrons from heavy-flavour hadron decays at mid-rapidity in Pb-Pb collisions at $\sqrt{s_{NN}} = 2.76$ TeV, J. High Energy Phys. 09 (2016) 028.

[82] M. He, R. J. Fries, and R. Rapp, Heavy Flavor at the Large Hadron Collider in a Strong Coupling Approach, Phys. Lett. B **735**, 445 (2014).

[83] C. A. G. Prado, J. Noronha-Hostler, R. Katz, A. A. P. Suaide, J. Noronha, and M. G. Munhoz, Event-by-event correlations of soft hadrons and D^0 mesons in 5.02 TeV PbPb collisions at the CERN Large Hadron Collider, Phys. Rev. C **96**, 064903 (2017).

[84] B. Alver *et al.* (PHOBOS Collaboration), System Size, Energy, Pseudorapidity, and Centrality Dependence of Elliptic Flow, Phys. Rev. Lett. **98**, 242302 (2007).

[85] ATLAS Collaboration, ATLAS Computing Acknowledgements, ATL-GEN-PUB-2016-002, https://cds.cern.ch/record/2202407

M. Aaboud,[34d] G. Aad,[99] B. Abbott,[124] O. Abdinov,[13,*] B. Abeloos,[128] D. K. Abhayasinghe,[91] S. H. Abidi,[165]
O. S. AbouZeid,[143] N. L. Abraham,[153] H. Abramowicz,[159] H. Abreu,[158] Y. Abulaiti,[6] B. S. Acharya,[64a,64b,p] S. Adachi,[161]
L. Adamczyk,[81a] J. Adelman,[119] M. Adersberger,[112] A. Adiguzel,[12c,aj] T. Adye,[141] A. A. Affolder,[143] Y. Afik,[158]
C. Agheorghiesei,[27c] J. A. Aguilar-Saavedra,[136f,136a] F. Ahmadov,[77,ah] G. Aielli,[71a,71b] S. Akatsuka,[83] T. P. A. Åkesson,[94]
E. Akilli,[52] A. V. Akimov,[108] G. L. Alberghi,[23b,23a] J. Albert,[174] P. Albicocco,[49] M. J. Alconada Verzini,[86] S. Alderweireldt,[117]
M. Aleksa,[35] I. N. Aleksandrov,[77] C. Alexa,[27b] G. Alexander,[159] T. Alexopoulos,[10] M. Alhroob,[124] B. Ali,[138] G. Alimonti,[66a]

J. Alison,[36] S. P. Alkire,[145] C. Allaire,[128] B. M. M. Allbrooke,[153] B. W. Allen,[127] P. P. Allport,[21] A. Aloisio,[67a,67b] A. Alonso,[39] F. Alonso,[86] C. Alpigiani,[145] A. A. Alshehri,[55] M. I. Alstaty,[99] B. Alvarez Gonzalez,[35] D. Álvarez Piqueras,[172] M. G. Alviggi,[67a,67b] B. T. Amadio,[18] Y. Amaral Coutinho,[78b] L. Ambroz,[131] C. Amelung,[26] D. Amidei,[103] S. P. Amor Dos Santos,[136a,136c] S. Amoroso,[35] C. S. Amrouche,[52] C. Anastopoulos,[146] L. S. Ancu,[52] N. Andari,[21] T. Andeen,[11] C. F. Anders,[59b] J. K. Anders,[20] K. J. Anderson,[36] A. Andreazza,[66a,66b] V. Andrei,[59a] C. R. Anelli,[174] S. Angelidakis,[37] I. Angelozzi,[118] A. Angerami,[38] A. V. Anisenkov,[120b,120a] A. Annovi,[69a] C. Antel,[59a] M. T. Anthony,[146] M. Antonelli,[49] D. J. A. Antrim,[169] F. Anulli,[70a] M. Aoki,[79] L. Aperio Bella,[35] G. Arabidze,[104] Y. Arai,[79] J. P. Araque,[136a] V. Araujo Ferraz,[78b] R. Araujo Pereira,[78b] A. T. H. Arce,[47] R. E. Ardell,[91] F. A. Arduh,[86] J-F. Arguin,[107] S. Argyropoulos,[75] A. J. Armbruster,[35] L. J. Armitage,[90] A. Armstrong,[169] O. Arnaez,[165] H. Arnold,[118] M. Arratia,[31] O. Arslan,[24] A. Artamonov,[109,*] G. Artoni,[131] S. Artz,[97] S. Asai,[161] N. Asbah,[44] A. Ashkenazi,[159] E. M. Asimakopoulou,[170] L. Asquith,[153] K. Assamagan,[29] R. Astalos,[28a] R. J. Atkin,[32a] M. Atkinson,[171] N. B. Atlay,[148] K. Augsten,[138] G. Avolio,[35] R. Avramidou,[58a] B. Axen,[18] M. K. Ayoub,[15a] G. Azuelos,[107,aw] A. E. Baas,[59a] M. J. Baca,[21] H. Bachacou,[142] K. Bachas,[65a,65b] M. Backes,[131] P. Bagnaia,[70a,70b] M. Bahmani,[82] H. Bahrasemani,[149] A. J. Bailey,[172] J. T. Baines,[141] M. Bajic,[39] C. Bakalis,[10] O. K. Baker,[181] P. J. Bakker,[118] D. Bakshi Gupta,[93] E. M. Baldin,[120b,120a] P. Balek,[178] F. Balli,[142] W. K. Balunas,[133] E. Banas,[82] A. Bandyopadhyay,[24] S. Banerjee,[179,1] A. A. E. Bannoura,[180] L. Barak,[159] W. M. Barbe,[37] E. L. Barberio,[102] D. Barberis,[53b,53a] M. Barbero,[99] T. Barillari,[113] M-S. Barisits,[35] J. Barkeloo,[127] T. Barklow,[150] N. Barlow,[31] R. Barnea,[158] S. L. Barnes,[58c] B. M. Barnett,[141] R. M. Barnett,[18] Z. Barnovska-Blenessy,[58a] A. Baroncelli,[72a] G. Barone,[26] A. J. Barr,[131] L. Barranco Navarro,[172] F. Barreiro,[96] J. Barreiro Guimarães da Costa,[15a] R. Bartoldus,[150] A. E. Barton,[87] P. Bartos,[28a] A. Basalaev,[134] A. Bassalat,[128] R. L. Bates,[55] S. J. Batista,[165] S. Batlamous,[34e] J. R. Batley,[31] M. Battaglia,[143] M. Bauce,[70a,70b] F. Bauer,[142] K. T. Bauer,[169] H. S. Bawa,[150,n] J. B. Beacham,[122] M. D. Beattie,[87] T. Beau,[132] P. H. Beauchemin,[168] P. Bechtle,[24] H. C. Beck,[51] H. P. Beck,[20,t] K. Becker,[50] M. Becker,[97] C. Becot,[44] A. Beddall,[12d] A. J. Beddall,[12a] V. A. Bednyakov,[77] M. Bedognetti,[118] C. P. Bee,[152] T. A. Beermann,[35] M. Begalli,[78b] M. Begel,[29] A. Behera,[152] J. K. Behr,[44] A. S. Bell,[92] G. Bella,[159] L. Bellagamba,[23b] A. Bellerive,[33] M. Bellomo,[158] K. Belotskiy,[110] N. L. Belyaev,[110] O. Benary,[159,*] D. Benchekroun,[34a] M. Bender,[112] N. Benekos,[10] Y. Benhammou,[159] E. Benhar Noccioli,[181] J. Benitez,[75] D. P. Benjamin,[47] M. Benoit,[52] J. R. Bensinger,[26] S. Bentvelsen,[118] L. Beresford,[131] M. Beretta,[49] D. Berge,[44] E. Bergeaas Kuutmann,[170] N. Berger,[5] L. J. Bergsten,[26] J. Beringer,[18] S. Berlendis,[7] N. R. Bernard,[100] G. Bernardi,[132] C. Bernius,[150] F. U. Bernlochner,[24] T. Berry,[91] P. Berta,[97] C. Bertella,[15a] G. Bertoli,[43a,43b] I. A. Bertram,[87] G. J. Besjes,[39] O. Bessidskaia Bylund,[43a,43b] M. Bessner,[44] N. Besson,[142] A. Bethani,[98] S. Bethke,[113] A. Betti,[24] A. J. Bevan,[90] J. Beyer,[113] R. M. Bianchi,[135] O. Biebel,[112] D. Biedermann,[19] R. Bielski,[98] K. Bierwagen,[97] N. V. Biesuz,[69a,69b] M. Biglietti,[72a] T. R. V. Billoud,[107] M. Bindi,[51] A. Bingul,[12d] C. Bini,[70a,70b] S. Biondi,[23b,23a] T. Bisanz,[51] J. P. Biswal,[159] C. Bittrich,[46] D. M. Bjergaard,[47] J. E. Black,[150] K. M. Black,[25] R. E. Blair,[6] T. Blazek,[28a] I. Bloch,[44] C. Blocker,[26] A. Blue,[55] U. Blumenschein,[90] Dr. Blunier,[144a] G. J. Bobbink,[118] V. S. Bobrovnikov,[120b,120a] S. S. Bocchetta,[94] A. Bocci,[47] D. Boerner,[180] D. Bogavac,[112] A. G. Bogdanchikov,[120b,120a] C. Bohm,[43a] V. Boisvert,[91] P. Bokan,[170] T. Bold,[81a] A. S. Boldyrev,[111] A. E. Bolz,[59b] M. Bomben,[132] M. Bona,[90] J. S. Bonilla,[127] M. Boonekamp,[142] A. Borisov,[140] G. Borissov,[87] J. Bortfeldt,[35] D. Bortoletto,[131] V. Bortolotto,[71a,61b,61c,71b] D. Boscherini,[23b] M. Bosman,[14] J. D. Bossio Sola,[30] K. Bouaouda,[34a] J. Boudreau,[135] E. V. Bouhova-Thacker,[87] D. Boumediene,[37] C. Bourdarios,[128] S. K. Boutle,[55] A. Boveia,[122] J. Boyd,[35] I. R. Boyko,[77] A. J. Bozson,[91] J. Bracinik,[21] N. Brahimi,[99] A. Brandt,[8] G. Brandt,[180] O. Brandt,[59a] F. Braren,[44] U. Bratzler,[162] B. Brau,[100] J. E. Brau,[127] W. D. Breaden Madden,[55] K. Brendlinger,[44] A. J. Brennan,[102] L. Brenner,[44] R. Brenner,[170] S. Bressler,[178] B. Brickwedde,[97] D. L. Briglin,[21] D. Britton,[55] D. Britzger,[59b] I. Brock,[24] R. Brock,[104] G. Brooijmans,[38] T. Brooks,[91] W. K. Brooks,[144b] E. Brost,[119] J. H Broughton,[21] P. A. Bruckman de Renstrom,[82] D. Bruncko,[28b] A. Bruni,[23b] G. Bruni,[23b] L. S. Bruni,[118] S. Bruno,[71a,71b] B. H. Brunt,[31] M. Bruschi,[23b] N. Bruscino,[135] P. Bryant,[36] L. Bryngemark,[44] T. Buanes,[17] Q. Buat,[35] P. Buchholz,[148] A. G. Buckley,[55] I. A. Budagov,[77] F. Buehrer,[50] M. K. Bugge,[130] O. Bulekov,[110] D. Bullock,[8] T. J. Burch,[119] S. Burdin,[88] C. D. Burgard,[118] A. M. Burger,[5] B. Burghgrave,[119] K. Burka,[82] S. Burke,[141] I. Burmeister,[45] J. T. P. Burr,[131] D. Büscher,[50] V. Büscher,[97] E. Buschmann,[51] P. Bussey,[55] J. M. Butler,[25] C. M. Buttar,[55] J. M. Butterworth,[92] P. Butti,[35] W. Buttinger,[35] A. Buzatu,[155] A. R. Buzykaev,[120b,120a] G. Cabras,[23b,23a] S. Cabrera Urbán,[172] D. Caforio,[138] H. Cai,[171] V. M. M. Cairo,[2] O. Cakir,[4a] N. Calace,[52] P. Calafiura,[18] A. Calandri,[99] G. Calderini,[132] P. Calfayan,[63] G. Callea,[40b,40a] L. P. Caloba,[78b] S. Calvente Lopez,[96] D. Calvet,[37] S. Calvet,[37] T. P. Calvet,[152] M. Calvetti,[69a,69b] R. Camacho Toro,[132] S. Camarda,[35] P. Camarri,[71a,71b] D. Cameron,[130] R. Caminal Armadans,[100] C. Camincher,[35] S. Campana,[35] M. Campanelli,[92] A. Camplani,[39] A. Campoverde,[148] V. Canale,[67a,67b] M. Cano Bret,[58c] J. Cantero,[125] T. Cao,[159] Y. Cao,[171] M. D. M. Capeans Garrido,[35] I. Caprini,[27b] M. Caprini,[27b] M. Capua,[40b,40a] R. M. Carbone,[38] R. Cardarelli,[71a] F. C. Cardillo,[50] I. Carli,[139] T. Carli,[35] G. Carlino,[67a] B. T. Carlson,[135] L. Carminati,[66a,66b] R. M. D. Carney,[43a,43b] S. Caron,[117] E. Carquin,[144b] S. Carrá,[66a,66b] G. D. Carrillo-Montoya,[35] D. Casadei,[32b] M. P. Casado,[14,h] A. F. Casha,[165] M. Casolino,[14] D. W. Casper,[169] R. Castelijn,[118] F. L. Castillo,[172] V. Castillo Gimenez,[172] N. F. Castro,[136a,136e] A. Catinaccio,[35] J. R. Catmore,[130] A. Cattai,[35] J. Caudron,[24] V. Cavaliere,[29] E. Cavallaro,[14] D. Cavalli,[66a] M. Cavalli-Sforza,[14] V. Cavasinni,[69a,69b] E. Celebi,[12b] F. Ceradini,[72a,72b] L. Cerda Alberich,[172] A. S. Cerqueira,[78a] A. Cerri,[153] L. Cerrito,[71a,71b] F. Cerutti,[18] A. Cervelli,[23b,23a] S. A. Cetin,[12b] A. Chafaq,[34a] D. Chakraborty,[119] S. K. Chan,[57] W. S. Chan,[118] Y. L. Chan,[61a] P. Chang,[171] J. D. Chapman,[31] D. G. Charlton,[21] C. C. Chau,[33] C. A. Chavez Barajas,[153] S. Che,[122] A. Chegwidden,[104] S. Chekanov,[6] S. V. Chekulaev,[166a] G. A. Chelkov,[77,av] M. A. Chelstowska,[35] C. Chen,[58a] C. H. Chen,[76] H. Chen,[29] J. Chen,[58a] J. Chen,[38] S. Chen,[133] S. J. Chen,[15c] X. Chen,[15b,au] Y. Chen,[80] Y-H. Chen,[44] H. C. Cheng,[103] H. J. Cheng,[15d] A. Cheplakov,[77]

E. Cheremushkina,[140] R. Cherkaoui El Moursli,[34e] E. Cheu,[7] K. Cheung,[62] L. Chevalier,[142] V. Chiarella,[49] G. Chiarelli,[69a] G. Chiodini,[65a] A. S. Chisholm,[35] A. Chitan,[27b] I. Chiu,[161] Y. H. Chiu,[174] M. V. Chizhov,[77] K. Choi,[63] A. R. Chomont,[128] S. Chouridou,[160] Y. S. Chow,[118] V. Christodoulou,[92] M. C. Chu,[61a] J. Chudoba,[137] A. J. Chuinard,[101] J. J. Chwastowski,[82] L. Chytka,[126] D. Cinca,[45] V. Cindro,[89] I. A. Cioară,[24] A. Ciocio,[18] F. Cirotto,[67a,67b] Z. H. Citron,[178] M. Citterio,[66a] A. Clark,[52] M. R. Clark,[38] P. J. Clark,[48] C. Clement,[43a,43b] Y. Coadou,[99] M. Cobal,[64a,64c] A. Coccaro,[53b,53a] J. Cochran,[76] A. E. C. Coimbra,[178] L. Colasurdo,[117] B. Cole,[38] A. P. Colijn,[118] J. Collot,[56] P. Conde Muiño,[136a,136b] E. Coniavitis,[50] S. H. Connell,[32b] I. A. Connelly,[98] S. Constantinescu,[27b] F. Conventi,[67a,ax] A. M. Cooper-Sarkar,[131] F. Cormier,[173] K. J. R. Cormier,[165] M. Corradi,[70a,70b] E. E. Corrigan,[94] F. Corriveau,[101,af] A. Cortes-Gonzalez,[35] M. J. Costa,[172] D. Costanzo,[146] G. Cottin,[31] G. Cowan,[91] B. E. Cox,[98] J. Crane,[98] K. Cranmer,[121] S. J. Crawley,[55] R. A. Creager,[133] G. Cree,[33] S. Crépé-Renaudin,[56] F. Crescioli,[132] M. Cristinziani,[24] V. Croft,[121] G. Crosetti,[40b,40a] A. Cueto,[96] T. Cuhadar Donszelmann,[146] A. R. Cukierman,[150] M. Curatolo,[49] J. Cúth,[97] S. Czekierda,[82] P. Czodrowski,[35] M. J. Da Cunha Sargedas De Sousa,[58b,136b] C. Da Via,[98] W. Dabrowski,[81a] T. Dado,[28a,aa] S. Dahbi,[34e] T. Dai,[103] F. Dallaire,[107] C. Dallapiccola,[100] M. Dam,[39] G. D'amen,[23b,23a] J. R. Dandoy,[133] M. F. Daneri,[30] N. P. Dang,[179,l] N. D Dann,[98] M. Danninger,[173] V. Dao,[35] G. Darbo,[53b] S. Darmora,[8] O. Dartsi,[5] A. Dattagupta,[127] T. Daubney,[44] S. D'Auria,[55] W. Davey,[24] C. David,[44] T. Davidek,[139] D. R. Davis,[47] E. Dawe,[102] I. Dawson,[146] K. De,[8] R. De Asmundis,[67a] A. De Benedetti,[124] S. De Castro,[23b,23a] S. De Cecco,[70a,70b] N. De Groot,[117] P. de Jong,[118] H. De la Torre,[104] F. De Lorenzi,[76] A. De Maria,[51,v] D. De Pedis,[70a] A. De Salvo,[70a] U. De Sanctis,[71a,71b] A. De Santo,[153] K. De Vasconcelos Corga,[99] J. B. De Vivie De Regie,[128] C. Debenedetti,[143] D. V. Dedovich,[77] N. Dehghanian,[3] M. Del Gaudio,[40b,40a] J. Del Peso,[96] D. Delgove,[128] F. Deliot,[142] C. M. Delitzsch,[7] M. Della Pietra,[67a,67b] D. Della Volpe,[52] A. Dell'Acqua,[35] L. Dell'Asta,[25] M. Delmastro,[5] C. Delporte,[128] P. A. Delsart,[56] D. A. DeMarco,[165] S. Demers,[181] M. Demichev,[77] S. P. Denisov,[140] D. Denysiuk,[118] L. D'Eramo,[132] D. Derendarz,[82] J. E. Derkaoui,[34d] F. Derue,[132] P. Dervan,[88] K. Desch,[24] C. Deterre,[44] K. Dette,[165] M. R. Devesa,[30] P. O. Deviveiros,[35] A. Dewhurst,[141] S. Dhaliwal,[26] F. A. Di Bello,[52] A. Di Ciaccio,[71a,71b] L. Di Ciaccio,[5] W. K. Di Clemente,[133] C. Di Donato,[67a,67b] A. Di Girolamo,[35] B. Di Micco,[72a,72b] R. Di Nardo,[35] K. F. Di Petrillo,[57] A. Di Simone,[50] R. Di Sipio,[165] D. Di Valentino,[33] C. Diaconu,[99] M. Diamond,[165] F. A. Dias,[39] T. Dias Do Vale,[136a] M. A. Diaz,[144a] J. Dickinson,[18] E. B. Diehl,[103] J. Dietrich,[19] S. Díez Cornell,[44] A. Dimitrievska,[18] J. Dingfelder,[24] F. Dittus,[35] F. Djama,[99] T. Djobava,[157b] J. I. Djuvsland,[59a] M. A. B. Do Vale,[78c] M. Dobre,[27b] D. Dodsworth,[26] C. Doglioni,[94] J. Dolejsi,[139] Z. Dolezal,[139] M. Donadelli,[78d] J. Donini,[37] A. D'onofrio,[90] M. D'Onofrio,[88] J. Dopke,[141] A. Doria,[67a] M. T. Dova,[86] A. T. Doyle,[55] E. Drechsler,[51] E. Dreyer,[149] T. Dreyer,[51] M. Dris,[10] Y. Du,[58b] J. Duarte-Campderros,[159] F. Dubinin,[108] A. Dubreuil,[52] E. Duchovni,[178] G. Duckeck,[112] A. Ducourthial,[132] O. A. Ducu,[107,z] D. Duda,[113] A. Dudarev,[35] A. C. Dudder,[97] E. M. Duffield,[18] L. Duflot,[128] M. Dührssen,[35] C. Dülsen,[180] M. Dumancic,[178] A. E. Dumitriu,[27b,f] A. K. Duncan,[55] M. Dunford,[59a] A. Duperrin,[99] H. Duran Yildiz,[4a] M. Düren,[54] A. Durglishvili,[157b] D. Duschinger,[46] B. Dutta,[44] D. Duvnjak,[1] M. Dyndal,[44] B. S. Dziedzic,[82] B. Dysch,[98] C. Eckardt,[44] K. M. Ecker,[113] R. C. Edgar,[103] T. Eifert,[35] G. Eigen,[17] K. Einsweiler,[18] T. Ekelof,[170] M. El Kacimi,[34c] R. El Kosseifi,[99] V. Ellajosyula,[99] M. Ellert,[170] F. Ellinghaus,[180] A. A. Elliot,[90] N. Ellis,[35] J. Elmsheuser,[29] M. Elsing,[35] D. Emeliyanov,[141] Y. Enari,[161] J. S. Ennis,[176] M. B. Epland,[47] J. Erdmann,[45] A. Ereditato,[20] S. Errede,[171] M. Escalier,[128] C. Escobar,[172] B. Esposito,[49] O. Estrada Pastor,[172] A. I. Etienvre,[142] E. Etzion,[159] H. Evans,[63] A. Ezhilov,[134] M. Ezzi,[34e] F. Fabbri,[55] L. Fabbri,[23b,23a] V. Fabiani,[117] G. Facini,[92] R. M. Faisca Rodrigues Pereira,[136a] R. M. Fakhrutdinov,[140] S. Falciano,[70a] P. J. Falke,[5] S. Falke,[5] J. Faltova,[139] Y. Fang,[15a] M. Fanti,[66a,66b] A. Farbin,[8] A. Farilla,[72a] E. M. Farina,[68a,68b] T. Farooque,[104] S. Farrell,[18] S. M. Farrington,[176] P. Farthouat,[35] F. Fassi,[34e] P. Fassnacht,[35] D. Fassouliotis,[9] M. Faucci Giannelli,[48] A. Favareto,[53b,53a] W. J. Fawcett,[52] L. Fayard,[128] O. L. Fedin,[134,r] W. Fedorko,[173] M. Feickert,[41] S. Feigl,[130] L. Feligioni,[99] C. Feng,[58b] E. J. Feng,[35] M. Feng,[47] M. J. Fenton,[55] A. B. Fenyuk,[140] L. Feremenga,[8] J. Ferrando,[44] A. Ferrari,[170] P. Ferrari,[118] R. Ferrari,[68a] D. E. Ferreira de Lima,[59b] A. Ferrer,[172] D. Ferrere,[52] C. Ferretti,[103] F. Fiedler,[97] A. Filipčič,[89] F. Filthaut,[117] K. D. Finelli,[25] M. C. N. Fiolhais,[136a,136c,b] L. Fiorini,[172] C. Fischer,[14] W. C. Fisher,[104] N. Flaschel,[44] I. Fleck,[148] P. Fleischmann,[103] R. R. M. Fletcher,[133] T. Flick,[180] B. M. Flierl,[112] L. M. Flores,[133] L. R. Flores Castillo,[61a] N. Fomin,[17] G. T. Forcolin,[98] A. Formica,[142] F. A. Förster,[14] A. C. Forti,[98] A. G. Foster,[21] D. Fournier,[128] H. Fox,[87] S. Fracchia,[146] P. Francavilla,[69a,69b] M. Franchini,[23b,23a] S. Franchino,[59a] D. Francis,[35] L. Franconi,[130] M. Franklin,[57] M. Frate,[169] M. Fraternali,[68a,68b] D. Freeborn,[92] S. M. Fressard-Batraneanu,[35] B. Freund,[107] W. S. Freund,[78b] D. Froidevaux,[35] J. A. Frost,[131] C. Fukunaga,[162] T. Fusayasu,[114] J. Fuster,[172] O. Gabizon,[158] A. Gabrielli,[23b,23a] A. Gabrielli,[18] G. P. Gach,[81a] S. Gadatsch,[52] P. Gadow,[113] G. Gagliardi,[53b,53a] L. G. Gagnon,[107] C. Galea,[27b] B. Galhardo,[136a,136c] E. J. Gallas,[131] B. J. Gallop,[141] P. Gallus,[138] G. Galster,[39] R. Gamboa Goni,[90] K. K. Gan,[122] S. Ganguly,[178] Y. Gao,[88] Y. S. Gao,[150,n] C. García,[172] J. E. García Navarro,[172] J. A. García Pascual,[15a] M. Garcia-Sciveres,[18] R. W. Gardner,[36] N. Garelli,[150] V. Garonne,[130] K. Gasnikova,[44] A. Gaudiello,[53b,53a] G. Gaudio,[68a] I. L. Gavrilenko,[108] A. Gavrilyuk,[109] C. Gay,[173] G. Gaycken,[24] E. N. Gazis,[10] C. N. P. Gee,[141] J. Geisen,[51] M. Geisen,[97] M. P. Geisler,[59a] K. Gellerstedt,[43a,43b] C. Gemme,[53b] M. H. Genest,[56] C. Geng,[103] S. Gentile,[70a,70b] C. Gentsos,[160] S. George,[91] D. Gerbaudo,[14] G. Gessner,[45] S. Ghasemi,[148] M. Ghasemi Bostanabad,[174] M. Ghneimat,[24] B. Giacobbe,[23b] S. Giagu,[70a,70b] N. Giangiacomi,[23b,23a] P. Giannetti,[69a] S. M. Gibson,[91] M. Gignac,[143] D. Gillberg,[33] G. Gilles,[180] D. M. Gingrich,[3,aw] M. P. Giordani,[64a,64c] F. M. Giorgi,[23b] P. F. Giraud,[142] P. Giromini,[57] G. Giugliarelli,[64a,64c] D. Giugni,[66a] F. Giuli,[131] M. Giulini,[59b] S. Gkaitatzis,[160] I. Gkialas,[9,k] E. L. Gkougkousis,[14] P. Gkountoumis,[10] L. K. Gladilin,[111] C. Glasman,[96] J. Glatzer,[14] P. C. F. Glaysher,[44] A. Glazov,[44] M. Goblirsch-Kolb,[26] J. Godlewski,[82] S. Goldfarb,[102] T. Golling,[52] D. Golubkov,[140] A. Gomes,[136a,136b,136d]

R. Goncalves Gama,[78a] R. Gonçalo,[136a] G. Gonella,[50] L. Gonella,[21] A. Gongadze,[77] F. Gonnella,[21] J. L. Gonski,[57] S. González de la Hoz,[172] S. Gonzalez-Sevilla,[52] L. Goossens,[35] P. A. Gorbounov,[109] H. A. Gordon,[29] B. Gorini,[35] E. Gorini,[65a,65b] A. Gorišek,[89] A. T. Goshaw,[47] C. Gössling,[45] M. I. Gostkin,[77] C. A. Gottardo,[24] C. R. Goudet,[128] D. Goujdami,[34c] A. G. Goussiou,[145] N. Govender,[32b,d] C. Goy,[5] E. Gozani,[158] I. Grabowska-Bold,[81a] P. O. J. Gradin,[170] E. C. Graham,[88] J. Gramling,[169] E. Gramstad,[130] S. Grancagnolo,[19] V. Gratchev,[134] P. M. Gravila,[27f] C. Gray,[55] H. M. Gray,[18] Z. D. Greenwood,[93,al] C. Grefe,[24] K. Gregersen,[92] I. M. Gregor,[44] P. Grenier,[150] K. Grevtsov,[44] J. Griffiths,[8] A. A. Grillo,[143] K. Grimm,[150,c] S. Grinstein,[14,ab] Ph. Gris,[37] J.-F. Grivaz,[128] S. Groh,[97] E. Gross,[178] J. Grosse-Knetter,[51] G. C. Grossi,[93] Z. J. Grout,[92] C. Grud,[103] A. Grummer,[116] L. Guan,[103] W. Guan,[179] J. Guenther,[35] A. Guerguichon,[128] F. Guescini,[166a] D. Guest,[169] R. Gugel,[50] B. Gui,[122] T. Guillemin,[5] S. Guindon,[35] U. Gul,[55] C. Gumpert,[35] J. Guo,[58c] W. Guo,[103] Y. Guo,[58a,u] Z. Guo,[99] R. Gupta,[41] S. Gurbuz,[12c] G. Gustavino,[124] B. J. Gutelman,[158] P. Gutierrez,[124] C. Gutschow,[92] C. Guyot,[142] M. P. Guzik,[81a] C. Gwenlan,[131] C. B. Gwilliam,[88] A. Haas,[121] C. Haber,[18] H. K. Hadavand,[8] N. Haddad,[34e] A. Hadef,[58a] S. Hageböck,[24] M. Hagihara,[167] H. Hakobyan,[182,*] M. Haleem,[175] J. Haley,[125] G. Halladjian,[104] G. D. Hallewell,[99] K. Hamacher,[180] P. Hamal,[126] K. Hamano,[174] A. Hamilton,[32a] G. N. Hamity,[146] K. Han,[58a,ak] L. Han,[58a] S. Han,[15d] K. Hanagaki,[79,x] M. Hance,[143] D. M. Handl,[112] B. Haney,[133] R. Hankache,[132] P. Hanke,[59a] E. Hansen,[94] J. B. Hansen,[39] J. D. Hansen,[39] M. C. Hansen,[24] P. H. Hansen,[39] K. Hara,[167] A. S. Hard,[179] T. Harenberg,[180] S. Harkusha,[105] P. F. Harrison,[176] N. M. Hartmann,[112] Y. Hasegawa,[147] A. Hasib,[48] S. Hassani,[142] S. Haug,[20] R. Hauser,[104] L. Hauswald,[46] L. B. Havener,[38] M. Havranek,[138] C. M. Hawkes,[21] R. J. Hawkings,[35] D. Hayden,[104] C. Hayes,[152] C. P. Hays,[131] J. M. Hays,[90] H. S. Hayward,[88] S. J. Haywood,[141] M. P. Heath,[48] V. Hedberg,[94] L. Heelan,[8] S. Heer,[24] K. K. Heidegger,[50] J. Heilman,[33] S. Heim,[44] T. Heim,[18] B. Heinemann,[44,ar] J. J. Heinrich,[112] L. Heinrich,[121] C. Heinz,[54] J. Hejbal,[137] L. Helary,[35] A. Held,[173] S. Hellesund,[130] S. Hellman,[43a,43b] C. Helsens,[35] R. C. W. Henderson,[87] Y. Heng,[179] S. Henkelmann,[173] A. M. Henriques Correia,[35] G. H. Herbert,[19] H. Herde,[26] V. Herget,[175] Y. Hernández Jiménez,[32c] H. Herr,[97] G. Herten,[50] R. Hertenberger,[112] L. Hervas,[35] T. C. Herwig,[133] G. G. Hesketh,[92] N. P. Hessey,[166a] J. W. Hetherly,[41] S. Higashino,[79] E. Higón-Rodriguez,[172] K. Hildebrand,[36] E. Hill,[174] J. C. Hill,[31] K. K. Hill,[29] K. H. Hiller,[44] S. J. Hillier,[21] M. Hils,[46] I. Hinchliffe,[18] M. Hirose,[129] D. Hirschbuehl,[180] B. Hiti,[89] O. Hladik,[137] D. R. Hlaluku,[32c] X. Hoad,[48] J. Hobbs,[152] N. Hod,[166a] M. C. Hodgkinson,[146] A. Hoecker,[35] M. R. Hoeferkamp,[116] F. Hoenig,[112] D. Hohn,[24] D. Hohov,[128] T. R. Holmes,[36] M. Holzbock,[112] M. Homann,[45] S. Honda,[167] T. Honda,[79] T. M. Hong,[135] A. Hönle,[113] B. H. Hooberman,[171] W. H. Hopkins,[127] Y. Horii,[115] P. Horn,[46] A. J. Horton,[149] L. A. Horyn,[36] J-Y. Hostachy,[56] A. Hostiuc,[145] S. Hou,[155] A. Hoummada,[34a] J. Howarth,[98] J. Hoya,[86] M. Hrabovsky,[126] J. Hrdinka,[35] I. Hristova,[19] J. Hrivnac,[128] A. Hrynevich,[106] T. Hryn'ova,[5] P. J. Hsu,[62] S.-C. Hsu,[145] Q. Hu,[29] S. Hu,[58c] Y. Huang,[15a] Z. Hubacek,[138] F. Hubaut,[99] M. Huebner,[24] F. Huegging,[24] T. B. Huffman,[131] E. W. Hughes,[38] M. Huhtinen,[35] R. F. H. Hunter,[33] P. Huo,[152] A. M. Hupe,[33] N. Huseynov,[77,ah] J. Huston,[104] J. Huth,[57] R. Hyneman,[103] G. Iacobucci,[52] G. Iakovidis,[29] I. Ibragimov,[148] L. Iconomidou-Fayard,[128] Z. Idrissi,[34e] P. Iengo,[35] R. Ignazzi,[39] O. Igonkina,[118,ad] R. Iguchi,[161] T. Iizawa,[52] Y. Ikegami,[79] M. Ikeno,[79] D. Iliadis,[160] N. Ilic,[150] F. Iltzsche,[46] G. Introzzi,[68a,68b] M. Iodice,[72a] K. Iordanidou,[38] V. Ippolito,[70a,70b] M. F. Isacson,[170] N. Ishijima,[129] M. Ishino,[161] M. Ishitsuka,[163] C. Issever,[131] S. Istin,[12c,aq] F. Ito,[167] J. M. Iturbe Ponce,[61a] R. Iuppa,[73a,73b] A. Ivina,[178] H. Iwasaki,[79] J. M. Izen,[42] V. Izzo,[67a] S. Jabbar,[3] P. Jacka,[137] P. Jackson,[1] R. M. Jacobs,[24] V. Jain,[2] G. Jäkel,[180] K. B. Jakobi,[97] K. Jakobs,[50] S. Jakobsen,[74] T. Jakoubek,[137] D. O. Jamin,[125] D. K. Jana,[93] R. Jansky,[52] J. Janssen,[24] M. Janus,[51] P. A. Janus,[81a] G. Jarlskog,[94] N. Javadov,[77,ah] T. Javůrek,[50] M. Javurkova,[50] F. Jeanneau,[142] L. Jeanty,[18] J. Jejelava,[157a,ai] A. Jelinskas,[176] P. Jenni,[50,e] J. Jeong,[44] C. Jeske,[176] S. Jézéquel,[5] H. Ji,[179] J. Jia,[152] H. Jiang,[76] Y. Jiang,[58a] Z. Jiang,[150,s] S. Jiggins,[50] F. A. Jimenez Morales,[37] J. Jimenez Pena,[172] S. Jin,[15c] A. Jinaru,[27b] O. Jinnouchi,[163] H. Jivan,[32c] P. Johansson,[146] K. A. Johns,[7] C. A. Johnson,[63] W. J. Johnson,[145] K. Jon-And,[43a,43b] R. W. L. Jones,[87] S. D. Jones,[153] S. Jones,[7] T. J. Jones,[88] J. Jongmanns,[59a] P. M. Jorge,[136a,136b] J. Jovicevic,[166a] X. Ju,[179] J. J. Junggeburth,[113] A. Juste Rozas,[14,ab] A. Kaczmarska,[82] M. Kado,[128] H. Kagan,[122] M. Kagan,[150] T. Kaji,[177] E. Kajomovitz,[158] C. W. Kalderon,[94] A. Kaluza,[97] S. Kama,[41] A. Kamenshchikov,[140] L. Kanjir,[89] Y. Kano,[161] V. A. Kantserov,[110] J. Kanzaki,[79] B. Kaplan,[121] L. S. Kaplan,[179] D. Kar,[32c] M. J. Kareem,[166b] E. Karentzos,[10] S. N. Karpov,[77] Z. M. Karpova,[77] V. Kartvelishvili,[87] A. N. Karyukhin,[140] K. Kasahara,[167] L. Kashif,[179] R. D. Kass,[122] A. Kastanas,[151] Y. Kataoka,[161] C. Kato,[161] J. Katzy,[44] K. Kawade,[80] K. Kawagoe,[85] T. Kawamoto,[161] G. Kawamura,[51] E. F. Kay,[88] V. F. Kazanin,[120b,120a] R. Keeler,[174] R. Kehoe,[41] J. S. Keller,[33] E. Kellermann,[94] J. J. Kempster,[21] J. Kendrick,[21] O. Kepka,[137] S. Kersten,[180] B. P. Keršévan,[89] R. A. Keyes,[101] M. Khader,[171] F. Khalil-Zada,[13] A. Khanov,[125] A. G. Kharlamov,[120b,120a] T. Kharlamova,[120b,120a] A. Khodinov,[164] T. J. Khoo,[52] E. Khramov,[77] J. Khubua,[157b] S. Kido,[80] M. Kiehn,[52] C. R. Kilby,[91] S. H. Kim,[167] Y. K. Kim,[36] N. Kimura,[64a,64c] O. M. Kind,[19] B. T. King,[88] D. Kirchmeier,[46] J. Kirk,[141] A. E. Kiryunin,[113] T. Kishimoto,[161] D. Kisielewska,[81a] V. Kitali,[44] O. Kivernyk,[5] E. Kladiva,[28b,*] T. Klapdor-Kleingrothaus,[50] M. H. Klein,[103] M. Klein,[88] U. Klein,[88] K. Kleinknecht,[97] P. Klimek,[119] A. Klimentov,[29] R. Klingenberg,[45,*] T. Klingl,[24] T. Klioutchnikova,[35] F. F. Klitzner,[112] P. Kluit,[118] S. Kluth,[113] E. Kneringer,[74] E. B. F. G. Knoops,[99] A. Knue,[50] A. Kobayashi,[161] D. Kobayashi,[85] T. Kobayashi,[161] M. Kobel,[46] M. Kocian,[150] P. Kodys,[139] T. Koffas,[33] E. Koffeman,[118] N. M. Köhler,[113] T. Koi,[150] M. Kolb,[59b] I. Koletsou,[5] T. Kondo,[79] N. Kondrashova,[58c] K. Köneke,[50] A. C. König,[117] T. Kono,[79] R. Konoplich,[121,an] V. Konstantinides,[92] N. Konstantinidis,[92] B. Konya,[94] R. Kopeliansky,[63] S. Koperny,[81a] K. Korcyl,[82] K. Kordas,[160] A. Korn,[92] I. Korolkov,[14] E. V. Korolkova,[146] O. Kortner,[113] S. Kortner,[113] T. Kosek,[139] V. V. Kostyukhin,[24] A. Kotwal,[47] A. Koulouris,[10] A. Kourkoumeli-Charalampidi,[68a,68b] C. Kourkoumelis,[9] E. Kourlitis,[146] V. Kouskoura,[29] A. B. Kowalewska,[82] R. Kowalewski,[174] T. Z. Kowalski,[81a] C. Kozakai,[161] W. Kozanecki,[142] A. S. Kozhin,[140] V. A. Kramarenko,[111] G. Kramberger,[89]

D. Krasnopevtsev,[110] M. W. Krasny,[132] A. Krasznahorkay,[35] D. Krauss,[113] J. A. Kremer,[81a] J. Kretzschmar,[88] P. Krieger,[165] K. Krizka,[18] K. Kroeninger,[45] H. Kroha,[113] J. Kroll,[137] J. Kroll,[133] J. Krstic,[16] U. Kruchonak,[77] H. Krüger,[24] N. Krumnack,[76] M. C. Kruse,[47] T. Kubota,[102] S. Kuday,[4b] J. T. Kuechler,[180] S. Kuehn,[35] A. Kugel,[59a] F. Kuger,[175] T. Kuhl,[44] V. Kukhtin,[77] R. Kukla,[99] Y. Kulchitsky,[105] S. Kuleshov,[144b] Y. P. Kulinich,[171] M. Kuna,[56] T. Kunigo,[83] A. Kupco,[137] T. Kupfer,[45] O. Kuprash,[159] H. Kurashige,[80] L. L. Kurchaninov,[166a] Y. A. Kurochkin,[105] M. G. Kurth,[15d] E. S. Kuwertz,[174] M. Kuze,[163] J. Kvita,[126] T. Kwan,[174] A. La Rosa,[113] J. L. La Rosa Navarro,[78d] L. La Rotonda,[40b,40a] F. La Ruffa,[40b,40a] C. Lacasta,[172] F. Lacava,[70a,70b] J. Lacey,[44] D. P. J. Lack,[98] H. Lacker,[19] D. Lacour,[132] E. Ladygin,[77] R. Lafaye,[5] B. Laforge,[132] T. Lagouri,[32c] S. Lai,[51] S. Lammers,[63] W. Lampl,[7] E. Lançon,[29] U. Landgraf,[50] M. P. J. Landon,[90] M. C. Lanfermann,[52] V. S. Lang,[44] J. C. Lange,[14] R. J. Langenberg,[35] A. J. Lankford,[169] F. Lanni,[29] K. Lantzsch,[24] A. Lanza,[68a] A. Lapertosa,[53b,53a] S. Laplace,[132] J. F. Laporte,[142] T. Lari,[66a] F. Lasagni Manghi,[23b,23a] M. Lassnig,[35] T. S. Lau,[61a] A. Laudrain,[128] A. T. Law,[143] P. Laycock,[88] M. Lazzaroni,[66a,66b] B. Le,[102] O. Le Dortz,[132] E. Le Guirriec,[99] E. P. Le Quilleuc,[142] M. LeBlanc,[7] T. LeCompte,[6] F. Ledroit-Guillon,[56] C. A. Lee,[29] G. R. Lee,[144a] L. Lee,[57] S. C. Lee,[155] B. Lefebvre,[101] M. Lefebvre,[174] F. Legger,[112] C. Leggett,[18] G. Lehmann Miotto,[35] W. A. Leight,[44] A. Leisos,[160,y] M. A. L. Leite,[78d] R. Leitner,[139] D. Lellouch,[178] B. Lemmer,[51] K. J. C. Leney,[92] T. Lenz,[24] B. Lenzi,[35] R. Leone,[7] S. Leone,[69a] C. Leonidopoulos,[48] G. Lerner,[153] C. Leroy,[107] R. Les,[165] A. A. J. Lesage,[142] C. G. Lester,[31] M. Levchenko,[134] J. Lévêque,[5] D. Levin,[103] L. J. Levinson,[178] D. Lewis,[90] B. Li,[103] C-Q. Li,[58a,am] H. Li,[58b] L. Li,[58c] Q. Li,[15d] Q. Y. Li,[58a] S. Li,[58d,58c] X. Li,[58c] Y. Li,[148] Z. Liang,[15a] B. Liberti,[71a] A. Liblong,[165] K. Lie,[61c] S. Liem,[118] A. Limosani,[154] C. Y. Lin,[31] K. Lin,[104] S. C. Lin,[156] T. H. Lin,[97] R. A. Linck,[63] B. E. Lindquist,[152] A. L. Lionti,[52] E. Lipeles,[133] A. Lipniacka,[17] M. Lisovyi,[59b] T. M. Liss,[171,at] A. Lister,[173] A. M. Litke,[143] J. D. Little,[8] B. Liu,[76] B. L Liu,[6] H. B. Liu,[29] H. Liu,[103] J. B. Liu,[58a] J. K. K. Liu,[131] K. Liu,[132] M. Liu,[58a] P. Liu,[18] Y. L. Liu,[58a] Y. W. Liu,[58a] M. Livan,[68a,68b] A. Lleres,[56] J. Llorente Merino,[15a] S. L. Lloyd,[90] C. Y. Lo,[61b] F. Lo Sterzo,[41] E. M. Lobodzinska,[44] P. Loch,[7] F. K. Loebinger,[98] K. M. Loew,[26] T. Lohse,[19] K. Lohwasser,[146] M. Lokajicek,[137] B. A. Long,[25] J. D. Long,[171] R. E. Long,[87] L. Longo,[65a,65b] K. A. Looper,[122] J. A. Lopez,[144b] I. Lopez Paz,[14] A. Lopez Solis,[132] J. Lorenz,[112] N. Lorenzo Martinez,[5] M. Losada,[22] P. J. Lösel,[112] A. Lösle,[50] X. Lou,[44] X. Lou,[15a] A. Lounis,[128] J. Love,[6] P. A. Love,[87] J. J. Lozano Bahilo,[172] H. Lu,[61a] N. Lu,[103] Y. J. Lu,[62] H. J. Lubatti,[145] C. Luci,[70a,70b] A. Lucotte,[56] C. Luedtke,[50] F. Luehring,[63] I. Luise,[132] W. Lukas,[74] L. Luminari,[70a] B. Lund-Jensen,[151] M. S. Lutz,[100] P. M. Luzi,[132] D. Lynn,[29] R. Lysak,[137] E. Lytken,[94] F. Lyu,[15a] V. Lyubushkin,[77] H. Ma,[29] L. L. Ma,[58b] Y. Ma,[58b] G. Maccarrone,[49] A. Macchiolo,[113] C. M. Macdonald,[146] J. Machado Miguens,[133,136b] D. Madaffari,[172] R. Madar,[37] W. F. Mader,[46] A. Madsen,[44] N. Madysa,[46] J. Maeda,[80] S. Maeland,[17] T. Maeno,[29] A. S. Maevskiy,[111] V. Magerl,[50] C. Maidantchik,[78b] T. Maier,[112] A. Maio,[136a,136b,136d] O. Majersky,[28a] S. Majewski,[127] Y. Makida,[79] N. Makovec,[128] B. Malaescu,[132] Pa. Malecki,[82] V. P. Maleev,[134] F. Malek,[56] U. Mallik,[75] D. Malon,[6] C. Malone,[31] S. Maltezos,[10] S. Malyukov,[35] J. Mamuzic,[172] G. Mancini,[49] I. Mandić,[89] J. Maneira,[136a] L. Manhaes de Andrade Filho,[78a] J. Manjarres Ramos,[46] K. H. Mankinen,[94] A. Mann,[112] A. Manousos,[74] B. Mansoulie,[142] J. D. Mansour,[15a] M. Mantoani,[51] S. Manzoni,[66a,66b] G. Marceca,[30] L. March,[52] L. Marchese,[131] G. Marchiori,[132] M. Marcisovsky,[137] C. A. Marin Tobon,[35] M. Marjanovic,[37] D. E. Marley,[103] F. Marroquim,[78b] Z. Marshall,[18] M. U. F Martensson,[170] S. Marti-Garcia,[172] C. B. Martin,[122] T. A. Martin,[176] V. J. Martin,[48] B. Martin dit Latour,[17] M. Martinez,[14,ab] V. I. Martinez Outschoorn,[100] S. Martin-Haugh,[141] V. S. Martoiu,[27b] A. C. Martyniuk,[92] A. Marzin,[35] L. Masetti,[97] T. Mashimo,[161] R. Mashinistov,[108] J. Masik,[98] A. L. Maslennikov,[120b,120a] L. H. Mason,[102] L. Massa,[71a,71b] P. Mastrandrea,[5] A. Mastroberardino,[40b,40a] T. Masubuchi,[161] P. Mättig,[180] J. Maurer,[27b] B. Maček,[89] S. J. Maxfield,[88] D. A. Maximov,[120b,120a] R. Mazini,[155] I. Maznas,[160] S. M. Mazza,[143] N. C. Mc Fadden,[116] G. Mc Goldrick,[165] S. P. Mc Kee,[103] A. McCarn,[103] T. G. McCarthy,[113] L. I. McClymont,[92] E. F. McDonald,[102] J. A. Mcfayden,[35] G. Mchedlidze,[51] M. A. McKay,[41] K. D. McLean,[174] S. J. McMahon,[141] P. C. McNamara,[102] C. J. McNicol,[176] R. A. McPherson,[174,af] J. E. Mdhluli,[32c] Z. A. Meadows,[100] S. Meehan,[145] T. M. Megy,[50] S. Mehlhase,[112] A. Mehta,[88] T. Meideck,[56] B. Meirose,[42] D. Melini,[172,i] B. R. Mellado Garcia,[32c] J. D. Mellenthin,[51] M. Melo,[28a] F. Meloni,[20] A. Melzer,[24] S. B. Menary,[98] L. Meng,[88] X. T. Meng,[103] A. Mengarelli,[23b,23a] S. Menke,[113] E. Meoni,[40b,40a] S. Mergelmeyer,[19] C. Merlassino,[20] P. Mermod,[52] L. Merola,[67a,67b] C. Meroni,[66a] F. S. Merritt,[36] A. Messina,[70a,70b] J. Metcalfe,[6] A. S. Mete,[169] C. Meyer,[133] J. Meyer,[158] J-P. Meyer,[142] H. Meyer Zu Theenhausen,[59a] F. Miano,[153] R. P. Middleton,[141] L. Mijović,[48] G. Mikenberg,[178] M. Mikestikova,[137] M. Mikuž,[89] M. Milesi,[102] A. Milic,[165] D. A. Millar,[90] D. W. Miller,[36] A. Milov,[178] D. A. Milstead,[43a,43b] A. A. Minaenko,[140] I. A. Minashvili,[157b] A. I. Mincer,[121] B. Mindur,[81a] M. Mineev,[77] Y. Minegishi,[161] Y. Ming,[179] L. M. Mir,[14] A. Mirto,[65a,65b] K. P. Mistry,[133] T. Mitani,[177] J. Mitrevski,[112] V. A. Mitsou,[172] A. Miucci,[20] P. S. Miyagawa,[146] A. Mizukami,[79] J. U. Mjörnmark,[94] T. Mkrtchyan,[182] M. Mlynarikova,[139] T. Moa,[43a,43b] K. Mochizuki,[107] P. Mogg,[50] S. Mohapatra,[38] S. Molander,[43a,43b] R. Moles-Valls,[24] M. C. Mondragon,[104] K. Mönig,[44] J. Monk,[39] E. Monnier,[99] A. Montalbano,[149] J. Montejo Berlingen,[35] F. Monticelli,[86] S. Monzani,[66a] R. W. Moore,[3] N. Morange,[128] D. Moreno,[22] M. Moreno Llácer,[35] P. Morettini,[53b] M. Morgenstern,[118] S. Morgenstern,[35] D. Mori,[149] T. Mori,[161] M. Morii,[57] M. Morinaga,[177] V. Morisbak,[130] A. K. Morley,[35] G. Mornacchi,[35] A. P. Morris,[92] J. D. Morris,[90] L. Morvaj,[152] P. Moschovakos,[10] M. Mosidze,[157b] H. J. Moss,[146] J. Moss,[150,o] K. Motohashi,[163] R. Mount,[150] E. Mountricha,[35] E. J. W. Moyse,[100] S. Muanza,[99] F. Mueller,[113] J. Mueller,[135] R. S. P. Mueller,[112] D. Muenstermann,[87] P. Mullen,[55] G. A. Mullier,[20] F. J. Munoz Sanchez,[98] P. Murin,[28b] W. J. Murray,[176,141] A. Murrone,[66a,66b] M. Muškinja,[89] C. Mwewa,[32a] A. G. Myagkov,[140,ao] J. Myers,[127] M. Myska,[138] B. P. Nachman,[18] O. Nackenhorst,[45] K. Nagai,[131] K. Nagano,[79] Y. Nagasaka,[60] K. Nagata,[167] M. Nagel,[50] E. Nagy,[99] A. M. Nairz,[35] Y. Nakahama,[115] K. Nakamura,[79] T. Nakamura,[161] I. Nakano,[123] H. Nanjo,[129] F. Napolitano,[59a]

R. F. Naranjo Garcia,[44] R. Narayan,[11] D. I. Narrias Villar,[59a] I. Naryshkin,[134] T. Naumann,[44] G. Navarro,[22] R. Nayyar,[7] H. A. Neal,[103,*] P. Y. Nechaeva,[108] T. J. Neep,[142] A. Negri,[68a,68b] M. Negrini,[23b] S. Nektarijevic,[117] C. Nellist,[51] M. E. Nelson,[131] S. Nemecek,[137] P. Nemethy,[121] M. Nessi,[35,g] M. S. Neubauer,[171] M. Neumann,[180] P. R. Newman,[21] T. Y. Ng,[61c] Y. S. Ng,[19] H. D. N. Nguyen,[99] T. Nguyen Manh,[107] E. Nibigira,[37] R. B. Nickerson,[131] R. Nicolaidou,[142] J. Nielsen,[143] N. Nikiforou,[11] V. Nikolaenko,[140,ao] I. Nikolic-Audit,[132] K. Nikolopoulos,[21] P. Nilsson,[29] Y. Ninomiya,[79] A. Nisati,[70a] N. Nishu,[58c] R. Nisius,[113] I. Nitsche,[45] T. Nitta,[177] T. Nobe,[161] Y. Noguchi,[83] M. Nomachi,[129] I. Nomidis,[132] M. A. Nomura,[29] T. Nooney,[90] M. Nordberg,[35] N. Norjoharuddeen,[131] T. Novak,[89] O. Novgorodova,[46] R. Novotny,[138] M. Nozaki,[79] L. Nozka,[126] K. Ntekas,[169] E. Nurse,[92] F. Nuti,[102] F. G. Oakham,[33,aw] H. Oberlack,[113] T. Obermann,[24] J. Ocariz,[132] A. Ochi,[80] I. Ochoa,[38] J. P. Ochoa-Ricoux,[144a] K. O'Connor,[26] S. Oda,[85] S. Odaka,[79] A. Oh,[98] S. H. Oh,[47] C. C. Ohm,[151] H. Oide,[53b,53a] H. Okawa,[167] Y. Okazaki,[83] Y. Okumura,[161] T. Okuyama,[79] A. Olariu,[27b] L. F. Oleiro Seabra,[136a] S. A. Olivares Pino,[144a] D. Oliveira Damazio,[29] J. L. Oliver,[1] M. J. R. Olsson,[36] A. Olszewski,[82] J. Olszowska,[82] D. C. O'Neil,[149] A. Onofre,[136a,136e] K. Onogi,[115] P. U. E. Onyisi,[11] H. Oppen,[130] M. J. Oreglia,[36] Y. Oren,[159] D. Orestano,[72a,72b] E. C. Orgill,[98] N. Orlando,[61b] A. A. O'Rourke,[44] R. S. Orr,[165] B. Osculati,[53b,53a,*] V. O'Shea,[55] R. Ospanov,[58a] G. Otero y Garzon,[30] H. Otono,[85] M. Ouchrif,[34d] F. Ould-Saada,[130] A. Ouraou,[142] Q. Ouyang,[15a] M. Owen,[55] R. E. Owen,[21] V. E. Ozcan,[12c] N. Ozturk,[8] J. Pacalt,[126] H. A. Pacey,[31] K. Pachal,[149] A. Pacheco Pages,[14] L. Pacheco Rodriguez,[142] C. Padilla Aranda,[14] S. Pagan Griso,[18] M. Paganini,[181] G. Palacino,[63] S. Palazzo,[40b,40a] S. Palestini,[35] M. Palka,[81b] D. Pallin,[37] I. Panagoulias,[10] C. E. Pandini,[35] J. G. Panduro Vazquez,[91] P. Pani,[35] G. Panizzo,[64a,64c] L. Paolozzi,[52] T. D. Papadopoulou,[10] K. Papageorgiou,[9,k] A. Paramonov,[6] D. Paredes Hernandez,[61b] B. Parida,[58c] A. J. Parker,[87] K. A. Parker,[44] M. A. Parker,[31] F. Parodi,[53b,53a] J. A. Parsons,[38] U. Parzefall,[50] V. R. Pascuzzi,[165] J. M. P. Pasner,[143] E. Pasqualucci,[70a] S. Passaggio,[53b] F. Pastore,[91] P. Pasuwan,[43a,43b] S. Pataraia,[97] J. R. Pater,[98] A. Pathak,[179,l] T. Pauly,[35] B. Pearson,[113] M. Pedersen,[130] L. Pedraza Diaz,[117] S. Pedraza Lopez,[172] R. Pedro,[136a,136b] S. V. Peleganchuk,[120b,120a] O. Penc,[137] C. Peng,[15d] H. Peng,[58a] B. S. Peralva,[78a] M. M. Perego,[142] A. P. Pereira Peixoto,[136a] D. V. Perepelitsa,[29] F. Peri,[19] L. Perini,[66a,66b] H. Pernegger,[35] S. Perrella,[67a,67b] V. D. Peshekhonov,[77,*] K. Peters,[44] R. F. Y. Peters,[98] B. A. Petersen,[35] T. C. Petersen,[39] E. Petit,[56] A. Petridis,[1] C. Petridou,[160] P. Petroff,[128] E. Petrolo,[70a] M. Petrov,[131] F. Petrucci,[72a,72b] M. Pettee,[181] N. E. Pettersson,[100] A. Peyaud,[142] R. Pezoa,[144b] T. Pham,[102] F. H. Phillips,[104] P. W. Phillips,[141] G. Piacquadio,[152] E. Pianori,[18] A. Picazio,[100] M. A. Pickering,[131] R. Piegaia,[30] J. E. Pilcher,[36] A. D. Pilkington,[98] M. Pinamonti,[71a,71b] J. L. Pinfold,[3] M. Pitt,[178] M-A. Pleier,[29] V. Pleskot,[139] E. Plotnikova,[77] D. Pluth,[76] P. Podberezko,[120b,120a] R. Poettgen,[94] R. Poggi,[52] L. Poggioli,[128] I. Pogrebnyak,[104] D. Pohl,[24] I. Pokharel,[51] G. Polesello,[68a] A. Poley,[44] A. Policicchio,[40b,40a] R. Polifka,[35] A. Polini,[23b] C. S. Pollard,[44] V. Polychronakos,[29] D. Ponomarenko,[110] L. Pontecorvo,[70a] G. A. Popeneciu,[27d] D. M. Portillo Quintero,[132] S. Pospisil,[138] K. Potamianos,[44] I. N. Potrap,[77] C. J. Potter,[31] H. Potti,[11] T. Poulsen,[94] J. Poveda,[35] T. D. Powell,[146] M. E. Pozo Astigarraga,[35] P. Pralavorio,[99] S. Prell,[76] D. Price,[98] M. Primavera,[65a] S. Prince,[101] N. Proklova,[110] K. Prokofiev,[61c] F. Prokoshin,[144b] S. Protopopescu,[29] J. Proudfoot,[6] M. Przybycien,[81a] A. Puri,[171] P. Puzo,[128] J. Qian,[103] Y. Qin,[98] A. Quadt,[51] M. Queitsch-Maitland,[44] A. Qureshi,[1] P. Rados,[102] F. Ragusa,[66a,66b] G. Rahal,[95] J. A. Raine,[98] S. Rajagopalan,[29] A. Ramirez Morales,[90] T. Rashid,[128] S. Raspopov,[5] M. G. Ratti,[66a,66b] D. M. Rauch,[44] F. Rauscher,[112] S. Rave,[97] B. Ravina,[146] I. Ravinovich,[178] J. H. Rawling,[98] M. Raymond,[35] A. L. Read,[130] N. P. Readioff,[56] M. Reale,[65a,65b] D. M. Rebuzzi,[68a,68b] A. Redelbach,[175] G. Redlinger,[29] R. Reece,[143] R. G. Reed,[32c] K. Reeves,[42] L. Rehnisch,[19] J. Reichert,[133] A. Reiss,[97] C. Rembser,[35] H. Ren,[15d] M. Rescigno,[70a] S. Resconi,[66a] E. D. Resseguie,[133] S. Rettie,[173] E. Reynolds,[21] O. L. Rezanova,[120b,120a] P. Reznicek,[139] R. Richter,[113] S. Richter,[92] E. Richter-Was,[81b] O. Ricken,[24] M. Ridel,[132] P. Rieck,[113] C. J. Riegel,[180] O. Rifki,[44] M. Rijssenbeek,[152] A. Rimoldi,[68a,68b] M. Rimoldi,[20] L. Rinaldi,[23b] G. Ripellino,[151] B. Ristić,[87] E. Ritsch,[35] I. Riu,[14] J. C. Rivera Vergara,[144a] F. Rizatdinova,[125] E. Rizvi,[90] C. Rizzi,[14] R. T. Roberts,[98] S. H. Robertson,[101,af] A. Robichaud-Veronneau,[101] D. Robinson,[31] J. E. M. Robinson,[44] A. Robson,[55] E. Rocco,[97] C. Roda,[69a,69b] Y. Rodina,[99] S. Rodriguez Bosca,[172] A. Rodriguez Perez,[14] D. Rodriguez Rodriguez,[172] A. M. Rodríguez Vera,[166b] S. Roe,[35] C. S. Rogan,[57] O. Røhne,[130] R. Röhrig,[113] C. P. A. Roland,[63] J. Roloff,[57] A. Romaniouk,[110] M. Romano,[23b,23a] N. Rompotis,[88] M. Ronzani,[121] L. Roos,[132] S. Rosati,[70a] K. Rosbach,[50] P. Rose,[143] N-A. Rosien,[51] E. Rossi,[67a,67b] L. P. Rossi,[53b] L. Rossini,[66a,66b] J. H. N. Rosten,[31] R. Rosten,[14] M. Rotaru,[27b] J. Rothberg,[145] D. Rousseau,[128] D. Roy,[32c] A. Rozanov,[99] Y. Rozen,[158] X. Ruan,[32c] F. Rubbo,[150] F. Rühr,[50] A. Ruiz-Martinez,[33] Z. Rurikova,[50] N. A. Rusakovich,[77] H. L. Russell,[101] J. P. Rutherfoord,[7] N. Ruthmann,[35] E. M. Rüttinger,[44,m] Y. F. Ryabov,[134] M. Rybar,[171] G. Rybkin,[128] S. Ryu,[6] A. Ryzhov,[140] G. F. Rzehorz,[51] P. Sabatini,[51] G. Sabato,[118] S. Sacerdoti,[128] H. F-W. Sadrozinski,[143] R. Sadykov,[77] F. Safai Tehrani,[70a] P. Saha,[119] M. Sahinsoy,[59a] A. Sahu,[180] M. Saimpert,[44] M. Saito,[161] T. Saito,[161] H. Sakamoto,[161] A. Sakharov,[121,an] D. Salamani,[52] G. Salamanna,[72a,72b] J. E. Salazar Loyola,[144b] D. Salek,[118] P. H. Sales De Bruin,[170] D. Salihagic,[113] A. Salnikov,[150] J. Salt,[172] D. Salvatore,[40b,40a] F. Salvatore,[153] A. Salvucci,[61a,61b,61c] A. Salzburger,[35] D. Sammel,[50] D. Sampsonidis,[160] D. Sampsonidou,[160] J. Sánchez,[172] A. Sanchez Pineda,[64a,64c] H. Sandaker,[130] C. O. Sander,[44] M. Sandhoff,[180] C. Sandoval,[22] D. P. C. Sankey,[141] M. Sannino,[53b,53a] Y. Sano,[115] A. Sansoni,[49] C. Santoni,[37] H. Santos,[136a] I. Santoyo Castillo,[153] A. Sapronov,[77] J. G. Saraiva,[136a,136d] O. Sasaki,[79] K. Sato,[167] E. Sauvan,[5] P. Savard,[165,aw] N. Savic,[113] R. Sawada,[161] C. Sawyer,[141] L. Sawyer,[93,al] C. Sbarra,[23b] A. Sbrizzi,[23b,23a] T. Scanlon,[92] J. Schaarschmidt,[145] P. Schacht,[113] B. M. Schachtner,[112] D. Schaefer,[36] L. Schaefer,[133] J. Schaeffer,[97] S. Schaepe,[35] U. Schäfer,[97] A. C. Schaffer,[128] D. Schaile,[112] R. D. Schamberger,[152] N. Scharmberg,[98] V. A. Schegelsky,[134] D. Scheirich,[139] F. Schenck,[19] M. Schernau,[169] C. Schiavi,[53b,53a] S. Schier,[143] L. K. Schildgen,[24] Z. M. Schillaci,[26] E. J. Schioppa,[35] M. Schioppa,[40b,40a] K. E. Schleicher,[50] S. Schlenker,[35]

K. R. Schmidt-Sommerfeld,[113] K. Schmieden,[35] C. Schmitt,[97] S. Schmitt,[44] S. Schmitz,[97] U. Schnoor,[50] L. Schoeffel,[142] A. Schoening,[59b] E. Schopf,[24] M. Schott,[97] J. F. P. Schouwenberg,[117] J. Schovancova,[35] S. Schramm,[52] A. Schulte,[97] H-C. Schultz-Coulon,[59a] M. Schumacher,[50] B. A. Schumm,[143] Ph. Schune,[142] A. Schwartzman,[150] T. A. Schwarz,[103] H. Schweiger,[98] Ph. Schwemling,[142] R. Schwienhorst,[104] A. Sciandra,[24] G. Sciolla,[26] M. Scornajenghi,[40b,40a] F. Scuri,[69a] F. Scutti,[102] L. M. Scyboz,[113] J. Searcy,[103] C. D. Sebastiani,[70a,70b] P. Seema,[24] S. C. Seidel,[116] A. Seiden,[143] T. Seiss,[36] J. M. Seixas,[78b] G. Sekhniaidze,[67a] K. Sekhon,[103] S. J. Sekula,[41] N. Semprini-Cesari,[23b,23a] S. Sen,[47] S. Senkin,[37] C. Serfon,[130] L. Serin,[128] L. Serkin,[64a,64b] M. Sessa,[72a,72b] H. Severini,[124] F. Sforza,[168] A. Sfyrla,[52] E. Shabalina,[51] J. D. Shahinian,[143] N. W. Shaikh,[43a,43b] L. Y. Shan,[15a] R. Shang,[171] J. T. Shank,[25] M. Shapiro,[18] A. S. Sharma,[1] A. Sharma,[131] P. B. Shatalov,[109] K. Shaw,[153] S. M. Shaw,[98] A. Shcherbakova,[134] Y. Shen,[124] N. Sherafati,[33] A. D. Sherman,[25] P. Sherwood,[92] L. Shi,[155,as] S. Shimizu,[80] C. O. Shimmin,[181] M. Shimojima,[114] I. P. J. Shipsey,[131] S. Shirabe,[85] M. Shiyakova,[77] J. Shlomi,[178] A. Shmeleva,[108] D. Shoaleh Saadi,[107] M. J. Shochet,[36] S. Shojaii,[102] D. R. Shope,[124] S. Shrestha,[122] E. Shulga,[110] P. Sicho,[137] A. M. Sickles,[171] P. E. Sidebo,[151] E. Sideras Haddad,[32c] O. Sidiropoulou,[175] A. Sidoti,[23b,23a] F. Siegert,[46] Dj. Sijacki,[16] J. Silva,[136a] M. Silva, Jr.,[179] S. B. Silverstein,[43a] L. Simic,[77] S. Simion,[128] E. Simioni,[97] M. Simon,[97] P. Sinervo,[165] N. B. Sinev,[127] M. Sioli,[23b,23a] G. Siragusa,[175] I. Siral,[103] S. Yu. Sivoklokov,[111] J. Sjölin,[43a,43b] M. B. Skinner,[87] P. Skubic,[124] M. Slater,[21] T. Slavicek,[138] M. Slawinska,[82] K. Sliwa,[168] R. Slovak,[139] V. Smakhtin,[178] B. H. Smart,[5] J. Smiesko,[28a] N. Smirnov,[110] S. Yu. Smirnov,[110] Y. Smirnov,[110] L. N. Smirnova,[111] O. Smirnova,[94] J. W. Smith,[51] M. N. K. Smith,[38] R. W. Smith,[38] M. Smizanska,[87] K. Smolek,[138] A. A. Snesarev,[108] I. M. Snyder,[127] S. Snyder,[29] R. Sobie,[174,af] A. M. Soffa,[169] A. Soffer,[159] A. Søgaard,[48] D. A. Soh,[155] G. Sokhrannyi,[89] C. A. Solans Sanchez,[35] M. Solar,[138] E. Yu. Soldatov,[110] U. Soldevila,[172] A. A. Solodkov,[140] A. Soloshenko,[77] O. V. Solovyanov,[140] V. Solovyev,[134] P. Sommer,[146] H. Son,[168] W. Song,[141] A. Sopczak,[138] F. Sopkova,[28b] D. Sosa,[59b] C. L. Sotiropoulou,[69a,69b] S. Sottocornola,[68a,68b] R. Soualah,[64a,64c,j] A. M. Soukharev,[120b,120a] D. South,[44] B. C. Sowden,[91] S. Spagnolo,[65a,65b] M. Spalla,[113] M. Spangenberg,[176] F. Spanò,[91] D. Sperlich,[19] F. Spettel,[113] T. M. Spieker,[59a] R. Spighi,[23b] G. Spigo,[35] L. A. Spiller,[102] D. P. Spiteri,[55] M. Spousta,[139] A. Stabile,[66a,66b] R. Stamen,[59a] S. Stamm,[19] E. Stanecka,[82] R. W. Stanek,[6] C. Stanescu,[72a] M. M. Stanitzki,[44] B. Stapf,[118] S. Stapnes,[130] E. A. Starchenko,[140] G. H. Stark,[36] J. Stark,[56] S. H Stark,[39] P. Staroba,[137] P. Starovoitov,[59a] S. Stärz,[35] R. Staszewski,[82] M. Stegler,[44] P. Steinberg,[29] B. Stelzer,[149] H. J. Stelzer,[35] O. Stelzer-Chilton,[166a] H. Stenzel,[54] T. J. Stevenson,[90] G. A. Stewart,[55] M. C. Stockton,[127] G. Stoicea,[27b] P. Stolte,[51] S. Stonjek,[113] A. Straessner,[46] J. Strandberg,[151] S. Strandberg,[43a,43b] M. Strauss,[124] P. Strizenec,[28b] R. Ströhmer,[175] D. M. Strom,[127] R. Stroynowski,[41] A. Strubig,[48] S. A. Stucci,[29] B. Stugu,[17] J. Stupak,[124] N. A. Styles,[44] D. Su,[150] J. Su,[135] S. Suchek,[59a] Y. Sugaya,[129] M. Suk,[138] V. V. Sulin,[108] D. M. S. Sultan,[52] S. Sultansoy,[4c] T. Sumida,[83] S. Sun,[103] X. Sun,[3] K. Suruliz,[153] C. J. E. Suster,[154] M. R. Sutton,[153] S. Suzuki,[79] M. Svatos,[137] M. Swiatlowski,[36] S. P. Swift,[2] A. Sydorenko,[97] I. Sykora,[28a] T. Sykora,[139] D. Ta,[97] K. Tackmann,[44,ac] J. Taenzer,[159] A. Taffard,[169] R. Tafirout,[166a] E. Tahirovic,[90] N. Taiblum,[159] H. Takai,[29] R. Takashima,[84] E. H. Takasugi,[113] K. Takeda,[80] T. Takeshita,[147] Y. Takubo,[79] M. Talby,[99] A. A. Talyshev,[120b,120a] J. Tanaka,[161] M. Tanaka,[163] R. Tanaka,[128] R. Tanioka,[80] B. B. Tannenwald,[122] S. Tapia Araya,[144b] S. Tapprogge,[97] A. Tarek Abouelfadl Mohamed,[132] S. Tarem,[158] G. Tarna,[27b,f] G. F. Tartarelli,[66a] P. Tas,[139] M. Tasevsky,[137] T. Tashiro,[83] E. Tassi,[40b,40a] A. Tavares Delgado,[136a,136b] Y. Tayalati,[34e] A. C. Taylor,[116] A. J. Taylor,[48] G. N. Taylor,[102] P. T. E. Taylor,[102] W. Taylor,[166b] A. S. Tee,[87] P. Teixeira-Dias,[91] D. Temple,[149] H. Ten Kate,[35] P. K. Teng,[155] J. J. Teoh,[129] F. Tepel,[180] S. Terada,[79] K. Terashi,[161] J. Terron,[96] S. Terzo,[14] M. Testa,[49] R. J. Teuscher,[165,af] S. J. Thais,[181] T. Theveneaux-Pelzer,[44] F. Thiele,[39] J. P. Thomas,[21] A. S. Thompson,[55] P. D. Thompson,[21] L. A. Thomsen,[181] E. Thomson,[133] Y. Tian,[38] R. E. Ticse Torres,[51] V. O. Tikhomirov,[108,ap] Yu. A. Tikhonov,[120b,120a] S. Timoshenko,[110] P. Tipton,[181] S. Tisserant,[99] K. Todome,[163] S. Todorova-Nova,[5] S. Todt,[46] J. Tojo,[85] S. Tokár,[28a] K. Tokushuku,[79] E. Tolley,[122] K. G. Tomiwa,[32c] M. Tomoto,[115] L. Tompkins,[150,s] K. Toms,[116] B. Tong,[57] P. Tornambe,[50] E. Torrence,[127] H. Torres,[46] E. Torró Pastor,[145] C. Tosciri,[131] J. Toth,[99,ae] F. Touchard,[99] D. R. Tovey,[146] C. J. Treado,[121] T. Trefzger,[175] F. Tresoldi,[153] A. Tricoli,[29] I. M. Trigger,[166a] S. Trincaz-Duvoid,[132] M. F. Tripiana,[14] W. Trischuk,[165] B. Trocmé,[56] A. Trofymov,[128] C. Troncon,[66a] M. Trovatelli,[174] F. Trovato,[153] L. Truong,[32b] M. Trzebinski,[82] A. Trzupek,[82] F. Tsai,[44] J. C-L. Tseng,[131] P. V. Tsiareshka,[105] N. Tsirintanis,[9] V. Tsiskaridze,[152] E. G. Tskhadadze,[157a] I. I. Tsukerman,[109] V. Tsulaia,[18] S. Tsuno,[79] D. Tsybychev,[152] Y. Tu,[61b] A. Tudorache,[27b] V. Tudorache,[27b] T. T. Tulbure,[27a] A. N. Tuna,[57] S. Turchikhin,[77] D. Turgeman,[178] I. Turk Cakir,[4b,w] R. Turra,[66a] P. M. Tuts,[38] E. Tzovara,[97] G. Ucchielli,[23b,23a] I. Ueda,[79] M. Ughetto,[43a,43b] F. Ukegawa,[167] G. Unal,[35] A. Undrus,[29] G. Unel,[169] F. C. Ungaro,[102] Y. Unno,[79] K. Uno,[161] J. Urban,[28b] P. Urquijo,[102] P. Urrejola,[97] G. Usai,[8] J. Usui,[79] L. Vacavant,[99] V. Vacek,[138] B. Vachon,[101] K. O. H. Vadla,[130] A. Vaidya,[92] C. Valderanis,[112] E. Valdes Santurio,[43a,43b] M. Valente,[52] S. Valentinetti,[23b,23a] A. Valero,[172] L. Valéry,[44] R. A. Vallance,[21] A. Vallier,[5] J. A. Valls Ferrer,[172] T. R. Van Daalen,[14] W. Van Den Wollenberg,[118] H. Van der Graaf,[118] P. Van Gemmeren,[6] J. Van Nieuwkoop,[149] I. Van Vulpen,[118] M. C. van Woerden,[118] M. Vanadia,[71a,71b] W. Vandelli,[35] A. Vaniachine,[164] P. Vankov,[118] R. Vari,[70a] E. W. Varnes,[7] C. Varni,[53b,53a] T. Varol,[41] D. Varouchas,[128] A. Vartapetian,[8] K. E. Varvell,[154] G. A. Vasquez,[144b] J. G. Vasquez,[181] F. Vazeille,[37] D. Vazquez Furelos,[14] T. Vazquez Schroeder,[101] J. Veatch,[51] V. Vecchio,[72a,72b] L. M. Veloce,[165] F. Veloso,[136a,136c] S. Veneziano,[70a] A. Ventura,[65a,65b] M. Venturi,[174] N. Venturi,[35] V. Vercesi,[68a] M. Verducci,[72a,72b] C. M. Vergel Infante,[76] W. Verkerke,[118] A. T. Vermeulen,[118] J. C. Vermeulen,[118] M. C. Vetterli,[149,aw] N. Viaux Maira,[144b] O. Viazlo,[94] I. Vichou,[171,*] T. Vickey,[146] O. E. Vickey Boeriu,[146] G. H. A. Viehhauser,[131] S. Viel,[18] L. Vigani,[131] M. Villa,[23b,23a] M. Villaplana Perez,[66a,66b] E. Vilucchi,[49] M. G. Vincter,[33] V. B. Vinogradov,[77] A. Vishwakarma,[44] C. Vittori,[23b,23a] I. Vivarelli,[153] S. Vlachos,[10] M. Vogel,[180] P. Vokac,[138] G. Volpi,[14]

S. E. von Buddenbrock,[32c] E. Von Toerne,[24] V. Vorobel,[139] K. Vorobev,[110] M. Vos,[172] J. H. Vossebeld,[88] N. Vranjes,[16] M. Vranjes Milosavljevic,[16] V. Vrba,[138] M. Vreeswijk,[118] T. Šfiligoj,[89] R. Vuillermet,[35] I. Vukotic,[36] T. Ženiš,[28a] L. Živković,[16] P. Wagner,[24] W. Wagner,[180] J. Wagner-Kuhr,[112] H. Wahlberg,[86] S. Wahrmund,[46] K. Wakamiya,[80] V. M. Walbrecht,[113] J. Walder,[87] R. Walker,[112] W. Walkowiak,[148] V. Wallangen,[43a,43b] A. M. Wang,[57] C. Wang,[58b,f] F. Wang,[179] H. Wang,[18] H. Wang,[3] J. Wang,[154] J. Wang,[59b] P. Wang,[41] Q. Wang,[124] R.-J. Wang,[132] R. Wang,[58a] R. Wang,[6] S. M. Wang,[155] W. T. Wang,[58a] W. Wang,[155,q] W. X. Wang,[58a,ag] Y. Wang,[58a,am] Z. Wang,[58c] C. Wanotayaroj,[44] A. Warburton,[101] C. P. Ward,[31] D. R. Wardrope,[92] A. Washbrook,[48] P. M. Watkins,[21] A. T. Watson,[21] M. F. Watson,[21] G. Watts,[145] S. Watts,[98] B. M. Waugh,[92] A. F. Webb,[11] S. Webb,[97] C. Weber,[181] M. S. Weber,[20] S. A. Weber,[33] S. M. Weber,[59a] J. S. Webster,[6] A. R. Weidberg,[131] B. Weinert,[63] J. Weingarten,[51] M. Weirich,[97] C. Weiser,[50] P. S. Wells,[35] T. Wenaus,[29] T. Wengler,[35] S. Wenig,[35] N. Wermes,[24] M. D. Werner,[76] P. Werner,[35] M. Wessels,[59a] T. D. Weston,[20] K. Whalen,[127] N. L. Whallon,[145] A. M. Wharton,[87] A. S. White,[103] A. White,[8] M. J. White,[1] R. White,[144b] D. Whiteson,[169] B. W. Whitmore,[87] F. J. Wickens,[141] W. Wiedenmann,[179] M. Wielers,[141] C. Wiglesworth,[39] L. A. M. Wiik-Fuchs,[50] A. Wildauer,[113] F. Wilk,[98] H. G. Wilkens,[35] L. J. Wilkins,[91] H. H. Williams,[133] S. Williams,[31] C. Willis,[104] S. Willocq,[100] J. A. Wilson,[21] I. Wingerter-Seez,[5] E. Winkels,[153] F. Winklmeier,[127] O. J. Winston,[153] B. T. Winter,[24] M. Wittgen,[150] M. Wobisch,[93] A. Wolf,[97] T. M. H. Wolf,[118] R. Wolff,[99] M. W. Wolter,[82] H. Wolters,[136a,136c] V. W. S. Wong,[173] N. L. Woods,[143] S. D. Worm,[21] B. K. Wosiek,[82] K. W. Woźniak,[82] K. Wraight,[55] M. Wu,[36] S. L. Wu,[179] X. Wu,[52] Y. Wu,[58a] T. R. Wyatt,[98] B. M. Wynne,[48] S. Xella,[39] Z. Xi,[103] L. Xia,[176] D. Xu,[15a] H. Xu,[58a,f] L. Xu,[29] T. Xu,[142] W. Xu,[103] B. Yabsley,[154] S. Yacoob,[32a] K. Yajima,[129] D. P. Yallup,[92] D. Yamaguchi,[163] Y. Yamaguchi,[163] A. Yamamoto,[79] T. Yamanaka,[161] F. Yamane,[80] M. Yamatani,[161] T. Yamazaki,[161] Y. Yamazaki,[80] Z. Yan,[25] H. J. Yang,[58c,58d] H. T. Yang,[18] S. Yang,[75] Y. Yang,[161] Y. Yang,[155] Z. Yang,[17] W-M. Yao,[18] Y. C. Yap,[44] Y. Yasu,[79] E. Yatsenko,[58c] J. Ye,[41] S. Ye,[29] I. Yeletskikh,[77] E. Yigitbasi,[25] E. Yildirim,[97] K. Yorita,[177] K. Yoshihara,[133] C. J. S. Young,[35] C. Young,[150] J. Yu,[8] J. Yu,[76] X. Yue,[59a] S. P. Y. Yuen,[24] I. Yusuff,[31,a] B. Zabinski,[82] G. Zacharis,[10] E. Zaffaroni,[52] R. Zaidan,[14] A. M. Zaitsev,[140,ao] N. Zakharchuk,[44] J. Zalieckas,[17] S. Zambito,[57] D. Zanzi,[35] D. R. Zaripovas,[55] S. V. Zeißner,[45] C. Zeitnitz,[180] G. Zemaityte,[131] J. C. Zeng,[171] Q. Zeng,[150] O. Zenin,[140] D. Zerwas,[128] M. Zgubič,[131] D. F. Zhang,[58b] D. Zhang,[103] F. Zhang,[179] G. Zhang,[58a,ag] H. Zhang,[15c] J. Zhang,[6] L. Zhang,[50] L. Zhang,[58a] M. Zhang,[171] P. Zhang,[15c] R. Zhang,[58a,f] R. Zhang,[24] X. Zhang,[58b] Y. Zhang,[15d] Z. Zhang,[128] P. Zhao,[47] X. Zhao,[41] Y. Zhao,[58b,128,ak] Z. Zhao,[58a] A. Zhemchugov,[77] B. Zhou,[103] C. Zhou,[179] L. Zhou,[41] M. S. Zhou,[15d] M. Zhou,[152] N. Zhou,[58c] Y. Zhou,[7] C. G. Zhu,[58b] H. L. Zhu,[58a] H. Zhu,[15a] J. Zhu,[103] Y. Zhu,[58a] X. Zhuang,[15a] K. Zhukov,[108] V. Zhulanov,[120b,120a] A. Zibell,[175] D. Zieminska,[63] N. I. Zimine,[77] S. Zimmermann,[50] Z. Zinonos,[113] M. Zinser,[97] M. Ziolkowski,[148] G. Zobernig,[179] A. Zoccoli,[23b,23a] K. Zoch,[51] T. G. Zorbas,[146] R. Zou,[36] M. Zur Nedden,[19] and L. Zwalinski[35]

(ATLAS Collaboration)

[1]*Department of Physics, University of Adelaide, Adelaide, Australia*
[2]*Physics Department, SUNY Albany, Albany, New York, USA*
[3]*Department of Physics, University of Alberta, Edmonton, Alberta, Canada*
[4a]*Department of Physics, Ankara University, Ankara, Turkey*
[4b]*Istanbul Aydin University, Istanbul, Turkey*
[4c]*Division of Physics, TOBB University of Economics and Technology, Ankara, Turkey*
[5]*LAPP, Université Grenoble Alpes, Université Savoie Mont Blanc, CNRS/IN2P3, Annecy, France*
[6]*High Energy Physics Division, Argonne National Laboratory, Argonne, Illinois, USA*
[7]*Department of Physics, University of Arizona, Tucson, Arizona, USA*
[8]*Department of Physics, University of Texas at Arlington, Arlington, Texas, USA*
[9]*Physics Department, National and Kapodistrian University of Athens, Athens, Greece*
[10]*Physics Department, National Technical University of Athens, Zografou, Greece*
[11]*Department of Physics, University of Texas at Austin, Austin, Texas, USA*
[12a]*Bahcesehir University, Faculty of Engineering and Natural Sciences, Istanbul, Turkey*
[12b]*Istanbul Bilgi University, Faculty of Engineering and Natural Sciences, Istanbul, Turkey*
[12c]*Department of Physics, Bogazici University, Istanbul, Turkey*
[12d]*Department of Physics Engineering, Gaziantep University, Gaziantep, Turkey*
[13]*Institute of Physics, Azerbaijan Academy of Sciences, Baku, Azerbaijan*
[14]*Institut de Física d'Altes Energies (IFAE), Barcelona Institute of Science and Technology, Barcelona, Spain*
[15a]*Institute of High Energy Physics, Chinese Academy of Sciences, Beijing, China*
[15b]*Physics Department, Tsinghua University, Beijing, China*
[15c]*Department of Physics, Nanjing University, Nanjing, China*
[15d]*University of Chinese Academy of Science (UCAS), Beijing, China*
[16]*Institute of Physics, University of Belgrade, Belgrade, Serbia*
[17]*Department for Physics and Technology, University of Bergen, Bergen, Norway*
[18]*Physics Division, Lawrence Berkeley National Laboratory and University of California, Berkeley, California, USA*

[19]*Institut für Physik, Humboldt Universität zu Berlin, Berlin, Germany*

[20]*Albert Einstein Center for Fundamental Physics and Laboratory for High Energy Physics, University of Bern, Bern, Switzerland*

[21]*School of Physics and Astronomy, University of Birmingham, Birmingham, United Kingdom*

[22]*Centro de Investigaciónes, Universidad Antonio Nariño, Bogota, Colombia*

[23a]*Dipartimento di Fisica e Astronomia, Università di Bologna, Bologna, Italy*

[23b]*INFN Sezione di Bologna, Italy*

[24]*Physikalisches Institut, Universität Bonn, Bonn, Germany*

[25]*Department of Physics, Boston University, Boston, Massachusetts, USA*

[26]*Department of Physics, Brandeis University, Waltham, Massachusetts, USA*

[27a]*Transilvania University of Brasov, Brasov, Romania*

[27b]*Horia Hulubei National Institute of Physics and Nuclear Engineering, Bucharest, Romania*

[27c]*Department of Physics, Alexandru Ioan Cuza University of Iasi, Iasi, Romania*

[27d]*National Institute for Research and Development of Isotopic and Molecular Technologies, Physics Department, Cluj-Napoca, Romania*

[27e]*University Politehnica Bucharest, Bucharest, Romania*

[27f]*West University in Timisoara, Timisoara, Romania*

[28a]*Faculty of Mathematics, Physics and Informatics, Comenius University, Bratislava, Slovak Republic*

[28b]*Department of Subnuclear Physics, Institute of Experimental Physics of the Slovak Academy of Sciences, Kosice, Slovak Republic*

[29]*Physics Department, Brookhaven National Laboratory, Upton, New York, USA*

[30]*Departamento de Física, Universidad de Buenos Aires, Buenos Aires, Argentina*

[31]*Cavendish Laboratory, University of Cambridge, Cambridge, United Kingdom*

[32a]*Department of Physics, University of Cape Town, Cape Town, South Africa*

[32b]*Department of Mechanical Engineering Science, University of Johannesburg, Johannesburg, South Africa*

[32c]*School of Physics, University of the Witwatersrand, Johannesburg, South Africa*

[33]*Department of Physics, Carleton University, Ottawa, Ontario, Canada*

[34a]*Faculté des Sciences Ain Chock, Réseau Universitaire de Physique des Hautes Energies - Université Hassan II, Casablanca, Morocco*

[34b]*Centre National de l'Energie des Sciences Techniques Nucleaires (CNESTEN), Rabat, Morocco*

[34c]*Faculté des Sciences Semlalia, Université Cadi Ayyad, LPHEA-Marrakech, Morocco*

[34d]*Faculté des Sciences, Université Mohamed Premier and LPTPM, Oujda, Morocco*

[34e]*Faculté des Sciences, Université Mohammed V, Rabat, Morocco*

[35]*CERN, Geneva, Switzerland*

[36]*Enrico Fermi Institute, University of Chicago, Chicago, Illinois, USA*

[37]*LPC, Université Clermont Auvergne, CNRS/IN2P3, Clermont-Ferrand, France*

[38]*Nevis Laboratory, Columbia University, Irvington, New York, USA*

[39]*Niels Bohr Institute, University of Copenhagen, Copenhagen, Denmark*

[40a]*Dipartimento di Fisica, Università della Calabria, Rende, Italy*

[40b]*INFN Gruppo Collegato di Cosenza, Laboratori Nazionali di Frascati, Italy*

[41]*Physics Department, Southern Methodist University, Dallas, Texas, USA*

[42]*Physics Department, University of Texas at Dallas, Richardson TX, United States of America*

[43a]*Department of Physics, Stockholm University, Sweden*

[43b]*Oskar Klein Centre, Stockholm, Sweden*

[44]*Deutsches Elektronen-Synchrotron DESY, Hamburg and Zeuthen, Germany*

[45]*Lehrstuhl für Experimentelle Physik IV, Technische Universität Dortmund, Dortmund, Germany*

[46]*Institut für Kern- und Teilchenphysik, Technische Universität Dresden, Dresden, Germany*

[47]*Department of Physics, Duke University, Durham, North Carolina, USA*

[48]*SUPA - School of Physics and Astronomy, University of Edinburgh, Edinburgh, United Kingdom*

[49]*INFN e Laboratori Nazionali di Frascati, Frascati, Italy*

[50]*Physikalisches Institut, Albert-Ludwigs-Universität Freiburg, Freiburg, Germany*

[51]*II. Physikalisches Institut, Georg-August-Universität Göttingen, Göttingen, Germany*

[52]*Département de Physique Nucléaire et Corpusculaire, Université de Genève, Genève, Switzerland*

[53a]*Dipartimento di Fisica, Università di Genova, Genova, Italy*

[53b]*INFN Sezione di Genova, Italy*

[54]*II. Physikalisches Institut, Justus-Liebig-Universität Giessen, Giessen, Germany*

[55]*SUPA - School of Physics and Astronomy, University of Glasgow, Glasgow, United Kingdom*

[56]*LPSC, Université Grenoble Alpes, CNRS/IN2P3, Grenoble INP, Grenoble, France*

[57]*Laboratory for Particle Physics and Cosmology, Harvard University, Cambridge, Massachusetts, USA*

[58a]*Department of Modern Physics and State Key Laboratory of Particle Detection and Electronics, University of Science and Technology of China, Hefei, China*

[58b]*Institute of Frontier and Interdisciplinary Science and Key Laboratory of Particle Physics and Particle Irradiation (MOE), Shandong University, Qingdao, China*

[58c] *School of Physics and Astronomy, Shanghai Jiao Tong University, KLPPAC-MoE, SKLPPC, Shanghai, China*
[58d] *Tsung-Dao Lee Institute, Shanghai, China*
[59a] *Kirchhoff-Institut für Physik, Ruprecht-Karls-Universität Heidelberg, Heidelberg, Germany*
[59b] *Physikalisches Institut, Ruprecht-Karls-Universität Heidelberg, Heidelberg, Germany*
[60] *Faculty of Applied Information Science, Hiroshima Institute of Technology, Hiroshima, Japan*
[61a] *Department of Physics, Chinese University of Hong Kong, Shatin, N.T., Hong Kong, China*
[61b] *Department of Physics, University of Hong Kong, Hong Kong, China*
[61c] *Department of Physics and Institute for Advanced Study, Hong Kong University of Science and Technology,*
Clear Water Bay, Kowloon, Hong Kong, China
[62] *Department of Physics, National Tsing Hua University, Hsinchu, Taiwan*
[63] *Department of Physics, Indiana University, Bloomington, Indiana, USA*
[64a] *INFN Gruppo Collegato di Udine, Sezione di Trieste, Udine, Italy*
[64b] *ICTP, Trieste, Italy*
[64c] *Dipartimento di Chimica, Fisica e Ambiente, Università di Udine, Udine, Italy*
[65a] *INFN Sezione di Lecce, Italy*
[65b] *Dipartimento di Matematica e Fisica, Università del Salento, Lecce, Italy*
[66a] *INFN Sezione di Milano, Italy*
[66b] *Dipartimento di Fisica, Università di Milano, Milano, Italy*
[67a] *INFN Sezione di Napoli, Italy*
[67b] *Dipartimento di Fisica, Università di Napoli, Napoli, Italy*
[68a] *INFN Sezione di Pavia, Italy*
[68b] *Dipartimento di Fisica, Università di Pavia, Pavia, Italy*
[69a] *INFN Sezione di Pisa, Italy*
[69b] *Dipartimento di Fisica E. Fermi, Università di Pisa, Pisa, Italy*
[70a] *INFN Sezione di Roma, Italy*
[70b] *Dipartimento di Fisica, Sapienza Università di Roma, Roma, Italy*
[71a] *INFN Sezione di Roma Tor Vergata, Italy*
[71b] *Dipartimento di Fisica, Università di Roma Tor Vergata, Roma, Italy*
[72a] *INFN Sezione di Roma Tre, Italy*
[72b] *Dipartimento di Matematica e Fisica, Università Roma Tre, Roma, Italy*
[73a] *INFN-TIFPA, Italy*
[73b] *Università degli Studi di Trento, Trento, Italy*
[74] *Institut für Astro- und Teilchenphysik, Leopold-Franzens-Universität, Innsbruck, Austria*
[75] *University of Iowa, Iowa City, Iowa, USA*
[76] *Department of Physics and Astronomy, Iowa State University, Ames, Iowa, USA*
[77] *Joint Institute for Nuclear Research, Dubna, Russia*
[78a] *Departamento de Engenharia Elétrica, Universidade Federal de Juiz de Fora (UFJF), Juiz de Fora, Brazil*
[78b] *Universidade Federal do Rio De Janeiro COPPE/EE/IF, Rio de Janeiro, Brazil*
[78c] *Universidade Federal de São João del Rei (UFSJ), São João del Rei, Brazil*
[78d] *Instituto de Física, Universidade de São Paulo, São Paulo, Brazil*
[79] *KEK, High Energy Accelerator Research Organization, Tsukuba, Japan*
[80] *Graduate School of Science, Kobe University, Kobe, Japan*
[81a] *AGH University of Science and Technology, Faculty of Physics and Applied Computer Science, Krakow, Poland*
[81b] *Marian Smoluchowski Institute of Physics, Jagiellonian University, Krakow, Poland*
[82] *Institute of Nuclear Physics Polish Academy of Sciences, Krakow, Poland*
[83] *Faculty of Science, Kyoto University, Kyoto, Japan*
[84] *Kyoto University of Education, Kyoto, Japan*
[85] *Research Center for Advanced Particle Physics and Department of Physics, Kyushu University, Fukuoka, Japan*
[86] *Instituto de Física La Plata, Universidad Nacional de La Plata and CONICET, La Plata, Argentina*
[87] *Physics Department, Lancaster University, Lancaster, United Kingdom*
[88] *Oliver Lodge Laboratory, University of Liverpool, Liverpool, United Kingdom*
[89] *Department of Experimental Particle Physics, Jožef Stefan Institute and Department of Physics, University of Ljubljana, Ljubljana, Slovenia*
[90] *School of Physics and Astronomy, Queen Mary University of London, London, United Kingdom*
[91] *Department of Physics, Royal Holloway University of London, Egham, United Kingdom*
[92] *Department of Physics and Astronomy, University College London, London, United Kingdom*
[93] *Louisiana Tech University, Ruston, Louisiana, USA*
[94] *Fysiska Institutionen, Lunds Universitet, Lund, Sweden*
[95] *Centre de Calcul de l'Institut National de Physique Nucléaire et de Physique des Particules (IN2P3), Villeurbanne, France*
[96] *Departamento de Física Teorica C-15 and CIAFF, Universidad Autónoma de Madrid, Madrid, Spain*

[97]*Institut für Physik, Universität Mainz, Mainz, Germany*

[98]*School of Physics and Astronomy, University of Manchester, Manchester, United Kingdom*

[99]*CPPM, Aix-Marseille Université, CNRS/IN2P3, Marseille, France*

[100]*Department of Physics, University of Massachusetts, Amherst, Massachusetts, USA*

[101]*Department of Physics, McGill University, Montreal, Quebec, Canada*

[102]*School of Physics, University of Melbourne, Victoria, Australia*

[103]*Department of Physics, University of Michigan, Ann Arbor, Michigan, USA*

[104]*Department of Physics and Astronomy, Michigan State University, East Lansing, Michigan, USA*

[105]*B.I. Stepanov Institute of Physics, National Academy of Sciences of Belarus, Minsk, Belarus*

[106]*Research Institute for Nuclear Problems of Byelorussian State University, Minsk, Belarus*

[107]*Group of Particle Physics, University of Montreal, Montreal, Quebec, Canada*

[108]*P.N. Lebedev Physical Institute of the Russian Academy of Sciences, Moscow, Russia*

[109]*Institute for Theoretical and Experimental Physics (ITEP), Moscow, Russia*

[110]*National Research Nuclear University MEPhI, Moscow, Russia*

[111]*D.V. Skobeltsyn Institute of Nuclear Physics, M.V. Lomonosov Moscow State University, Moscow, Russia*

[112]*Fakultät für Physik, Ludwig-Maximilians-Universität München, München, Germany*

[113]*Max-Planck-Institut für Physik (Werner-Heisenberg-Institut), München, Germany*

[114]*Nagasaki Institute of Applied Science, Nagasaki, Japan*

[115]*Graduate School of Science and Kobayashi-Maskawa Institute, Nagoya University, Nagoya, Japan*

[116]*Department of Physics and Astronomy, University of New Mexico, Albuquerque, New Mexico, USA*

[117]*Institute for Mathematics, Astrophysics and Particle Physics, Radboud University Nijmegen/Nikhef, Nijmegen, Netherlands*

[118]*Nikhef National Institute for Subatomic Physics and University of Amsterdam, Amsterdam, Netherlands*

[119]*Department of Physics, Northern Illinois University, DeKalb, Illinois, USA*

[120a]*Budker Institute of Nuclear Physics, SB RAS, Novosibirsk, Russia*

[120b]*Novosibirsk State University Novosibirsk, Russia*

[121]*Department of Physics, New York University, New York, NY, United States of America*

[122]*Ohio State University, Columbus, Ohio, USA*

[123]*Faculty of Science, Okayama University, Okayama, Japan*

[124]*Homer L. Dodge Department of Physics and Astronomy, University of Oklahoma, Norman, Oklahoma, USA*

[125]*Department of Physics, Oklahoma State University, Stillwater, Oklahoma, USA*

[126]*Palacký University, RCPTM, Joint Laboratory of Optics, Olomouc, Czech Republic*

[127]*Center for High Energy Physics, University of Oregon, Eugene, Oregon, USA*

[128]*LAL, Université Paris-Sud, CNRS/IN2P3, Université Paris-Saclay, Orsay, France*

[129]*Graduate School of Science, Osaka University, Osaka, Japan*

[130]*Department of Physics, University of Oslo, Oslo, Norway*

[131]*Department of Physics, Oxford University, Oxford, United Kingdom*

[132]*LPNHE, Sorbonne Université, Paris Diderot Sorbonne Paris Cité, CNRS/IN2P3, Paris, France*

[133]*Department of Physics, University of Pennsylvania, Philadelphia, Pennsylvania, USA*

[134]*Konstantinov Nuclear Physics Institute of National Research Centre "Kurchatov Institute," PNPI, St. Petersburg, Russia*

[135]*Department of Physics and Astronomy, University of Pittsburgh, Pittsburgh, Pennsylvania, USA*

[136a]*Laboratório de Instrumentação e Física Experimental de Partículas - LIP, Portugal*

[136b]*Departamento de Física, Faculdade de Ciências, Universidade de Lisboa, Lisboa, Portugal*

[136c]*Departamento de Física, Universidade de Coimbra, Coimbra, Portugal*

[136d]*Centro de Física Nuclear da Universidade de Lisboa, Lisboa, Portugal*

[136e]*Departamento de Física, Universidade do Minho, Braga, Portugal*

[136f]*Departamento de Física Teorica y del Cosmos, Universidad de Granada, Granada (Spain), Portugal*

[136g]*Dep Física and CEFITEC of Faculdade de Ciências e Tecnologia, Universidade Nova de Lisboa, Caparica, Portugal*

[137]*Institute of Physics, Academy of Sciences of the Czech Republic, Prague, Czech Republic*

[138]*Czech Technical University in Prague, Prague, Czech Republic*

[139]*Charles University, Faculty of Mathematics and Physics, Prague, Czech Republic*

[140]*State Research Center Institute for High Energy Physics, NRC KI, Protvino, Russia*

[141]*Particle Physics Department, Rutherford Appleton Laboratory, Didcot, United Kingdom*

[142]*IRFU, CEA, Université Paris-Saclay, Gif-sur-Yvette, France*

[143]*Santa Cruz Institute for Particle Physics, University of California Santa Cruz, Santa Cruz, California, USA*

[144a]*Departamento de Física, Pontificia Universidad Católica de Chile, Santiago, Chile*

[144b]*Departamento de Física, Universidad Técnica Federico Santa María, Valparaíso, Chile*

[145]*Department of Physics, University of Washington, Seattle, Washington, USA*

[146]*Department of Physics and Astronomy, University of Sheffield, Sheffield, United Kingdom*

[147]*Department of Physics, Shinshu University, Nagano, Japan*

[148]*Department Physik, Universität Siegen, Siegen, Germany*

[149]*Department of Physics, Simon Fraser University, Burnaby, British Columbia, Canada*

[150]*SLAC National Accelerator Laboratory, Stanford, California, USA*

[151]*Physics Department, Royal Institute of Technology, Stockholm, Sweden*

[152]*Departments of Physics and Astronomy, Stony Brook University, Stony Brook, New York, USA*

[153]*Department of Physics and Astronomy, University of Sussex, Brighton, United Kingdom*

[154]*School of Physics, University of Sydney, Sydney, Australia*

[155]*Institute of Physics, Academia Sinica, Taipei, Taiwan*

[156]*Academia Sinica Grid Computing, Institute of Physics, Academia Sinica, Taipei, Taiwan*

[157a]*E. Andronikashvili Institute of Physics, Iv. Javakhishvili Tbilisi State University, Tbilisi, Georgia*

[157b]*High Energy Physics Institute, Tbilisi State University, Tbilisi, Georgia*

[158]*Department of Physics, Technion, Israel Institute of Technology, Haifa, Israel*

[159]*Raymond and Beverly Sackler School of Physics and Astronomy, Tel Aviv University, Tel Aviv, Israel*

[160]*Department of Physics, Aristotle University of Thessaloniki, Thessaloniki, Greece*

[161]*International Center for Elementary Particle Physics and Department of Physics, University of Tokyo, Tokyo, Japan*

[162]*Graduate School of Science and Technology, Tokyo Metropolitan University, Tokyo, Japan*

[163]*Department of Physics, Tokyo Institute of Technology, Tokyo, Japan*

[164]*Tomsk State University, Tomsk, Russia*

[165]*Department of Physics, University of Toronto, Toronto, Ontario, Canada*

[166a]*TRIUMF, Vancouver, British Columbia, Canada*

[166b]*Department of Physics and Astronomy, York University, Toronto, Ontario, Canada*

[167]*Division of Physics and Tomonaga Center for the History of the Universe, Faculty of Pure and Applied Sciences, University of Tsukuba, Tsukuba, Japan*

[168]*Department of Physics and Astronomy, Tufts University, Medford, Massachusetts, USA*

[169]*Department of Physics and Astronomy, University of California Irvine, Irvine, California, USA*

[170]*Department of Physics and Astronomy, University of Uppsala, Uppsala, Sweden*

[171]*Department of Physics, University of Illinois, Urbana, Illinois, USA*

[172]*Instituto de Física Corpuscular (IFIC), Centro Mixto Universidad de Valencia - CSIC, Valencia, Spain*

[173]*Department of Physics, University of British Columbia, Vancouver, British Columbia, Canada*

[174]*Department of Physics and Astronomy, University of Victoria, Victoria, British Columbia, Canada*

[175]*Fakultät für Physik und Astronomie, Julius-Maximilians-Universität Würzburg, Würzburg, Germany*

[176]*Department of Physics, University of Warwick, Coventry, United Kingdom*

[177]*Waseda University, Tokyo, Japan*

[178]*Department of Particle Physics, Weizmann Institute of Science, Rehovot, Israel*

[179]*Department of Physics, University of Wisconsin, Madison, Wisconsin, USA*

[180]*Fakultät für Mathematik und Naturwissenschaften, Fachgruppe Physik, Bergische Universität Wuppertal, Wuppertal, Germany*

[181]*Department of Physics, Yale University, New Haven, Connecticut, USA*

[182]*Yerevan Physics Institute, Yerevan, Armenia*

[a]Also at Department of Physics, University of Malaya, Kuala Lumpur, Malaysia.

[b]Also at Borough of Manhattan Community College, City University of New York, NY, USA.

[c]Also at California State University, East Bay, CA, USA.

[d]Also at Centre for High Performance Computing, CSIR Campus, Rosebank, Cape Town, South Africa.

[e]Also at CERN, Geneva, Switzerland.

[f]Also at CPPM, Aix-Marseille Université, CNRS/IN2P3, Marseille, France.

[g]Also at Département de Physique Nucléaire et Corpusculaire, Université de Genève, Genève, Switzerland.

[h]Also at Departament de Fisica de la Universitat Autonoma de Barcelona, Barcelona, Spain.

[i]Also at Departamento de Física Teorica y del Cosmos, Universidad de Granada, Granada, Spain.

[j]Also at Department of Applied Physics and Astronomy, University of Sharjah, Sharjah, United Arab Emirates.

[k]Also at Department of Financial and Management Engineering, University of the Aegean, Chios, Greece.

[l]Also at Department of Physics and Astronomy, University of Louisville, Louisville, KY, USA.

[m]Also at Department of Physics and Astronomy, University of Sheffield, Sheffield, United Kingdom.

[n]Also at Department of Physics, California State University, Fresno, CA, USA.

[o]Also at Department of Physics, California State University, Sacramento, CA, USA.

[p]Also at Department of Physics, King's College London, London, United Kingdom.

[q]Also at Department of Physics, Nanjing University, Nanjing, China.

[r]Also at Department of Physics, St. Petersburg State Polytechnical University, St. Petersburg, Russia.

[s]Also at Department of Physics, Stanford University, Stanford, CA, USA.

[t]Also at Department of Physics, University of Fribourg, Fribourg, Switzerland.

[u]Also at Department of Physics, University of Michigan, Ann Arbor, MI, USA.

[v]Also at Dipartimento di Fisica E. Fermi, Università di Pisa, Pisa, Italy.

[w]Also at Giresun University, Faculty of Engineering, Giresun, Turkey.

[x]Also at Graduate School of Science, Osaka University, Osaka, Japan.

[y]Also at Hellenic Open University, Patras, Greece.

[z]Also at Horia Hulubei National Institute of Physics and Nuclear Engineering, Bucharest, Romania.

[aa]Also at II. Physikalisches Institut, Georg-August-Universität Göttingen, Göttingen, Germany.

[ab]Also at Institucio Catalana de Recerca i Estudis Avancats, ICREA, Barcelona, Spain.

[ac]Also at Institut für Experimentalphysik, Universität Hamburg, Hamburg, Germany.

[ad]Also at Institute for Mathematics, Astrophysics and Particle Physics, Radboud University Nijmegen/Nikhef, Nijmegen, Netherlands.

[ae]Also at Institute for Particle and Nuclear Physics, Wigner Research Centre for Physics, Budapest, Hungary.

[af]Also at Institute of Particle Physics (IPP), Canada.

[ag]Also at Institute of Physics, Academia Sinica, Taipei, Taiwan.

[ah]Also at Institute of Physics, Azerbaijan Academy of Sciences, Baku, Azerbaijan.

[ai]Also at Institute of Theoretical Physics, Ilia State University, Tbilisi, Georgia.

[aj]Also at Istanbul University, Dept. of Physics, Istanbul, Turkey.

[ak]Also at LAL, Université Paris-Sud, CNRS/IN2P3, Université Paris-Saclay, Orsay, France.

[al]Also at Louisiana Tech University, Ruston, LA, USA.

[am]Also at LPNHE, Sorbonne Université, Paris Diderot Sorbonne Paris Cité, CNRS/IN2P3, Paris, France.

[an]Also at Manhattan College, New York, NY, USA.

[ao]Also at Moscow Institute of Physics and Technology State University, Dolgoprudny, Russia.

[ap]Also at National Research Nuclear University MEPhI, Moscow, Russia.

[aq]Also at Near East University, Nicosia, North Cyprus, Mersin, Turkey.

[ar]Also at Physikalisches Institut, Albert-Ludwigs-Universität Freiburg, Freiburg, Germany.

[as]Also at School of Physics, Sun Yat-sen University, Guangzhou, China.

[at]Also at The City College of New York, New York, NY, USA.

[au]Also at The Collaborative Innovation Center of Quantum Matter (CICQM), Beijing, China.

[av]Also at Tomsk State University, Tomsk, and Moscow Institute of Physics and Technology State University, Dolgoprudny, Russia.

[aw]Also at TRIUMF, Vancouver, British Columbia, Canada.

[ax]Also at Universita di Napoli Parthenope, Napoli, Italy.

[*]Deceased.